

Mechanics-based Monotonic Load-Deformation Curves of Beam to Column Joints for Nonlinear Seismic Analysis of Steel Moment Frame Buildings

Arnav Anuj Kasar



**DEPARTMENT OF CIVIL ENGINEERING
MALAVIYA NATIONAL INSTITUTE OF TECHNOLOGY JAIPUR
INDIA
July, 2016**

**Mechanics-based Monotonic Load-Deformation Curves of
Beam to Column Joints for Nonlinear Seismic Analysis of
Steel Moment Frame Buildings**

By

Arnav Anuj Kasar

DEPARTMENT OF CIVIL ENGINEERING

Dr. S. D. Bharti
(Supervisor)

Prof. M. K. Shrimali
(Supervisor)

Dr. Rupen Goswami
(Supervisor, External)

Submitted

in fulfillment of the requirements of the degree of Doctor of Philosophy

to the



MALAVIYA NATIONAL INSTITUTE OF TECHNOLOGY JAIPUR

INDIA

July, 2016

© Malaviya National Institute of Technology Jaipur, 2016
All rights reserved

Certificate

It is certified that the work contained in this thesis entitled "*Mechanics-based Monotonic Load-Deformation Curves of Beam to Column Joints for Nonlinear Seismic Analysis of Steel Moment Frame Buildings*", by Mr. Arnav Anuj Kasar (2012RCE9025), has been carried out under our joint supervision. This work has not been submitted elsewhere for a degree.

July 2016

(S. D. Bharti)
Associate Professor
Civil Engineering
MNIT Jaipur

(M. K. Shrimali)
Professor
Civil Engineering
MNIT Jaipur

(R. Goswami)
Assistant Professor
Civil Engineering
IIT Madras

Abstract

Steel moment frame buildings are not expected to sustain irreparable damages during minor to moderate levels of ground shaking intensities. However, inelastic deformations incur in Joint Panel Zones (JPZs) even at low drift levels, leading to permanent overall deformations. Increasing strength of JPZ delays the onset of inelasticity. The strength of JPZ depends primarily on column to beam strength ratio (CBSR) of joint, and increases with increase in CBSR. To determine the minimum value of CBSR, at which the JPZ remain elastic, nonlinear finite element analysis (FEA) of a set of beam to column joint subassemblages has been carried out. Results suggest that inelastic action initiates in JPZ, upto a CBSR of 3.9.

The estimation of a minimum CBSR requires an understanding of yield forces and drift levels for different components of beam to column joints a priori. This study further proposes a mechanics-based method, to develop load-deformation characteristics that help determine the sequence of yielding between the beam ends and JPZs, and corresponding drifts. The inelastic behaviour of beam to column joints, both interior and exterior are examined, by performing FEA of beam to column joint subassemblages. The CBSR of interior joints are varied from 1.2 to 10.99, and that of exterior joints from 2.4 to 21.98. The load-deformation characteristics of the beam to column joints considered in FEA are also developed using the proposed method. Results obtained from FEA suggest that the proposed method is able to predict the nonlinear force-deformation relationship of a beam to column joint reasonably well. The minimum value of CBSR required to prevent inelastic actions in JPZ is 8.0, in both interior and exterior beam to column moment joints. Also, simultaneous yielding of JPZ and beam ends occurs when CBSR is more than 2.5.

The efficacy of the proposed method is further confirmed, by performing Nonlinear Dynamic Time History Analyses (THA) of a six storey and a twenty storey benchmark frames reported in literature. THA has been carried out using two types of nonlinear hinge properties, which are, using the proposed method, and standard FEMA356 (2000) hinge properties. The THA responses, obtained using hinge properties based on the proposed method agrees more closely than standard FEMA hinges, with responses reported in literature.

Acknowledgement

I am grateful to Professors S. D. Bharti and M. K. Shrimali at MNIT Jaipur, and Professor Rupen Goswami at IIT Madras, my thesis supervisors, for their invaluable guidance and continuous support throughout the course of my Doctoral Programme. They have been an infinite source of encouragement for me, and their technical prowess nourished this thesis. I express my sincere gratitude towards Professor C. V. R. Murty, who always remain available for technical discussions and guidance. He has always been, and will be, a source of inspiration for me, both on technical and personal fronts. The insight provided by Professor T. K. Datta needs a special mention, and his unending support is gratefully acknowledged.

I also thank all faculty members of Structural Engineering Laboratory at IIT Madras, for their welcoming gestures and extending computing facilities, during my research work at IIT Madras. I am also thankful to Ms. Sunitha P. Menon and other research scholars at IIT Madras, for the technical discussions I had with them. I cannot thank them enough for their support.

I would also like to express sincere gratitude towards my teachers, friends, faculty members, and staff members, at MNIT Jaipur. Their unending encouragement has been a source of positive energy, which helped me to have a better outlook, not only in terms of technical matters, but also in interpersonal learning and growth. The caring gestures of Dr. U. Brighu and Dr. N. Rohatgi have always led me to a better path. The efforts of Mr. Chandresh Choudhary, Ms. Ambika Singh and Mr. Rahul Dubey, in proof-reading certain portions of the thesis have been supplemental. The peer group at MNIT Jaipur, especially, Mr. Pankaj Kumar, Mr. Vishisht Bhaiya, Mr. Shashi Narayan, Mr. Jitendra Kr. Goyal, Mr. Sumit Devlekar, Ms. A. Ramya and Mr. Mahdi Abdeddaim are acknowledged.

I am grateful to my parents and sisters for all their love and support. Their trust in me has been the primary driving force and support for this work. No words can describe my gratitude towards my family and friends, who have always been there for me. Their unstinted and constant support has made this cruise enjoyable. At last, I would like to express gratitude towards almighty God, for showering grace on me, by giving an opportunity to pursue this enriching journey...

Table of Contents

Certificate.....	i
Abstract.....	ii
Acknowledgement.....	iii
Table of Contents.....	iv
List of Tables	vii
List of Figures	viii
Nomenclature	xii
Chapter 1 Introduction.....	1
1.1 Overview	1
1.2 Beam to Column Joints	1
1.3 Column to Beam Strength Ratio.....	2
1.4 Panel Zone Behaviour.....	3
1.5 Organization of the Thesis	3
Chapter 2 Literature Review.....	7
2.1 Overview	7
2.2 Steel Moment Resistant Frames: A Historical Perspective.....	7
2.3 Performance of Steel MRFs in Past Earthquakes	9
2.3.1 Mexico City Earthquake of 19 September 1985.....	9
2.3.2 Loma Prieta Earthquake of 17 October 1989	10
2.3.3 Northridge Earthquake of 17 January 1994.....	11
2.3.4 Great Hanshin (Kobe) Earthquake of 17 January 1995	13
2.4 Seismic Behaviour of Steel MRFs	14
2.4.1 Concept of Capacity Design: Strong Column Weak Beam Design Philosophy	14
2.4.2 Significance of Column to Beam Strength Ratio.....	15
2.4.3 Joint Panel Zone Behaviour	17
2.4.4 Performance of Welds.....	23

2.4.5	Connection Configuration	29
2.5	Objectives.....	31
2.6	Organization of the Thesis	31
2.7	Scope of Present Work	32
Chapter 3	Effect of Column to Beam Strength Ratio on Inelastic Behavior of Strong Axis Beam to Column Joints	43
3.1	Overview	43
3.2	Introduction.....	43
3.3	Modelling and Analysis	44
3.4	Numerical Study.....	45
3.4.1	Direct Joints	46
3.4.2	Joints with Continuity Plates.....	46
3.4.3	Connections with Continuity and Doubler Plates.....	46
3.5	Results and Discussion	46
3.6	Conclusions	48
Chapter 4	Mechanics based Monotonic Load Deformation Curves of Beam to Column Joints.....	65
4.1	Overview	65
4.2	Introduction.....	65
4.3	Mechanics Based Method for Prediction of Force Deformation Behaviour	66
4.4	FEA Validation of proposed method.....	69
4.5	Conclusions	70
Chapter 5	Nonlinear Dynamic Analysis of Benchmark Steel Moment Resisting Frame.....	95
5.1	Overview	95
5.2	Introduction.....	95
5.3	Numerical Study of Benchmark Moment Frames	96
5.4	Modelling of Benchmark Moment Frames	98
5.4.1	Hinge Properties from the Proposed Method.....	99

5.4.2 FEMA 356 Hinge Properties	99
5.5 Results and Discussion	100
5.6 Conclusion.....	101
Chapter 6 Summary and Conclusion.....	112
6.1 Overview	112
6.2 Summary.....	112
6.3 Conclusions	114
6.4 Recommendations	115
6.5 Limitations.....	115
6.6 Scope of Future Work	116
References	117
Appendix-A	127

List of Tables

<i>Table 3.1: Properties of selected Column and Beam Sections.....</i>	<i>49</i>
<i>Table 4.1: List of Column and Beam sections used to model the subassemblages. 25.....</i>	<i>71</i>
<i>Table 4.2: Yield Drifts as obtained through Proposed Method and FEA for both Interior and Exterior Joints</i>	<i>72</i>
<i>Table 5.1: Modelling parameters (Nonlinear Hinges) for Beam Elements [Table 5-6, FEMA 356, 2000].....</i>	<i>102</i>
<i>Table 5.2: Modelling Parameters (Nonlinear Hinges) for Panel Zone Element [Table 5-6, FEMA 356, 2000]</i>	<i>102</i>
<i>Table 5.3: Manual (Proposed) Hinge Property Definitions for Exterior and Interior Joints for Six Storey Frame</i>	<i>102</i>
<i>Table 5.4: Manual (Proposed) Hinge Property Definitions for Exterior and Interior Joints for twenty Storey Frame</i>	<i>103</i>
<i>Table 5.5: Modelling parameters (Nonlinear Hinges) for Column Elements [Table 5-6, FEMA 356, 2000].....</i>	<i>103</i>

List of Figures

Figure 1.1: Schematic of an MRF along with its BMD under lateral forces. Both Interior and Exterior joints are also marked.	5
Figure 1.2: Beam to Column Joints in Steel MRF (a) Strong Axis (b) Weak Axis.....	5
Figure 1.3: Components of a typical beam to column joint.	6
Figure 2.1: Prescriptive Moment Connection: Specified between beam and column in steel MRF buildings.....	33
Figure 2.2: Failure modes at welded beam to column strong axis connections observed in the 1994 Northridge Earthquake.	33
Figure 2.3: Joint Panel Zone, Loads and Deformations. (a) Loads acting on a typical interior JPZ; and (b) Possible modes of deformation of JPZ.	34
Figure 2.4: Interstorey Drift Components.....	35
Figure 2.5: Effects of JPZ shear distortion.....	35
Figure 2.6: Balanced JPZ Design.	36
Figure 2.7: Stress Strain Behaviour for Structural Steel.	36
Figure 2.8: Effect of Slenderness Ratio on developable member capacity.....	37
Figure 2.9: Effect of tri-axial restraints to the welds at the column face [Blodgett,1995; FEMA 355c, 2000].....	37
Figure 2.10: Beam flange to Column interface.	38
Figure 2.11: Beam to Column Joint with flange cover plates	38
Figure 2.12: Beam to Column joint with RBS connection.	39
Figure 2.13: Beam to Column Joint with Slotted Beam Connection.	40
Figure 2.14: Non-seismic beam to column connections.	40
Figure 2.15: Connection Rigidity. [adapted from Mazzolani and Piluso, 1996].....	41
Figure 2.16: Typical Behaviour of Moment Resisting Connections [adapted from Mazzolani and Piluso, 1996].....	42
Figure 3.1: Interior and Exterior Beam Column Joints in a MRF.	50
Figure 3.2: Beam-Column Joint Subassembly.....	50
Figure 3.3: Stress Strain Curves for A36 Steel and E70 welds as modelled.	51
Figure 3.4: SAC's Standard Loading Protocol [ANSI/AISC 341-10].....	51
Figure 3.5: Hysteretic Curves and Backbone Curves for CFSR of 3.89.....	52
Figure 3.6: (a) von Mises Stress contours at final step and (b) Shear Stress contours at initiation of yielding, for direct joints.....	55
Figure 3.7: (a) von Mises Stress contours at final step and (b) Shear Stress contours at initiation of yielding, with Continuity Plates..	58
Figure 3.8: ((a) von Mises Stress contours at final step and (b) Shear Stress contours at initiation of yielding, with Doubler and Continuity Plates.	61
Figure 3.9: Normalized Force Deformation Behaviour of Prequalified Beam to Column Joint Subassemblages (Normalized by the Capacity of individual member).....	62

Figure 3.10: Normalized Force Deformation Behaviour of Prequalified Beam to Column Joint Subassemblages with Continuity Plates (Normalized by the Capacity of individual member).....	63
Figure 3.11: Normalized Force Deformation Behaviour of Prequalified Beam to Column Joint Subassemblages with Doubler and Continuity Plates (Normalized by the Capacity of individual member).....	64
Figure 44.1: A schematic of an exterior beam to column joint depicting the three probable yield locations.	74
Figure 4.2: Adopted Force Deformation Behaviour of Joint Panel Zone Region..	75
Figure 4.3: (a) von Mises stress contour at 4 % drift (b) Shear stress contours at initiation of yield.....	80
Figure 4.4: (a) von Mises stress contour at 4 % drift (b) Shear stress contours at initiation of yield.....	85
Figure 4.5: Column Shear Force versus Beam End Drift relationships for Exterior Beam to Column Joints.....	89
Figure 4.6: Column Shear Force versus Beam End Drift relationships for Interior Beam to Column Joints.	93
Figure 5.1: Plan of 6 Storey Building Frame.....	104
Figure 5.2: Plan of 20 Storey Building Frame	104
Figure 5.3: 6 Storey Benchmark Frame [Tsai and Popov, 1988].....	105
Figure 5.4: 20-Storey Benchmark Frame [Tsai and Popov, 1988]	106
Figure 5.5: Typical Beam compound element modelling.....	107
Figure 5.6: General Force Deformation Curve	107
Figure 5.7: Typical Column compound element	107
Figure 5.8: Ground Acceleration time history for 3× TAFT earthquake. The Six Storied Building frames is analysed using this ground motion.....	108
Figure 5.9: Ground Acceleration time history for Mexico City earthquake.	109
Figure 5.10: Displacement Profile at Maximum Roof Displacement for Six storied frame..	109
Figure 5.11: Floor Displacement Histories for Six storied frame.....	110
Figure 5.12: Roof Displacement History for Twenty storied frame	111
Figure 5.13: Base Shear History for Twenty storied frame	111
Figure A-1: Force Deformation Behaviour of an interior beam to column joint subassemblage.	133

Nomenclature

b_{bf}	Width of Beam Flange
b_{cf}	Width of Column Flange
b_p	Width of Joint Panel Zone
d_b	Depth of Beam Section
d_c	Depth of Column Section
d_p	Depth of Joint Panel Zone
E	Modulus of Elasticity of Steel
E_b	Modulus of Elasticity of beam material
E_c	Modulus of Elasticity of column material
E_t	Tangent stiffness of column section
$F_{p,bf}$	Beam Flange Force corresponding to formation of Beam Plastic Hinges
F_{pb}	Beam end force required to develop beam plastic hinge
f_y	Yield Strength of Steel
$F_{y,bf}$	Beam Flange Yield Strength
f_{yb}	Yield Strength of Beam steel
f_{yc}	Yield Strength of Column steel
G	Shear Modulus of Steel (Column and Beam material)
H	Horizontal shear in Joint Panel Zone
I_b	Moment of Inertia of Beam Section
I_c	Moment of Inertia of Column Section
K_{b1}	Beam Stiffness post beam flange yielding
K_{b2}	Beam Stiffness post formation of plastic hinge
K_{pz1}	Panel Zone Stiffness immediately after initiation of yielding ($\gamma_y < \gamma < 3\gamma_y$)
K_{pz2}	Panel Zone Stiffness post significant yield ($\gamma > 3\gamma_y$)
L_b	Length of beam, between supports
L_c	Storey height, support to support height of column
$M_{c,1}$	Column moment at first yield event
M_e	Beam end moment resulting from code specified seismic forces
M_g	Beam moment due to gravity loads
M_l	Beam end moment for left hand side beam
M_{pB}, M_{pb}	Plastic Moment Capacity of Beam Section
M_{pC}, M_{pc}	Plastic Moment Capacity of Column Section
M_r	Beam end moment for right hand side beam
P_u	Factored axial force in column
P_y	Axial yield capacity of column section
R_v	Strength of JPZ as recommended by AISC 1999
S_b	Shape Factor for Beam Section
S_c	Shape Factor for Column Section
t_{bf}	Thickness of Beam Flange
t_{bw}	Thickness of Beam Web

t_{cf}	Thickness of Column Flange
t_{cw}	Thickness of Column Web
t_{dp}	Total Thickness of Doubler Plates provided
$t_{p,reqd.}$	Minimum required thickness of Joint Panel Zone based on Slenderness
t_{pz}	Thickness of Joint Panel Zone
V_n	Nominal shear strength of joint panel zone
V_{pB}	Beam end force corresponding to plastic flexural strength of Beam
$V_{pz,1}$	Shear force in Joint Panel Zone at first yield event.
V_u	Ultimate shear strength of joint panel zone
$V_{y,pz}$	Panel Zone Yield Strength
V_{y1}	Beam end force corresponding to mode of first yield
V_{y2}	Beam end force corresponding to mode of second yield
V_{y3}	Beam end force corresponding to mode of third yield
Z_{eb}	Elastic Section Modulus of Beam Section
Z_{ec}	Elastic Section Modulus of Column Section
Z_{pb}	Plastic Section Modulus of Beam Section
Z_{pc}	Plastic Section Modulus of Column Section
a	Ratio of depth of beam to storey height
a_{gb}	reduction factor for gravity moment
β	Column to Beam Strength Ratio for a Beam to Column Joint
γ	Joint Panel Zone Rotation
γ_{avg}	Average Shear Strain in Joint Panel Zone
$\gamma_{pz,1}$	Joint Panel Zone Rotation at first yield event
γ_y	Yield Rotation of Joint Panel Zone
δ	Total storey drift
$\Delta_{b,1}$	Beam rotation at first yield
δ_c	Drift owing to flexural deformation of columns
δ_c	Drift owing to shear distortion of joint panel zone
$\Delta_{c,1}$	Column rotation at first yield
ΔM	Design unbalanced moment
$\Delta_{pz,1}$	Joint Panel Zone rotation at first yield event
δr	Drift owing to rigid body rotation of joint panel zone
$\Delta_{total,1}$	Total rotation of a joint at first yield vent
ε	Strain at any instant
ε_{sh}	Strain at initiation of strain-hardening
ε_u	Ultimate strain
ε_y	Strain at yield
$\theta_{c,1}$	Column rotation at first yield event
λ	Slenderness ratio of a cross-section
λ_p	Slenderness limit for non-compact elements

λ_{pd}	Limiting slenderness ratio for compact sections, to ensure plastic rotation ductility.
λ_r	Slenderness limit for compact elements
σ_1	maximum principal stress in a tri-axially loaded specimen
σ_3	minimum principal stress in a tri-axially loaded specimen
ΣM_{pb}	Sum of plastic moment capacities of beams framing at a joint
ΣM_y	Moment required to cause panel zone shear yielding
σ_y	Yield stress of column material
τ_{avg}	Average shear stress in Joint Panel Zone
τ_{max}	Maximum Shear Stress in a tri-axially loaded specimen
τ_w	Shearing stress in joint panel zone
ν	Poisson's Ratio of Steel (Column and Beam material)
Ω	Ratio of distortional moment to design seismic moment
Ω_0	Structural overstrength factor
Ω_{bal}	Overstrength factor for balanced Joint Panel Zone design
ϕ_v	resistance factor to incorporate initiation of yield in joint panel zone

Chapter 1

Introduction

1.1 Overview

Large scale damages to civil engineering structures in general, and buildings in particular, during major earthquakes have underlined the importance of a viable approach to earthquake resistant design (ERD). The earthquake resistant design philosophy, as envisaged by various international standards stipulates that, the structure should not suffer any structural damage under minor (but frequent) earthquakes, repairable structural damage under moderate (but occasional) earthquakes, and shall not collapse under severe (but rare earthquakes). The essence of earthquake resistant design (ERD) is in efficient and effective dissipation of seismic energy, the inelastic hysteretic energy dissipation should be such it is able to exploit the energy dissipation capacity of the system without endangering the safety. The concept of Capacity Design [Penelis and Kappos, 1997], envisages maximum utilization of ductile energy dissipation capacity of structure without collapse. Collapse prevention implies that the structure continues to maintain its gravitational load carrying capacity in the event of a strong earthquake.

Steel is the most highly regarded civil engineering construction material. The inherent ductility and low weight to strength ratio makes it an ideal material for ERD. Some of the commonly used structural systems for steel construction are, Moment Resisting Frames (MRFs), Braced Frames (eccentric and concentric) and Frames with Structural Walls. Among these, steel MRFs provide highest flexibility in terms of space utilization, as they provide unobstructed space between columns. An MRF is a rectilinear assembly of columns and beams, typically welded and/or bolted together. Lateral load resistance in MRFs is achieved by flexural and shearing actions in beams and columns.

1.2 Beam to Column Joints

Steel MRF buildings usually have frames oriented in orthogonal directions and having both interior and exterior joints (Figure 1.1). When I-sections are used as structural members, two sets of beam to column joints are possible, namely, (a) strong-

axis joints, where the beam(s) frames into the column flange(s), and (b) weak-axis joints, where beam(s) frame into the web of column (Figure 1.2). Since the moment of inertia and the plastic moment capacity of I-sections are usually higher along their strong-axis, the strong-axis orientation is preferred in case of joints that need to transfer moments as well as shear forces.

The seismic behaviour of steel MRF buildings critically depends on the performance of beam to column joints, in terms of plastic energy dissipation at beam ends without any brittle failure. Parts of a typical beam to column joint are: (i) beam ends, (ii) column ends, (iii) connections and (iv) joint panel zone (JPZ) (Figure 1.3).

The Capacity Design Concept [Penelis and Kappos, 1997], which is regarded as the basis for design of an MRF, enlists the strength hierarchy of the members as, (a) the beam to column joint has to be stronger than the beam, (b) the column has to be stronger than the beams, and (c) the column base connection has to be stronger than the column. The Capacity Design translates into strong column weak beam (SCWB) design, but there are no guidelines to ascertain the factor or number, by which, the strength of column has to be greater than that of the beam. Also, the strength hierarchy between JPZ and the column, remains unspecified.

1.3 Column to Beam Strength Ratio

Since the disclosure of serious damages to modern steel MRFs during 1994 Northridge and 1995 Hyogoken-Nanbu (Kobe) Earthquakes, extensive research is underway on various issues concerning performance of steel moment frames. One of the related research subjects is 'how to design a SCWB frame in order to ensure a beam hinging mechanism' during the response. A specific research target along this line is the Column to Beam Strength Ratio (CBSR, represented by β) needed to secure beam-hinging response. The current SCWB seismic design criterion presents a single value as the acceptance limit of strength ratios for steel MRFs. The SCWB design philosophy can be realized by designing the columns as per capacity design approach. The CBSR should be larger than unity, by some margin of safety for each joint, with the assumption that columns remain elastic, even after the formation of plastic hinges in beams.

1.4 Panel Zone Behaviour

The behaviour of beam to column joints in welded steel MRFs is strongly affected by the performance of joint panel zone (JPZ); which is the portion of column web area delineated by the extension of beam and column flanges through the connection. The transfer of moments between beams and columns causes a complicated state of stress and strain in the panel zone. Under the action of lateral forces, the panel zone deforms in three modes: axial, shear, and bending, however, the shear deformation of panel zone has significant effect on the behavior of steel MRFs.

Since late 1960s, a number of experimental and analytical investigations have been carried out to understand the behaviour of JPZ [Fielding and Huang, 1972, Krawinkler, 1978; Popov et al., 1987]. These studies suggest that, when subjected to repeated cyclic distortions, yielding of JPZ is a stable phenomenon, and can be helpful in dissipating the energy induced. But, it is also evident from these studies that the overall frame stiffness is greatly influenced by the stiffness of the JPZ.

Till early 1980s, AISC recommended a strong JPZ design approach to prevent inelastic actions in the JPZ region. However, on the basis of researches carried out during late 1970s a balanced JPZ was recommended. Thus, a balanced JPZ design approach was adopted, which aims at simultaneous onset of flexural hinging in beams and shear yielding in JPZ [FEMA 355D, 2000]. Further, in cases where the columns are not strong enough, weak JPZ causes large inelastic drifts and loss of overall stiffness of frames. This often leads to kinking of column flanges at the level of beam flanges. This increases curvature and causes failure of welded connections due to large concentration of stresses.

1.5 Organization of the Thesis

The study proposes a mechanics based, analytical, closed form approximations of the beam to column joint force deformation behaviour. The thesis comprises of six chapters; the first chapter provides a introduction to steel MRFs and its components. The second chapter presents a review of relevant literature and the performance of MRFs during past major earthquakes.

The effects of CFSR on the behaviour of SCWB strong axis beam to column joints, on the basis of flow of inelastic stresses in interior beam to column joint subassemblages has been investigated in chapter three.

In the fourth chapter, a mechanics based hand calculation approach has been proposed to determine the drift levels at which inelastic actions initiate in strong axis beam to column joint subassemblages. This method takes into consideration, the effects of column web doubler plates. Using the proposed method, force deformation behaviour of strong axis interior as well as exterior joints can be predicted. Nonlinear Finite Element Analyses of 25 SCWB strong axis joint subassemblages has been carried out, for both interior and exterior joints, to validate the proposed method.

The effectiveness of the proposed method is further validated in chapter five by carrying out Nonlinear Dynamic Time History Analyses (NLDTHA) of two benchmark steel MRFs [Tsai and Popov, 1988]. The nonlinear moment rotation properties of joints of the frame are obtained using the proposed method. The suitability of the proposed method over nonlinear moment rotation properties as prescribed in FEMA 356 (2000) is also presented.

Chapter six presents the summary of the work carried out in the thesis and the conclusions. In addition to this some recommendations and scope of future work have been discussed.

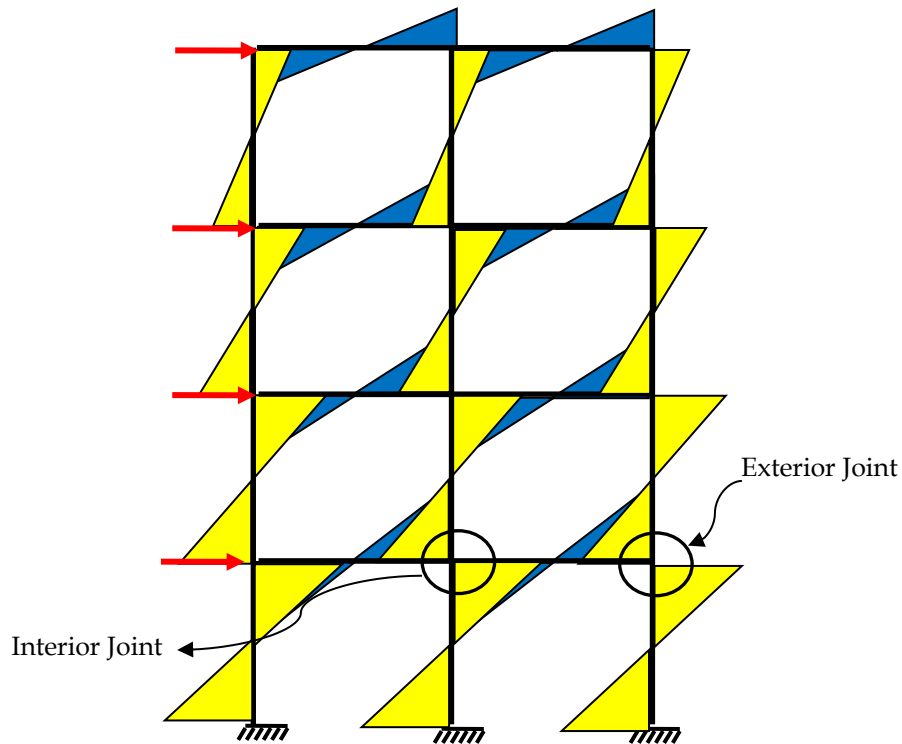


Figure 1.1: Schematic of an MRF along with its BMD under lateral forces. Both Interior and Exterior joints are also marked. Linear Static Analysis of frames suggests that point of contraflexure lies at mid height of columns and at center of beams.

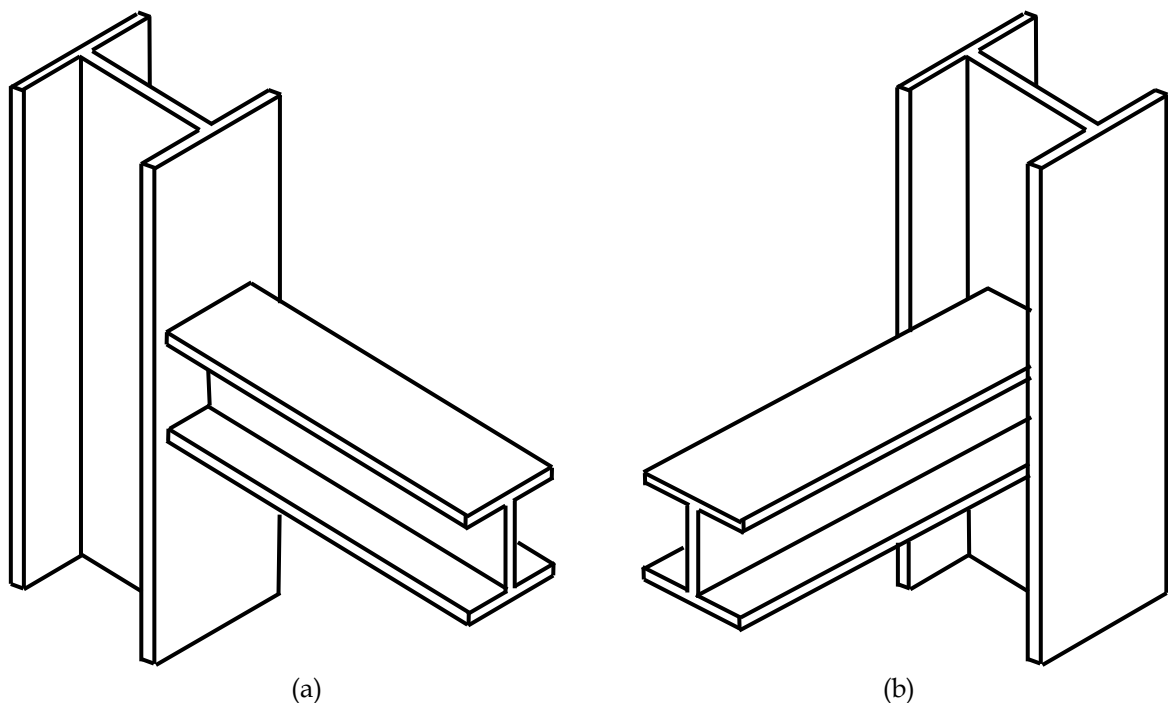


Figure 1.2: Beam to Column Joints in Steel MRF (a) Strong Axis (b) Weak Axis. For seismic design of MRFs, strong axis joints are preferred over weak axis joints. Weak Axis joints are usually designed to transfer Shear Forces.

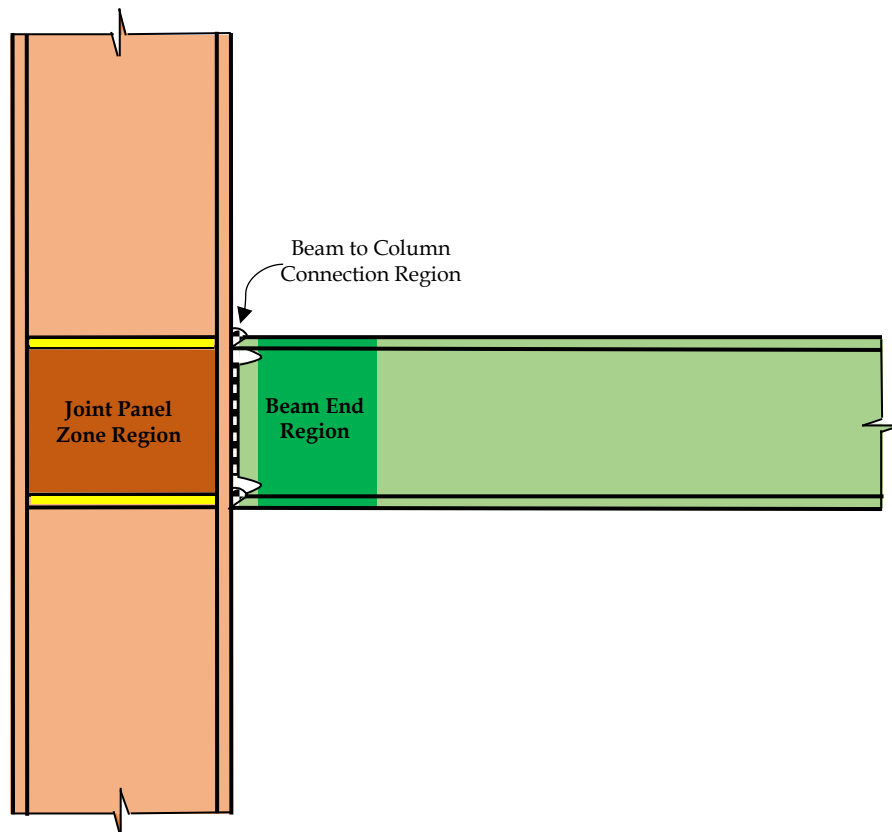


Figure 1.3: Components of a typical beam to column joint. The beam to column joint can be viewed in three parts, namely, (i) beam end region, (ii) beam to column connection and (iii) Joint Panel Zone (JPZ).

Chapter 2

Literature Review

2.1 Overview

Performances of steel moment resisting frame (MRF) buildings during strong ground shaking are greatly influenced by the behaviour of individual components and interaction thereof. Over the past couple of decades, the philosophy of seismic design of individual frame members (i.e., beams and columns), has not seen major changes. But, the seismic design of joints and their connections, particularly of the beam to column connections in steel MRF buildings, has undergone radical changes. While welded connections were considered to be the most efficient way of connecting members in all types of steel frames, recent findings indicate that stouter connections and shorter buildings perform better during large magnitude near-field ground motions [Hall, 1997]. The development of earthquake-resistant design has emphasized the importance of capacity design concept for structures. Employing a hierarchy of structural component strengths, capacity design of structures ensures that inelasticity is confined to predetermined and preferred structural components. Failure modes that result in non-ductile structural behaviour are avoided by providing higher resistance to such modes. Thus, columns are made stronger than beams to ensure that during strong earthquake shaking, energy dissipating plastic hinges are formed at the beam ends. In addition, the connection elements are required to remain elastic, so as to allow the adjoining beams to develop plastic hinges.

2.2 Steel Moment Resistant Frames: A Historical Perspective

Steel MRFs are commonly used for single-story and multi-storey buildings around the world. This structural system has the inherent advantage to accommodate a variety of functional and architectural requirements. Initially these frames utilized riveted moment-resisting connections designed to resist nominal wind loads, and cladding and unreinforced masonry provided substantial additional strength and stiffness for the resistance of lateral loads. This class of structure has generally provided life-saving performance, following a number of major earthquakes till the early years of twentieth century.

Gradually due to modernization of the steel building construction industry, engineers began to make modifications in the steel moment frame system. In the 1950s, high strength bolting replaced riveted construction, field welding procedures made the connection of large structural shapes a viable alternative in the late 1960s and early 1970s. Further, a movement towards much lighter and more flexible cladding systems for modern buildings meant that the steel frames would no longer benefit from the additional stiffness and strength provided by the masonry cladding used in the older buildings.

Early applications of steel MRFs usually included moment-resisting connections to all columns in both orthogonal directions. For interior columns, this would result in four-way moment connections. These connections were expensive to construct, and as a result, engineers began to seek ways to limit the number of these connections. The advent of larger rolled structural shapes in the post-World War II era allowed to achieve equivalent lateral stiffness and strength with fewer moment frames, leading some cost savings in the structural steel fabrication and erection. Initially, these less redundant frames incorporated the moment resisting connections at the building perimeter whereas simple connections at the interior columns. As engineers became more comfortable with this approach, they continued to minimize the number of lateral force resisting elements in these moment frames, eventually resulting in many buildings where only one or two bays of moment resisting connections were provided at the building perimeter. While this approach provided some cost savings, the use of a minimal number of frames required the use of very large member sizes, and therefore very large full penetration field welds to meet the drift requirements of the building code.

Early moment connections used full penetration welds between the entire beam section for both flanges and the web and the column. These welds were completed in the field as part of the erection of the steel frame. In the early 1970s, a series of tests on small W18 and W24 beam shapes conducted experimental studies demonstrated that connections with welded flanges and high strength bolted webs could achieve some inelastic rotation prior to fracturing the flange welds [Popov and Stephen, 1972]. Since these connections were more economical to fabricate and erect

than the welded beam detail, they quickly became the industry standard and were eventually codified into the Uniform Building Code (1988).

2.3 Performance of Steel MRFs in Past Earthquakes

The earthquakes that occurred up to the latter half of twentieth century validated the good performance of steel MRF buildings. In the 1964 Alaska earthquake, a number of steel MRFs with reinforced concrete shear walls performed well, with cracking observed in the concrete walls, but apparently little damage to the steel frames [Berg, 1973]. In the 1971 San Fernando earthquake, a number of more modern steel frame buildings survived the event and were analysed extensively to evaluate the demands imposed on the system by the ground motion. The only steel moment frame building shaken by the 1972 Managua, Nicaragua earthquake also appeared to have come through the event unscathed [EERI, 1973]. Finally, the lack of damage found in investigations immediately following the 1989 Loma Prieta earthquake apparently affirmed the notion that steel MRFs provide excellent seismic performance, however, incorrectly, as the reinvestigation of a number of buildings subsequent to the 1994 Northridge earthquake proved. Investigations have shown the presence of similar, though previously undetected, damage in welded steel MRF buildings shaken by the 1989 Loma Prieta, 1992 Landers and 1992 Big Bear earthquakes.

By the early 1990s, the performance in previous earthquakes and favourable results from early experimental and analytical investigations led building code developers and structural engineers in the United States to regard the welded steel moment frames as one of the best systems available for resisting the damaging effects of earthquakes. In the last quarter of the 20th century, a few but significant earthquakes that hit large and well-developed urban areas, led to a much better appreciation of the behaviour of steel MRF buildings. The performances of steel MRF buildings during these earthquakes are discussed in the following sub-sections.

2.3.1 Mexico City Earthquake of 19 September 1985

This was one of the most damaging earthquakes to have occurred at the subduction zone between the North American and Pacific plates. Majority of damages occurred in Mexico City, about 350 km away from the epicenter. During the post-

earthquake studies, 102 steel buildings were identified in the strongly shaken part of Mexico; these included 41 moment resisting frame (MRF) buildings [Osteraas and Krawinkler, 1989]. A typical MRF building frame consisted of box columns made of two channels welded with cover plates or of four welded plates; built-up and hot rolled H- sections were also found in some buildings. Beams were hot rolled H- sections, built-up H-sections or truss girders made of angles. Truss girders were used at a time when sections deeper than 450 mm were not manufactured in Mexico and structural steel was not imported.

Steel MRF buildings seemed to have performed well, in contrast to the RC MRF buildings. Only 5 of the 41 MRF buildings studied were damaged, and had sustained failures at the beam-to-column connections. The 44-storey steel MRF Torre Latinoamericana Building, built during 1948-1956, having H-sections columns with cover plates, beams of standard wide sections, and riveted beam-to-column connections showed no apparent damage [Osteraas and Krawinkler, 1989].

The 11-storey steel MRF Amsterdam Street Building, built in 1970, sustained severe cracks in the infill masonry walls and the beam-to-column connections of the first four storeys [Osteraas and Krawinkler, 1989]. The columns of this building were built up with two channels and cover plates, and the beams were plate girders welded from three plates. The beam-to-column connections were complete joint penetration welds connecting the beam flanges to column cover plate. These connections constituted the weak links in the entire beam to column joint subassemblage. Studies showed that the lower bound bending strength estimates of these connections barely matched the moments generated by gravity loads.

2.3.2 Loma Prieta Earthquake of 17 October 1989

The post-earthquake field surveys after the 17 October 1989 Loma Prieta earthquake indicated no structural damage to steel buildings. In fact, reports stated that steel buildings performed “excellently” during this earthquake, with damages limited to cracking of cladding and interior partitions, which was a result of large displacements of the flexible steel frames [EQE, 1989]. However, several months after the Northridge earthquake of 17 January 1994 in the Greater Los Angeles area, extensive damages to steel buildings in the San Francisco Bay Area were discovered

[SAC, 1996]. These damages during the 1989 Loma Prieta earthquake went unnoticed during the post-earthquake surveys in 1989, hidden away behind the architectural finishes and fireproofing material.

Typically, the damages were concentrated at the beam-column joints. Fractures initiated at or near the complete joint penetration welds. Some cracks progressed through the column flange, and a few of these also traversed the entire column cross-section. These cracks reduced both the lateral stiffness and strength of the building, to levels below that required to resist lateral forces induced by strong winds and subsequent earthquakes [SAC, 1996].

2.3.3 Northridge Earthquake of 17 January 1994

The 17 January 1994 Northridge Earthquake was the first earthquake where extensive damage was reported from steel MRF buildings subjected to strong earthquake ground motion. There were no collapses of steel MRF buildings. Initial field surveys indicated that steel MRF buildings performed well during this earthquake. It was more than two weeks later that problems with welded connections started surfacing; the damages to the structural steel members were hidden behind the architectural finishes and fire proofing material [Krawinkler, et al., 1996]. Many buildings in the affected area sustained significant distortions, which was apparent because of the large cracks in the column cladding. Damage to the non-structural components like fireproofing, facades, plaster, glazing, unreinforced infills and glass panels, was one of the primary reasons to begin investigations for structural damage [Hall, 1994]. A number of problems related to steel MRF buildings were noted, and their performance was unacceptable. These problems were not known prior to this earthquake [EQE, 1994].

One of the major signatures of the 1994 Northridge earthquake was the discovery of widespread brittle fractures in the critical beam to column joints in a number of welded steel MRF buildings. Damage was observed in a wide variety of MRF buildings, new, old, short and tall. A wide spectrum of brittle connection damage was discovered, ranging from minor cracking to completely severed beams and columns. The most commonly observed damage was located in or near the welded joint connecting a beam bottom flange to the supporting column flange. Interestingly,

connection fractures were detected in buildings located in regions of relatively modest ground shaking, that is, below 0.3g peak ground acceleration. In areas with more intense shaking, some buildings were discovered with fractures at all of the moment-resisting connections in one or more floors, resulting in significant permanent lateral displacements. No loss of life resulted from damage to steel MRF structures in the United States and none of these structures collapsed. However, little evidence of ductile yielding prior to fracture has been found in damaged buildings. Such brittle behaviour is contrary to the basic tenets of modern seismic-resistant design and the intent of contemporary building codes. This brittle behaviour has raised questions about the safety of steel MRF structures in the event of severe ground shaking.

The performance of steel MRF buildings during the 1994 Northridge earthquake has emphasized the vulnerability of moment resisting connections subjected to strong earthquake shaking. Many low and medium rise steel MRF buildings sustained structural damage in the beam to column joints. These buildings were designed and detailed according to the then existing building code requirements, which were intended to ensure ductile performance of the buildings during major earthquakes [Krawinkler and Popov, 1982]. The unintended overstrength due to underestimation of actual yield strengths of sections resulted in MRF buildings with far greater elastic strength than expected [Krawinkler, et al., 1996]. Further, analyses of the steel MRF buildings damaged during this earthquake showed that the code drift limits resulted in frames with large reserve elastic strengths. Although no steel building collapsed, the extensive damage to beam to column connections led designers and researchers to agree that the damage type is unacceptable.

The prescriptive MRF connection was extensively used in steel frames constructed prior to the 1994 Northridge earthquake (Figure 2.1). It was a common practice to design selected moment resisting frames to carry the entire lateral load, and the other frames for gravity load alone. This strategy minimized the number of moment resisting connections, resulting in buildings having low redundancy with only a few frames (in most cases only the two perimeter frames) resisting the lateral loads.

A survey report indicated that more than 100 steel MRF buildings had localized failures at the beam to column connections [Youssef, et al., 1995]. Fracture at the weldment connecting beam flange to the column flange was the most common failure. Other failure types observed, includes (a) separation of weld, (b) divot pull out from column flanges near beam flange CJP groove weld, (c) cracking in column flanges, column web and beam flanges, (d) cracking of shear tabs, (e) brittle failures of the beams flange weld connections, and (f) fracture of column flanges including portions of the column web, particularly near the beam bottom flange (Figure 2.2) [Degenklob, 1994; Krawinkler et al., 1996; Miller, 1998]. Most cracks initiated at the welds connecting the beam bottom flange and the column face; the top flange of the beam was embedded in the floor slabs and hence sustained lesser stress [Bertero, et al., 1994]. All these damages were not readily apparent as they were hidden behind the finishes and fireproofing material. Many failures of welded connections were reported in buildings located even as far as 30 kms from the epicenter [NIST, 1994]. This is an issue of concern as the magnitude of the 1994 Northridge earthquake was only 6.8.

2.3.4 Great Hanshin (Kobe) Earthquake of 17 January 1995

This magnitude 7.2 earthquake in Japan was similar to the 1994 Northridge earthquake in the USA in terms of low focal depth and high peak ground accelerations, particularly the vertical motion associated with the near-field type pulses. While Japanese construction practices differ from those used in the United States in several basic ways, steel MRF buildings in Kobe suffered more severe damage than that observed in California during 1994 Northridge earthquake; in fact, more than 10% of these structures collapsed. A large number of mid to high rise steel MRF buildings were affected. Typically, columns were of built-up or rolled box sections and beams of rolled I-sections. Beams were connected to columns by CJP welds. Steel buildings of around 20 storeys were estimated to have sustained inter-storey drifts between 2% and 4% [AIJ, 1995]. Post-earthquake surveys reported severe cracking and extensive fracturing of welds in these welded connections in the beam column joint region [JSCE, 1995].

2.4 Seismic Behaviour of Steel MRFs

Seismic behaviour of steel MRFs is controlled by the behaviour of individual members, their interconnection and interaction thereof. Various components of steel MRFs are: Beam, Column, Joint Panel Zone and connection elements (Figure 1.3). The general philosophy of earthquake-resistant design allows the inelastic behaviour of structures under severe earthquake ground motions. In addition, the design earthquake force is determined considering the ductility or energy dissipation capacity through inelastic structural responses. The global structure should remain stable and safe while these inelastic deformations occur. In this context, it is generally desirable to provide strong columns and to allow the yielding of the beams in flexure prior to possible yielding in columns.

2.4.1 *Concept of Capacity Design: Strong Column Weak Beam Design Philosophy*

The strong column weak beam (SCWB) design philosophy improves the seismic performance of MRF buildings, and most steel MRF buildings designed prior to the 1994 Northridge earthquake adopted this philosophy. There are two options for achieving SCWB designs, namely (a) by using steel of same grade in both beams and columns, and larger size columns, and (b) by using steel of higher grade in columns. The second option allows the use of beams and columns of similar sizes, and sometimes even columns of smaller sizes. In the pre-Northridge earthquake buildings, the second option with A572 Grade 50 steel for columns and A36 grade steel for beams was extensively used. However, for A36 grade steel, ASTM [ASTM, 1996] ensures only the lower bound value of yield strength; the upper limit of yield strength is not specified. A survey after the 1994 Northridge earthquake revealed that strengths of most beams of A36 grade steel were close to that of A572 Grade 50 steel [Miller, 1998; Malley and Frank, 2000]. This, in effect, made some of the intended SCWB designs to become the undesirable weak-column strong-beam (WCSB) designs.

Inappropriately large lateral drifts result in excessive straining and subsequent damage to both, the structural as well as non-structural components of MRF buildings. The overall building drifts under lateral loads can be controlled effectively by adopting the SCWB design for MRFs. Analytical estimates show that lateral drifts of WCSB frames can be up to 3-4 times larger than that of the corresponding SCWB

frames [e.g., Roeder, et al., 1993]. Similar experimental comparisons show that lateral drifts of WCSB frames are about 1.7 times larger than the corresponding SCWB frames [Schneider, et al., 1993]. In effect, to reduce lateral drifts of WCSB frames to levels of the corresponding SCWB frames, the WCSB buildings need to be designed for seismic loads that are up to twice as much as those used in the design of SCWB buildings. The behaviour of WCSB frames is also sensitive to the axial load in the columns; the overall frame cyclic load hysteretic loops deteriorate with increased column axial load.

The desirable performance of steel MRF buildings during strong earthquake shaking requires the input seismic energy to be dissipated without collapse of the structure. The WCSB frames have plastic deformation in a limited number of frame members, generally in the columns. This is detrimental to the structure since it results in large inter-storey drifts. Further, column hinging can lead to early collapse of the structure by the formation of panel or storey mechanism. But, in SCWB frames, the plastic deformation is distributed over a larger number of members across the structure, that too mostly in the beams [Roeder, et al. 1993]. Thus, large energy dissipation is possible in SCWB frames before collapse.

SCWB designs result in significant economy, and their seismic performance is superior to that of the WCSB frames. The 1997 Uniform Building Code [UBC, 1997] does not allow the use of WCSB design configuration when the column is to resist the seismic effects. Even in non-seismic columns of the frame, the use of WCSB is restricted and is permitted only when (a) the maximum axial load in column is less than 30% of its yield, and (b) column in a given storey has a ratio of design shear strength to design shear demand 50% higher than that of the storey above.

2.4.2 Significance of Column to Beam Strength Ratio

The strong column weak beam philosophy is based on the linear static analysis with the assumption that the inflection points of columns are located at the centre of columns. However, due to the influence of nonlinear behaviour, it is known that the real moment distribution of moment frames is different from that based on the linear static analysis and the column hinge mechanism may be induced even if the strong-column weak-beam condition is satisfied [Lee H., 1996]. A lot of studies have been

conducted to evaluate the column to beam strength ratios required for inducing the beam hinge mechanism [Lee H, 1996; Kuntz and Browning, 2003; Choi et al., 2013].

The desirable mechanism, for formation of hinges in a structures is such that all the inelasticity remain localised at beam ends. To ensure this behaviour, strong column weak beam design philosophy had been deemed sufficient. However, studies carried out during past decade have suggested that, the column to beam strength ratios depends on various factors. Nakashima and Sawaizumi analysed the strength ratios of an example structure, modelled such that plastic hinges occur only at beam ends and the bottom of the first-story columns. Based on the maximum moments of columns, it was found that the strength ratios ensuring the elastic behaviour of columns increased with the increment of the ground motion amplitude, and reached about 1.5 for the ground motion amplitude of 0.5 m/s [Nakashima and Sawaizumi, 2000]. Another study considered the number of storeys, the natural period, and the seismic level as parameters influencing on the strength ratios required for ensuring the beam hinge collapse mechanism [Medina and Krawinkler, 2005; Dooley and Bracci, 2001].

The current strong-column weak-beam design criterion presents a single value as the acceptance limit of strength ratios for MRFs. ANSI/AISC 341-05 suggests the strong column weak beam criterion to secure the ductility capacity of the steel MRFs. The criterion means that the ratio of the sum of plastic flexural strengths of columns to the sum of plastic flexural strengths of beams connected at a joint should be greater than unity. Choi and Park, 2012 [12] presented the optimal seismic design method for ensuring the beam hinge mechanism in steel frames. The energy dissipation capacity was maximized while minimizing the structural weight with the constraint on prevention of formation of plastic hinges at columns connected at joints. In addition to optimal solutions, it was found that the minimum strength ratios of optimal solutions with the beam hinge mechanism are larger than the limit value, 1.0, suggested in ANSI/AISC 341-05. The purpose of this criterion is to achieve a higher level of energy dissipation in a structural system through inducing the yielding of the beams rather than the columns. If a plastic hinge occurs at columns in advance, plastic deformation can be concentrated. This will eventually cause a column hinge

mechanism of the structure. In addition, the collapse of columns bearing a vertical load in a steel MRF increases the possibility of a sudden collapse due to the loss of the axial load carrying capacity.

2.4.3 Joint Panel Zone Behaviour

When subjected to lateral deformations, it is desirable that the joint remains elastic and all the inelastic actions occur at beam ends. Till early 1980's, it was recommended to design frames with stronger joints [AISC, 1980]. With improved understanding of behavior of joints under lateral loading, the JPZ region were designed to undergo controlled inelastic yielding. The simultaneous yielding of beams and JPZ leads to inelastic actions in JPZ region at a fairly low drift level. As, damage in JPZ essentially means a damage in the column, it is deemed irreparable in nature and shall be avoided.

Joint Panel Zones form important components of beam to column joints. Their behaviour and design have received considerable attention in the past. Experiments have shown that JPZ can be the weakest element in frames, and influences the behaviour of steel MRF buildings under strong seismic shaking. Controlling the behaviour of JPZ and hence of the structure through design specifications, still remains a field of active research [Brandonisio et al., 2011; Nasrabadi et al., 2013; Liu et al., 2014; Tuna et al., 2015; Pan et al., 2016].

The predominant shear behaviour of JPZ in steel MRFs is a direct outcome of its loading pattern. Figure 2.3 shows the forces acting on a typical interior beam column joint during earthquake shaking. The different deformation modes possible in a JPZ are rigid body deformations, i.e., (a) translations and (b) rotations, (c) extension, (d) shear distortion, and (e) bending [Fielding and Chen, 1973]. Under seismic actions, the JPZ undergoes predominant shear distortion behaviour. This shear distortion and the rigid body rotation together contribute to the most of the frame inter storey drift. The total storey drift δ comprises of contribution from column deformation, JPZ rotation, and JPZ shearing distortion (Figure 2.4), and can be written as

$$\delta = \delta_c + \delta_r + \delta_{pz} \quad (2.1)$$

where δ_c is the contribution due to the flexural bending of the column, δ_r is the contribution due to JPZ rigid body rotation, and δ_{pz} is the contribution due to JPZ shear

distortion. JPZs that are able to sustain high shear forces without significant shear distortion, undergo rigid body rotation and thereby impose high plastic demands at the beam ends (Figure 2.4(b)). On the other hand, JPZs that undergo large shear distortion impose smaller plastic demands at the beam ends (Figure 2.4(c)). But, the large deformations of JPZs cause high shear strains and stresses at the welds connecting the beam flange to the column, thereby making the welds more conducive to crack initiation [El-Tawil, et al., 1999]. Various models, to estimate the force deformation behaviour of JPZ, has also been proposed [Krawinkler, 1978; Castro et al., 2005; Castro et al., 2008]

During strong seismic shaking, the antisymmetric loading on the JPZ results in large inelasticity in the beam column joint, which reduces its overall stiffness and seismic moment carrying capacity [Dubina, et al., 2001; Popov, 1988]. JPZs can sustain large post-elastic shear deformations. Experiments on interior beam-column joint subassemblages showed that the panel zone shear deformation ductility of about 30-40 is easily achievable [Kato, 1982]. The post-elastic stiffness is in the range of 3-8% of the elastic stiffness. This stiffness is attributed to the resistance of the panel boundary elements, the strain-hardening of the column web in the JPZ, and the resistance offered by the adjoining frame members to the large deformation of the JPZ. Even when the strength of the JPZ is less than that of the adjoining frame members, it demonstrates adequate ductility and dissipates large energy with stable hysteretic loops and is thought to be beneficial to the frame behaviour. But, the excessive yielding of JPZ enhances its shear distortion further. This increases the storey drift, which in-turn results in more damage, greater susceptibility to $P-\Delta$ effects and large permanent offsets of building frames [Schneider, et al., 1993].

Excessive JPZ distortion can lead to local kinking of column, which can contribute to undesirable premature fractures at the beam-to-column interface [Popov, 1988]. Kinking of column also results in local buckling of the beam and column flanges near the joint region (Figure 2.5). These effects can be significantly reduced by using thick columns with thick flanges, which also reduces the joint distortion [Krawinkler, 1978; Schneider and Amidi, 1998; FEMA 355c, 2000; Calado and Luca, 2001]. Reinforcement of columns, along with adequate detailing has also

been recommended, as an effective measure, to attain adequate performance of JPZ [Lee et al., 2005; Jin and El-Tawil, 2005]

Buckling of JPZs is accentuated in beam column joints with large size members. Experimental studies on the behaviour of large size beam-column subassemblages showed that joints carry loads higher than the nominal beam yield strengths, and had stable hysteresis loops with some strain-hardening [e.g., Popov, et al., 1986]. Doubler plates, continuity plates and stiffeners contribute to increase in joint strength, and in specimen with stronger JPZs the inelasticity in beams is higher [Krawinkler, 1978; Popov, et al., 1986]. The participation of doubler plates is significant when the shearing strain in the JPZs reaches a value of three to four times its yield [Becker, 1975; Krawinkler, 1978]. The shear stress distribution in the JPZ is not uniform; the stress is highest at its centre [Tsai and Popov, 1990]. Also, the presence of axial load in the column reduces the shear capacity of JPZs [Fielding and Huang, 1971; Tsai and Popov, 1990].

2.4.3.1 Capacity of Joint Panel Zones

A reasonably accurate estimate of the elastic shear strength V_y of the JPZ, based on simple mechanics is

$$V_y = \frac{f_{yc}}{\sqrt{3}}(0.95t_{cw})d_c, \quad (2.2)$$

where, f_{yc} is the yield strength of column material, d_c is the depth of the column and t_{cw} is the thickness of column web. The area of the JPZ effective in resisting the shear is about 95% of the area of the column web. Early experiments on beam column joints showed that a weak JPZ is detrimental, and that for good inelastic performance of MRFs, the JPZs need to be designed for realistic beam plastic capacities; the use of doubler plates was recommended to strengthen the JPZs [Popov and Bertero, 1973].

The nonlinearity in the load-deformation behavior of JPZ starts at about $0.75V_y$ [Krawinkler, 1978]. Further, the ultimate strength V_u of the JPZ depends on the stiffness of the surrounding elements, and is given by

$$V_u = \frac{f_{yc}}{\sqrt{3}} \left((0.95 t_{cw}) d_c \right) \left[1 + \frac{3.45 b_{cf} t_{cf}^2}{d_b d_c t_{pz}} \right] \quad (2.3)$$

where b_{cf} is the width of column flange, t_{cf} is the thickness of column flange and d_b is the beam depth and t_{pz} is the overall thickness of JPZ. The JPZ strength that appears in the current AISC-LRFD [AISC, 1999] rounds off the numerals and expresses the shear capacity R_v as

$$R_v = \begin{cases} 0.6 f_{yc} d_c t_{cw} & \text{for } P_u \leq 0.4 P_y \\ 0.6 f_{yc} d_c t_{cw} \left(1.4 - \frac{P_u}{P_y} \right) & \text{for } P_u > 0.4 P_y \end{cases} \quad (2.4)$$

when the effect of JPZ deformation is not considered in the analysis, and

$$R_v = \begin{cases} 0.6 f_{yc} d_c t_{cw} \left(1 + \frac{3 b_{cf} t_{cf}^2}{d_b d_c t_{pz}} \right) & \text{for } P_u \leq 0.75 P_y \\ 0.6 f_y d_c t_{cw} \left(1 + \frac{3 b_{cf} t_{cf}^2}{d_b d_c t_{cw}} \right) \left(1.9 - \frac{1.2 P_u}{P_y} \right) & \text{for } P_u > 0.75 P_y \end{cases} \quad (2.5)$$

when the effect of JPZ deformation is considered in the analysis. Here, P_u is the factored axial load in the column, P_y is the yield capacity of the column. In Equations (2.4) and (2.5), the reduction in the shear capacity of the JPZ due to the presence of (factored) axial load P is approximated by a linear axial load - shear interaction, von Mises yield criterion suggests an axial load - shear interaction as

$$\left(\frac{P_u}{P_y} \right)^2 + \frac{3 \tau_w^2}{f_y^2} = 1 \quad (2.6)$$

where τ_w is the shearing stress in the JPZ [Fielding and Huang, 1971]. Thus, in frames with very high axial loads, the post-elastic reserve strength of the JPZ is not achievable [Fielding, 1994].

2.4.3.2 Demands for Joint Panel Zone Design

Over the years, the design of JPZs has undergone radical changes as their behavior was being understood better. Early codes required strong JPZs for all MRFs, with the JPZ being designed to remain elastic when the beams framing into the joints developed their plastic moment capacity [Tsai and Popov, 1990]. The design unbalanced moment ΔM for which the JPZ was being designed, is given by

$$\Delta M = M_l + M_r = \sum M_{pb} \quad (2.7)$$

where M_l and M_r are the end moments on the beams to the left and right of the JPZ, respectively, and M_{pb} is the plastic moment of the framing beams (Figure 2.8 (a)). A revised estimate for the design unbalanced moment considering the gravity load moments M_g on the beams is given by

$$\Delta M = M_l + M_r = \sum M_{pb} - \sum M_g \quad (2.8)$$

when the moments in the two beams due to the seismic action are equal. Assuming that the gravity moments M_g are a fraction of the beam plastic moment capacity M_{pb} , Equation (2.8) can be re-written as

$$\Delta M \cong \sum a_{gb} M_{pb} \quad (2.9)$$

where a_{gb} is the reduction factor to account for the gravity moments. Based on the findings reported in 1989 [Tsai and Popov, 1989], the early drafts of FEMA 350 recommended a value of 0.8 for a_{gb} [FEMA 267b, 1999]. This approach for the design of JPZ led to a reduction in the JPZ strength requirements over that specified in Equation (2.7), and as a consequence it was called the *intermediate-strength* JPZ design. In the 1997 UBC and FEMA 350 document [UCB, 1997; FEMA 350, 2000], a_{gb} is recommended as 0.9. In deriving the above expression, it is assumed that the beam moments due to the action of seismic lateral loads are equal on either side of the JPZ. This may not be true in general, particularly in frames with unequal beam spans and depths. Further investigations are required to improve the intermediate-strength JPZ provisions, particularly when the seismic beam moments on the either side of the JPZ are not equal.

The reduction in the design demands on JPZ, to a certain extent, was driven by the evidence reported in literature that panel zones could sustain large displacements with adequate ductility, resulting in large energy dissipation characteristics (e.g., Krawinkler, 1978; Tsai and Popov, 1990). Thus, *minimum-strength* JPZ design provisions were included in the 1990 AISC code, which resulted in a significant reduction in the strength requirement on JPZs [Tsai and Popov, 1990]. Here, the design unbalanced moment demand ΔM on the JPZ was obtained by applying a structural overstrength factor Ω_0 to the beam end moments M_e resulting from the code-specified seismic forces. Thus, the moment demand ΔM on the JPZ is

$$\Delta M = \sum (M_g + \Omega_0 M_e) \quad (2.10)$$

To encourage a balanced panel zone behavior, where both the JPZ and the beam ends participate in the seismic energy dissipation, the pre-Northridge code specifications resulted in weak panel zones. The use of weak JPZ design was one of the reasons for the poor performance on steel MRF connections during the 1994 Northridge earthquake. The situation was further aggravated by the higher actual yield strength of A36 grade steel than the minimum specified value of 36 ksi (250 MPa) [El-Tawil, 2000], which underestimated the shear demands on the JPZ.

2.4.3.3 *Balanced Joint Panel Zone Design*

Detailed investigation of the experimental data of the SAC Phase I tests indicated a definite trend of joints with weak JPZs resulting in lower flexural ductility compared to joints with strong JPZs [El-Tawil, 2000]. The principal stresses in the welds at the beam to column interface were shown to be significantly smaller in joints with strong JPZs. On the other hand, providing a strong JPZ requires additional welding, which results in residual stresses and large heat affected zones (HAZs). For this reason, there has been a growing consensus to develop a balanced JPZ design for steel MRFs, where the input seismic energy is dissipated by both the JPZ yielding and the plastification at beam ends. [Bertero, et al., 1972; Krawinkler, 1978; Popov, et al., 1986; El-Tawil, 2000]. Currently, codes do not have provisions on relative strengths of beams and JPZs, and since to satisfy the serviceability deflections criteria, the beam sizes can be larger than that required by seismic provisions, it may not be possible to restrict the plastification to the beams alone [FEMA 355c, 2000]. Thus, shear yielding of JPZs may not be completely avoidable, and a balanced panel zone behavior may be justifiable. This balanced panel zone design cannot be implemented at elastic force level, even with the factored loads. Its implementation requires a comprehensive understanding of the capacity design concept and an accurate assessment of member strengths [FEMA 355c, 2000]. The use of balanced panel zone design is likely to result in a significant reduction in the design forces for beam to column connections. It was shown that JPZs begin to yield at about 60% of their nominal strength, and that a resistance factor ϕ_v of 0.6 may be used for achieving a balanced panel zone design [Englekirk, 1999]. This essentially means that the strength of the panel zone should be associated with its yield and not the strain-hardened capacity, and that the JPZs

should be able to develop shear forces corresponding to ΣM_p [Englekirk, 1999; Popov, 1988]. The latest revision of AISC Seismic Provisions [AISC, 2010] uses a resistance factor of 1.0, which may not result in a balanced panel zone behavior.

The objective of balanced panel zone design is to exploit the positive features of JPZ yielding, i.e., the potential to dissipate energy effectively, while limiting its deformations. The extent of inelasticity in structural components (frame members or JPZs) can be quantified through (a) strength, (b) deformation, or (c) energy dissipation. Current codes use *strength* to control the level of inelasticity in JPZs. Further studies are necessary to develop deformation and energy based control of inelasticity.

A graphical representation (Figure 2.6) of the relative levels of inelasticity developed in the JPZ and at the beam ends, can be used to indicate probable trends. In Figure 2.6, Ω is the ratio of the distortional moment ΔM on the JPZ and seismic moment M_e at the beam end, i.e.,

$$\Omega = \frac{\Delta M}{M_e} \quad (2.11)$$

For fully rigid panel zone, Ω is equal to Ω_0 , the overstrength factor mentioned in Equation (2.10). Thus, the objective is to arrive at a value of Ω that will result in balanced panel zone behavior, i.e., M_p/V_n of 1.0. Improvements to Equation (2.11) can be made by including the effect of gravity loads. Also, inelasticity ratios based on deformation and energy can be evaluated corresponding to Ω_{bal} obtained from strength inelasticity.

2.4.4 Performance of Welds

Under increased compressive loading due to bending moment flexure and/or axial force, local buckling or lateral torsional buckling is inevitable. The stress-strain behavior of steel has a distinct linear elastic portion till yield strain ε_y , followed by a flat yield plateau till strain-hardening strain ε_{sh} , and a subsequent strain-hardening region beyond ε_{sh} (Figure 2.7). The section tangent stiffness E_t decreases as the structural member is compressed into the plastic or strain-hardened strain range. En-route, a state is reached where the member stiffness is no longer sufficient to carry the compressive load, and it buckles. Thus, according to this behavior, since $E_t = 0$ for $\varepsilon_y <$

$\varepsilon < \varepsilon_{sh}$, a steel member under pure compression should buckle as soon as $\varepsilon > \varepsilon_y$. However, in reality, such buckling is not observed on reaching yield strain.

The polycrystalline molecular structure of steel is such that it develops slip planes at 45° to the direction of loading, when strained beyond ε_y [Bruneau, et al., 1998]. These lines are also known as the *Lüder lines*, and are visible at axial strains beyond ε_y . At the slip plane, the polycrystalline molecules slip and the strain attains a value of ε_{sh} locally, even though the overall strain is maintained at ε_y . Depending on the distribution of imperfections within the polycrystalline structure, other planes also start forming Lüder lines randomly. The formation of Lüder lines continues till the entire length of the member is subjected to yield strain, attains the strain-hardening strain. Thus, even though along the yield plateau $E_t = 0$, it does not necessarily result in the buckling of the section.

A basic requirement of structural members to resist seismic loads is that they should have sufficient plastic deformation capacity while maintaining the plastic moment capacity M_p . The deformation capacity of a member is usually limited by its instability; in steel I-sections subjected to flexure, the different forms of instability are: (a) flange local buckling (FLB), (b) web local buckling (WLB), and (c) lateral-torsional buckling (LTB) [Bruneau, et al, 1998]. AISC codes [AISC, 1989b; AISC, 1994; AISC, 1997] use slenderness ratios to identify the stability limits of flange and web elements. These limits are (Figure 2.8(a)): (a) λ_p - slenderness limit for compact elements, and (b) λ_r - slenderness limit for non-compact elements, and (c) λ_{pd} - slenderness limit for compact elements with a minimum guaranteed develop plastic rotation ductility. The expected ductility level for λ_{pd} is 3 [Yura, 1988]. Structural members with non-compact flanges and web elements ($\lambda > \lambda_r$) cannot develop member plastic capacity before elastic buckling, while structural members with compact elements ($\lambda_{pd} < \lambda < \lambda_p$) are able to develop the member plastic capacity M_p with limited ductility. To develop full member plastic capacity M_p and sufficient rotation, the member elements need to have slenderness ratio λ less than λ_{pd} . The moment capacities developed in members with different slenderness limits are shown in Figure 2.8.

The 1997 AISC Seismic Provisions [AISC, 1997] allow a reduction in the beam to column connection design moments in SMFs and IMFs when the beam sections are

non-compact. Some studies proposed the use of non-compact beam sections to reduce the connection design moments [e.g., Yang and Popov, 1996]. However, non-compact sections have inadequate plastic rotation capacity, which limits the amount of energy dissipated during strong earthquake shaking. Thus, the use of non-compact sections is not recommended for seismic applications.

The good performance of steel welded beam to column connections during some experiments (e.g., Popov and Pinkney, 1969; Fielding and Huang, 1971; Popov, 1988; Popov and Tsai, 1989; Xue, et al., 1996; Zekioglu, et al., 1997; Englehardt and Sabol, 1998] led to a belief that the welds at the beam to column interface were adequate to transfer the loads corresponding to the beam capacity, to the column. Isolated reports of bad performance due to weld failure were attributed to lamellar tearing due to defects in steel material, and sub-standard welding [Hamburger, et al., 1998]. Higher beam moments were mobilized with increase in the thickness and length of connection welds [Engelhard and Hussain, 1993; Dubina, et al., 2001]. Further enhancement in performance was observed with (a) use of notch-tough weld, (b) improvement in welding procedures, and (c) removal of backup bars and grinding the copes to have smooth surfaces. But, the extremely poor performance of welded steel MRF buildings during the 1994 Northridge earthquake provided a completely different understanding.

At a tri-axially loaded material point, the maximum shear stress τ_{max} is given by

$$\tau_{max} = \frac{(\sigma_1 - \sigma_3)}{2} \quad (2.12)$$

where σ_1 and σ_3 are the maximum and minimum principal stresses, respectively. For uniaxial loading, i.e., $\sigma_1 = \sigma_3 = 0$ in Figure 2.9(a), yielding occurs when τ_{max} is equal to $\sigma_y/2$ (Figure 2.9(b)). For any other state of stress, yielding occurs when the difference between the maximum and minimum principal stresses reaches σ_y i.e., when the maximum shear stress τ_{max} reaches $\sigma_y/2$. For the tri-axially restrained configuration, like the one encountered in beam to column connection welds at the column face, due to the high restraints in the lateral directions (say directions 2 and 3), stress increase in the principal direction 1 is accompanied by stress increase in other two principal directions, due to the Poisson's effect (Figure 2.9 (c)). Further, these

stresses in the principal directions 1 and 2 have the same nature as that along the principal direction 1, i.e., tensile primary stress σ_1 induces tensile stresses σ_2 and σ_3 in the other two orthogonal principal directions. Thus, although the individual principal stresses reach a value of σ_y and more, τ_{max} never reaches $\sigma_y/2$, which precludes yielding and results in brittle rupture when the maximum principal stress reaches σ_u [Blodgett, 2000].

The toughness of weld material also influences its performance under severe earthquake loading. Fracture tough welds perform better with good ductility and energy dissipation capacity than other welds with low toughness [Xue, et al., 1996]. Materials like ferric steel and their weldment have a peculiar atomic structure that is vulnerable to brittle fracture at low stresses [Matos and Dodds, 2001]. Presence of micro-defects and in-homogeneities in the material microstructure strongly influence the fracture toughness of the weld material. High carbon content of steel and high heat input during welding, form a case for crack initiation [Bruneau and Mahin, 1991]. Welds are also known to result in shrinkage and associated restraints; higher heat input from the welds can result in reduced toughness of the heat affected zone [Miller, 1998]. Hence, along with good welding practices, it is also recommended to choose welding sequences to minimize the shrinkage and restraint [Engelhardt and Sabol, 1998; Miller, 1998]. With increase in plate thickness and the volume of weld material, other problems occur, like lamellar tearing, weld embrittlement, under-bead cracking, distortion, shrinkage and residual stresses [Bruneau and Mahin, 1991]. Experiments to study the performance of welds under direct tension and compression showed a reduction in tensile strength with increase in the weld size [Popov and Stephen, 1977]. Also, high cooling rates can result in a brittle microstructure. To avoid this situation, codes specify minimum weld size. Further, it is preferable to deposit the welds in a single pass, but pre-heating of the base metal can be utilized to ensure a slower rate of cooling where single pass welding is not possible [Miller, 1998].

As the welds are under a highly restrained state of stress, the frame members (beams and columns) are more reliable to sustain large inelastic strains without fracture. Thus, in welded MRFs for seismic forces, it is desirable to confine all plastic yielding to beams and columns, and not the welds. In addition, improved quality of

weld filler material, welds of high notch-toughness, and overmatched strength welds (i.e., weld with strength greater than that of the base metal) also help in pushing the inelasticity in to the connected members [Miller, 1997]. But, overmatched welds tend to aggravate the possibility of lamellar tearing in the base metal [AISC, 1973], and should be used only after evaluating its implications.

In beam-to-column connections, backup bars are used to hold the weld material in place while welding beam flanges or cover plates to the column face (Figure 2.2). In CJP welds with backup bars left in place, the un-fused interface between the backup bar and the column face acts as source for crack initiation (Figure 2.2(b)) [Yang and Popov, 1996]. Methods to reduce the detrimental effects of backup bars include (a) removal of backup bars, (b) use of grooved backup bars, (c) application of fillet welds under the bars to close the crack, and (d) application of weld overlays [Yang and Popov, 1996; Matos and Dodds, 2001; Anderson, et al., 2002]. Removal of backup bars is simple, but, incorrect removal can lead to cracks at the weld root. Grooved backup bars and application of fillet welds under the backup bar have shown superior performance [Matos and Dodds, 2001], Application of weld overlays showed very good inelasticity for shallow beams, but for intermediate size and deeper beams, weld overlays may need special design considerations since the strain demands on them are significantly higher than normal size beams [Anderson, et al., 2002].

Fabrication limitations require the CJP welds to be placed in the downhand position. Thus, the wedge-shaped welds at both the top and bottom flanges of the beam are loaded differently. At the bottom flange, the weld root is subjected to higher stress intensity than that at the top flange [Dubina, et al., 2001]. The quality of the weld at the bottom flange is further affected by the presence of the beam web, which interferes with the free movement of the welding electrode across the full width of the beam flange, and thereby interrupts the deposition of the weld in a single pass. The web access holes provided near the beam bottom flange to facilitate continuous welding, further increase the stress levels in the vicinity of the weld leading to a brittle response. Thus, the vulnerability of the lower beam flange region to crack initiation at the weld root is higher than that at the upper beam flange [Miller, 1998]. The stress concentration factor in CJP groove welds between the beam flange and column flange

could be as high as 4 [Richard, et al, 1995]. Poor performance of beam bottom flange-to-column flange welds were observed in experiments and they were attributed to the deposition of slag in the overlap region when downhand-position welding is interrupted due to the presence of the web and re-started from the other side of the web [Engelhardt and Hussain, 1993]. The damage to welded steel MRF connections was mostly concentrated at the beam bottom flange-to-column interface, which, in the aftermath of the 1994 Northridge earthquake was attributed to the presence of composite slab supporting the beam top flange-to-column interface connection [Uang, et al., 1996]. It was speculated that the presence of a composite slab at the top beam flange results in the shifting of the neutral axis towards the top flange, which in-turn increases the normal strains at the beam bottom flange. Subsequent experiments showed that the composite slab has a positive influence on the performance of steel beam to column connections, such as (a) increase in initial stiffness, (b) increased plastic rotation capacity, (c) reduced strains and stresses for the top beam flange-to-column welds, and (d) improved stability against lateral-torsional buckling of the beam [Civjan, et al., 2001].

An experimental study to assess the performance of partial and complete joint penetration welds to connect large sections showed that the former can develop and exceed their nominal design capacities, but due to severe stress concentration in the un-welded part, they are vulnerable to crack initiation [Bruneau and Mahin, 1991]. Also, a need to develop ductile CJP weld schemes was emphasized, wherein plasticity initiates near the welds and rapidly progresses into the connected member, leaving the weld free from excessive straining.

The welds in connections at the beam-to-column interface form important components of steel MRFs, and good performance of these welds is vital to ensure overall ductile behavior of the MRFs during strong earthquake shaking. FEMA 350 [FEMA 350, 2000] in conjunction with FEMA 353 [FEMA 353, 2000] recommends stringent quality control and quality assurance (QC/QA) requirements for welds at beam to column interface. Partial penetration welds exhibit low ductility [Popov and Stephen, 1977], and hence, are not recommended at beam-column interfaces [FEMA 350, 2000].

2.4.5 Connection Configuration

The flow of forces from the beam to column through the connections is influenced by the efficiency of the connections to carry out the transfer. Recent understanding has amply emphasized that the formation of plastic hinges at the column face is not possible [Goel et al., 1998, Arlekar and Murty, 2004]. Adequately proportioned connections help in the smooth flow of forces in the joint region, reducing the stress concentration and avoiding the undesirable brittle behavior of connections.

The 1989 AISC Manual of Steel Construction [AISC, 1989a] recommended a connection configuration where the beam flanges were fully welded to the column. This connection configuration is similar to the pre-Northridge prescriptive moment connection (Figure 2.1), which were designed for the nominal plastic moment M_p of the beam [AISC, 1989b; AISC, 1992]. Such connections with full penetration welds between the beam flange and column were experimentally found capable of developing the nominal plastic moment capacity $M_p (= f_y Z_p)$ [Popov and Stephen, 1977; Popov et al., 1986; Popov, 1988; Engelhardt and Hussian, 1993]. But, due to the unforeseen material uncertainty, the full plastic moment capacity ($= R_y f_y Z_p$) was not realized. In addition, inelastic energy dissipation was not realized through yielding of beam flanges at the face of the column. This incorrect estimation of the connection design forces was identified as one of the principal causes for the enormous damage to the beam to column connections during the 1994 Northridge earthquake [Miller, 1998; FEMA 355c, 2000].

The obvious improvement was to reinforce the joint, thus providing a connection region that is stronger than the rest of the beam. During strong earthquakes, this results in the development of plastic hinges in the portion of the beam adjoining the connection reinforcement region. Recent experimental evidence confirmed that reinforcing the beam near the column face not only protects the connection region, but also significantly improves the overall inelastic performance of MRFs. The appropriately chosen reinforcing plates provide for a smooth flow of forces from the beam to the column, and reduce stress concentration in the connection elements [Dubina, et al., 2001; Engelhardt and Sabol, 1998].

An alternative to reinforcing the joints region is the *Dogbone Connection* or the *Reduced Beam Section (RBS)*. In this connection configuration, portions of the beam flanges near the column face are trimmed (Figure 2.12). This intervention reduces the moment capacity of the beam and facilitates the formation of energy dissipating plastic hinges at the reduced section. The RBS connection results in some loss in the lateral strength of the structure. If this is acceptable, the large ductility and energy dissipating capabilities offer an excellent trade-off [Engelhardt, et al., 1996].

The *Slotted Beam Connection* is an alternative configuration that reduces the stress concentrations at the column face [Richard, et al., 1997]. In this connection, two horizontal beam web slots are introduced, one near the top flange and the other near the bottom flange. These slots separate the beam web from the beam flanges near the column face (Figure 2.13), and allow the web and flanges of the beam to deform independently. This lack of mutual constraints to the web and flanges reduces the stress concentration near the connection leading to enhanced ductility of the connection configuration. In this configuration, the web is expected to resist the entire beam shear. This is in contrast to other connection configurations, where beam shear is also carried by the beam flange and the connection elements present there. Finite element analyses have shown that, for slotted web connections, the stress concentration factor in the entire beam section is in the range 1.2-1.4, while it is as high as 4.0-4.5 for RBS and other pre-Northridge connections [Partridge, et al., 2002].

It has been a common practice to employ non-seismic connection configurations for gravity loads in frames (Figure 2.14). In an effort to reduce the moment demands at the column face of beam to column joints, different beam to column connection configurations, having different connection rigidity, have been suggested (Figure 2.15) [Engelhardt and Sabol, 1998]. Connections in a steel MRF can be categorized broadly under three heads, namely, simple connections, partially restrained connections and fully restrained connections. The characterization is based on the moment transfer capacity of the connections (Figure 2.16).

Immediately after the 1994 Northridge earthquake, thorough inspections of steel buildings lead to the identification of many cracked connections. The need for repair and upgrade of these connections was addressed in a few independent studies

[Xue, et al., 1996; Anderson, 1997; Allen, et al., 1998; Anderson and Xiao, 1998]. Typically, the seismic retrofit of damaged connections include the following options: (a) removal of damaged weld material and re-weld using notch-tough ductile weld material, (b) addition of horizontal reinforcing plates, and/or (c) addition of vertical rib plates [Anderson and Xiao, 1998]. The performance of re-welded connection is similar to the initial undamaged specimen. Reinforcing the beam flanges with cover plates improves the strength and energy dissipation capacity of connections [Anderson and Xiao, 1998; Anderson, 1997; Xue, et al., 1996]. In the retrofit scheme, the fractured beam flange along the weld line at the column face was reinforced with cover plates of slightly higher strength and thickness. The improvement in strength was due to the “reinforcing” effect provided by the cover plates. The slotted beam web connection is also an efficient scheme for retrofitting the undamaged pre-Northridge connections [Allen, et al., 1998].

2.5 Objectives

The broad objectives of present work are as under:

1. To determine the minimum value of CBSR required to ensure elastic behaviour of columns.
2. To propose a method for estimating the force deformation behaviour of strong axis beam to column joints.
3. To obtain tentative nonlinear hinge properties for beam to column joints, which can be used for analysis purposes.

2.6 Organization of the Thesis

The thesis comprises of six chapters, the first of which gives a basic introduction to steel MRFs, along with past performance of such frames during major earthquakes. The second chapter presents a review of relevant literature and point outs the gaps in prevalent design methodology for steel MRFs. Chapter three attempts to investigate the effects of CBSR on the behaviour of SCWB strong axis beam to column joints on the basis of flow of inelastic stresses in strong axis interior beam to column joint subassemblages.

In the fourth chapter, a hand calculation approach based on simple mechanics has been proposed to determine the drift levels at which inelastic actions initiates in

strong axis beam to column joint subassemblages. This method takes into consideration, the effects of column web doubler plates. Using the proposed method, force deformation behaviour of strong axis interior as well as exterior joints can be predicted.

In chapter five, the effectiveness of proposed method is validated by carrying out NLDTHA of two benchmark steel MRFs. The suitability of proposed method over nonlinear hinge properties as prescribed in FEMA 358 is also presented. Chapter six presents the summary of the results obtained and the conclusions arrived at.

2.7 Scope of Present Work

The present work attempts to investigate the suitability of steel MRFs in areas of high seismicity. The scope of this work can be summarized as follows

1. The behaviour of strong axis beam to column joints design according to strong column weak beam (SCWB) design philosophy is studied.
2. Drift capacities of different components of a joint are determined using a proposed method, based on simple mechanics. The force deformation behaviour obtained using proposed method are validated using Nonlinear Finite Element Analysis.
3. Two benchmark steel buildings having peripheral MRFs are analyzed to demonstrate the applicability and scope of the proposed method.

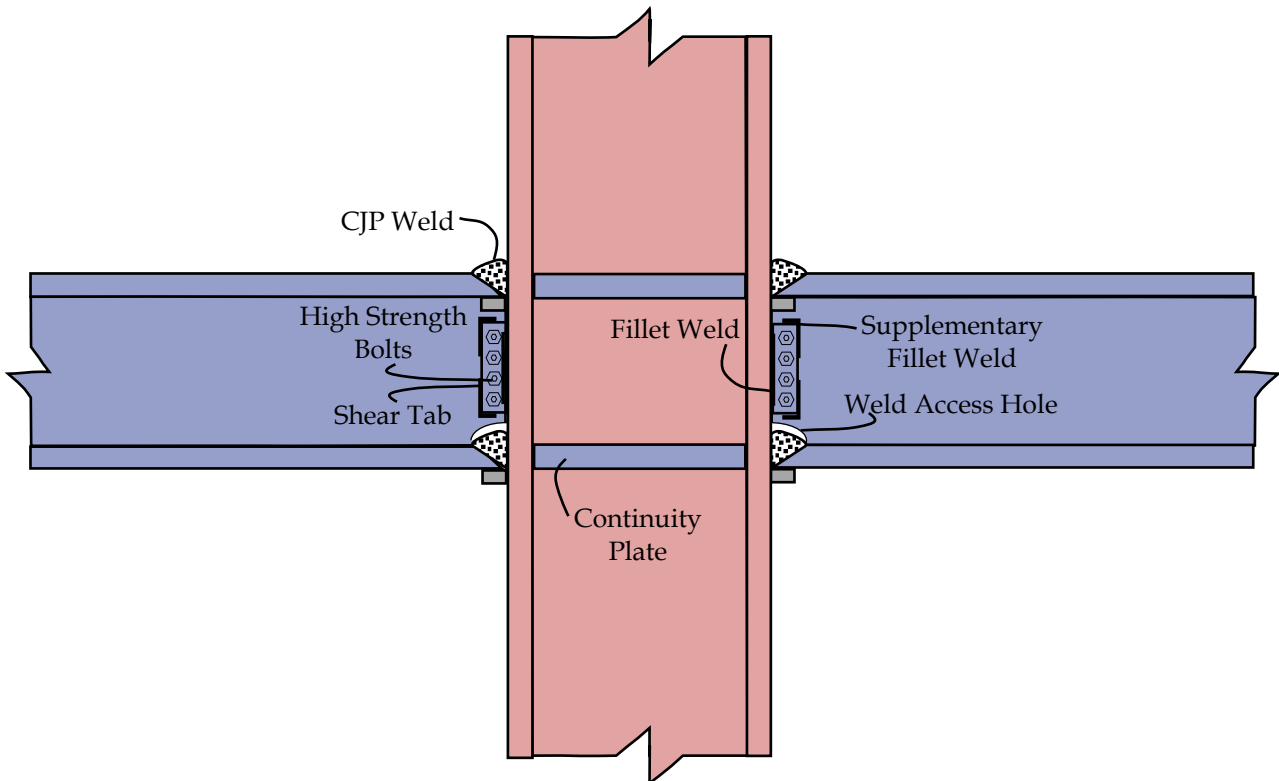


Figure 2.1: Prescriptive Moment Connection: Specified between beam and column in steel MRF buildings.

A combination of welding and high strength bolts is used for transfer of forces from beams to columns.

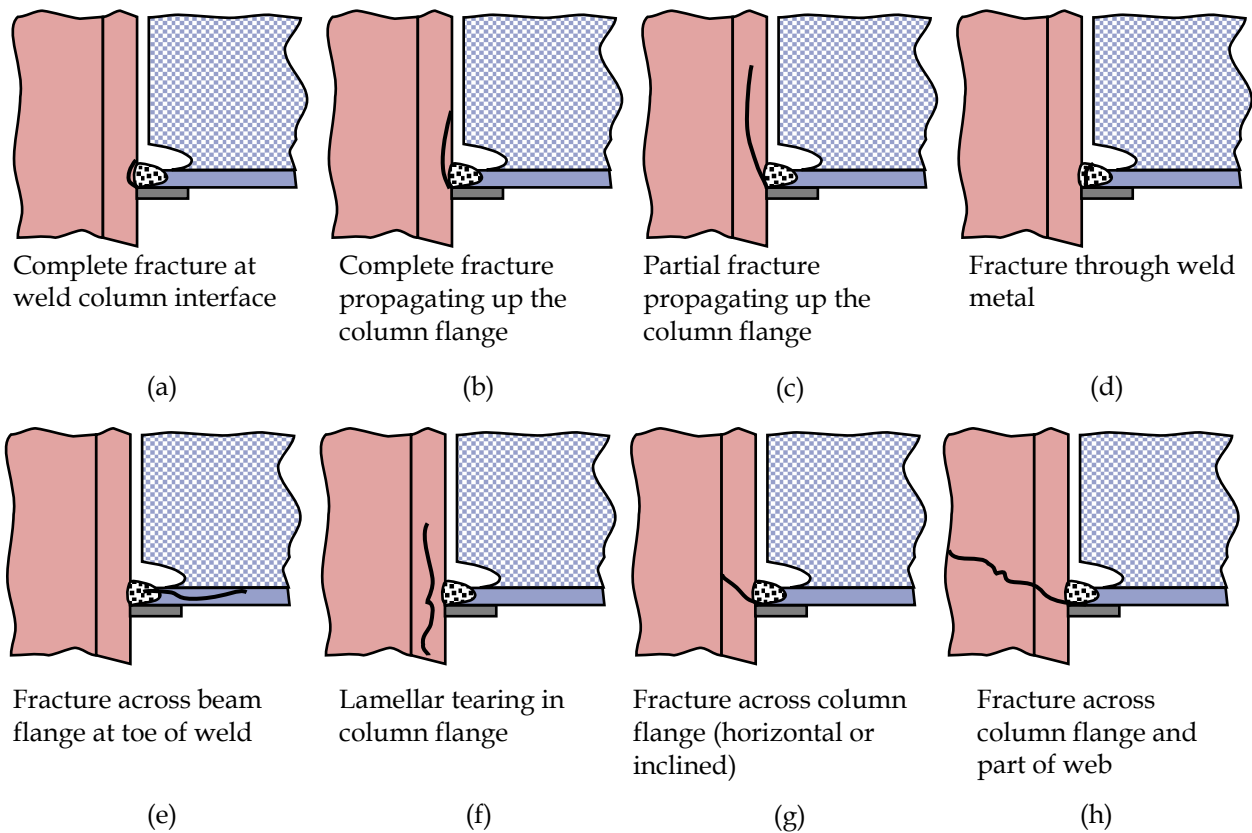


Figure 2.2: Failure modes at welded beam to column strong axis connections observed in the 1994 Northridge Earthquake.

The widespread failure of welded steel MRF connection initiated extensive research in the field. [adapted from Krawinkler et al.,1996]

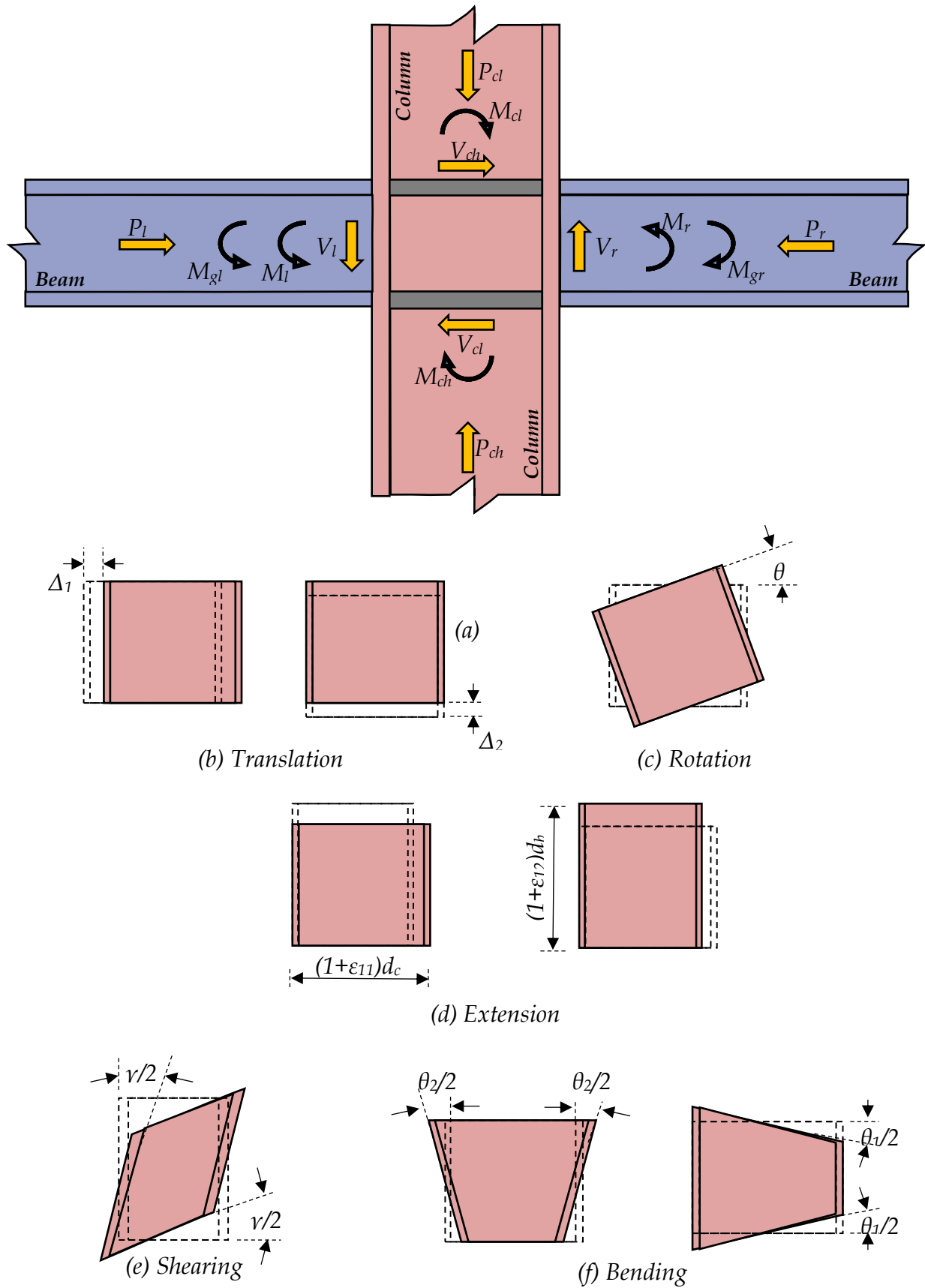


Figure 2.3: Joint Panel Zone, Loads and Deformations. (a) Loads acting on a typical interior JPZ; and (b) Possible modes of deformation of JPZ.

Seismic loads result in predominant shear distortion of the JPZ

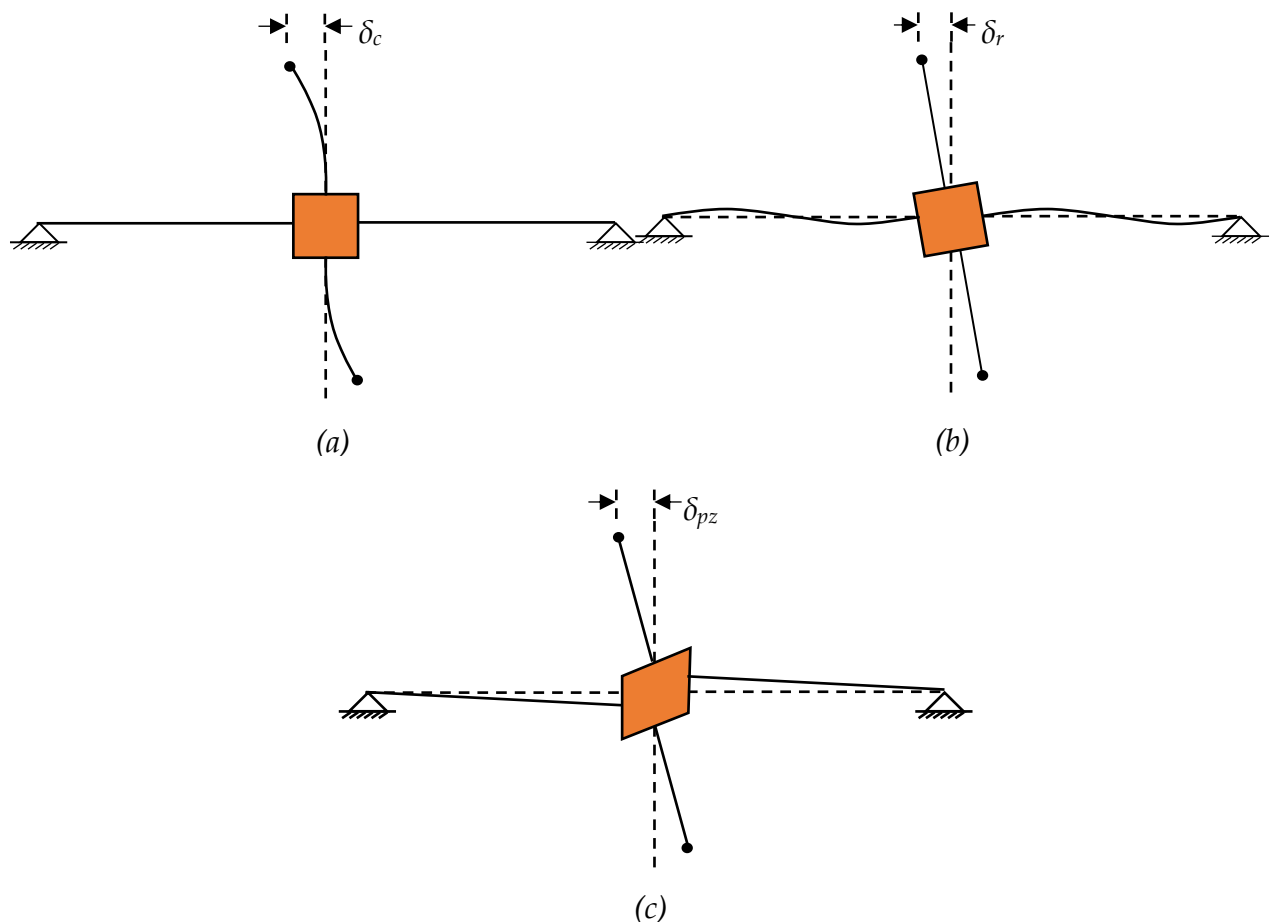


Figure 2.4: Interstorey Drift Components.

(a) δ_c from column deformation; (b) δ_r from JPZ rigid body rotation; and (c) δ_{pz} from JPZ shear distortion. Shear deformation in the JPZ reduces the rotation demands at the beam ends.

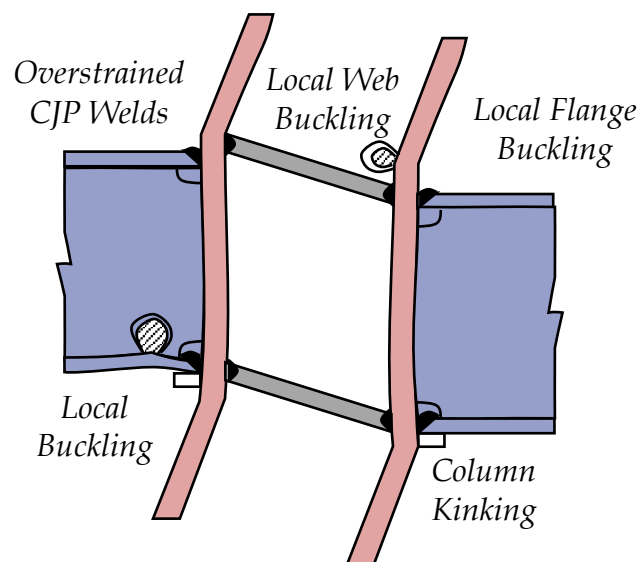


Figure 2.5: Effects of JPZ shear distortion.

Local Buckling in the beam and column flanges due to excessive distortion of the JPZ [Krawinkler, 1978]. The change in relative angle between the beam and the column flanges imposes high strains on the CJP groove welds, resulting in their brittle fracture.

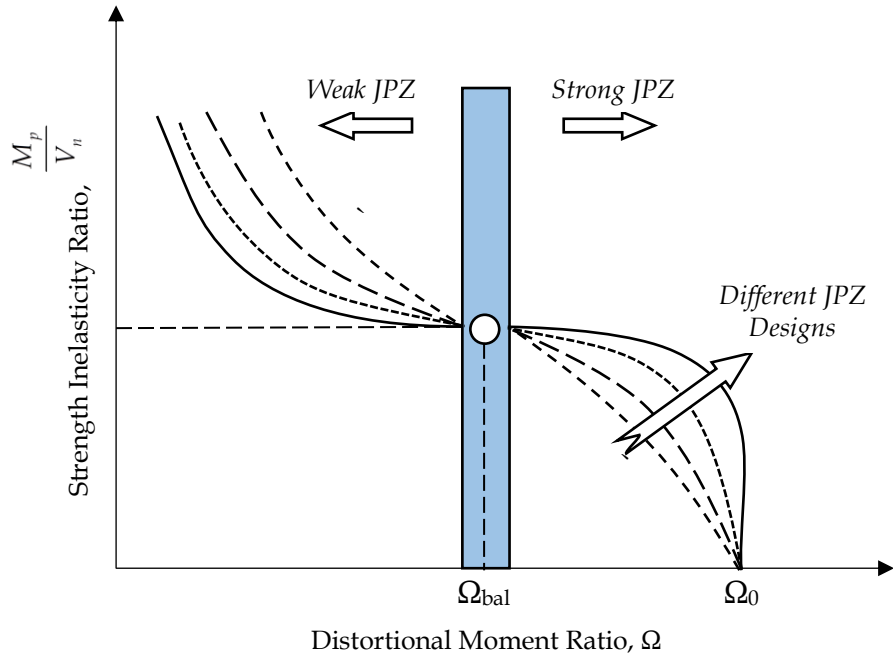


Figure 2.6: *Balanced JPZ Design.*

Probable trends of the relative inelasticity between JPZ and beam end. Further work is needed to estimate values of Ω_{bal} that will result in balanced panel zone behavior.

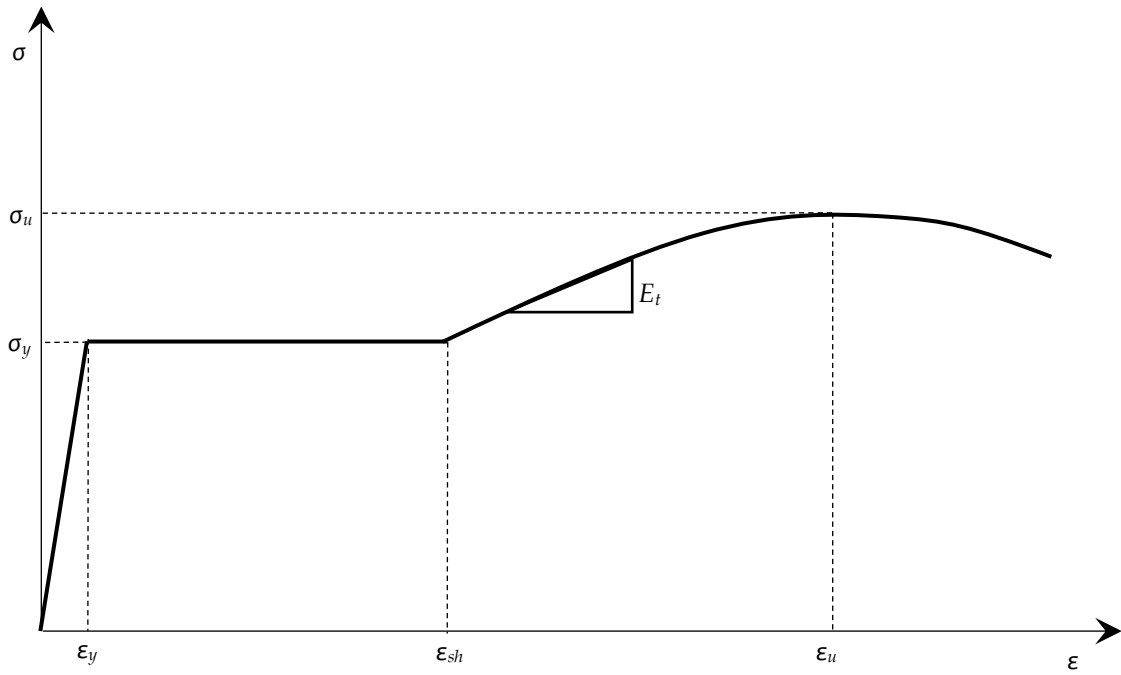


Figure 2.7: *Stress Strain Behaviour for Structural Steel.*

For strains between ϵ_y and ϵ_{sh} , the formation of slip planes (luder lines) results in a sudden increase in fiber strains from ϵ_y and ϵ_{sh} thus precluding buckling at yield strain, even though the tangent modulus $E_t=0$ [Bruneau, et al., 1998]

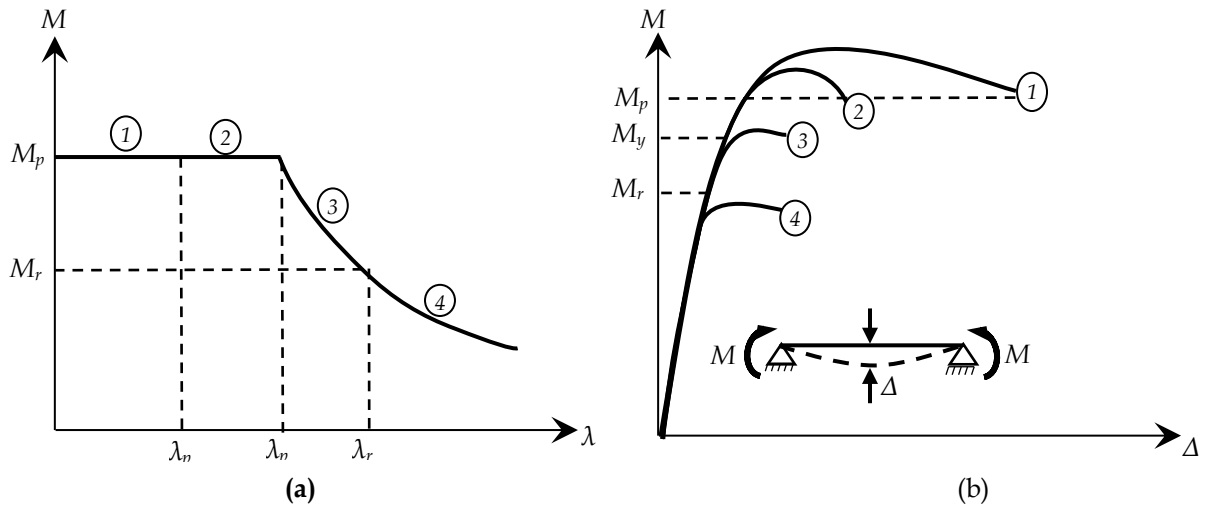


Figure 2.8: Effect of Slenderness Ratio on developable member capacity. (a) Buckling strength-slenderness ratio relationship; (b) Moment-deflection behaviour of I-sections, for different levels of slenderness. Inelastic buckling commences much before yield moment M_y , because of residual stresses.

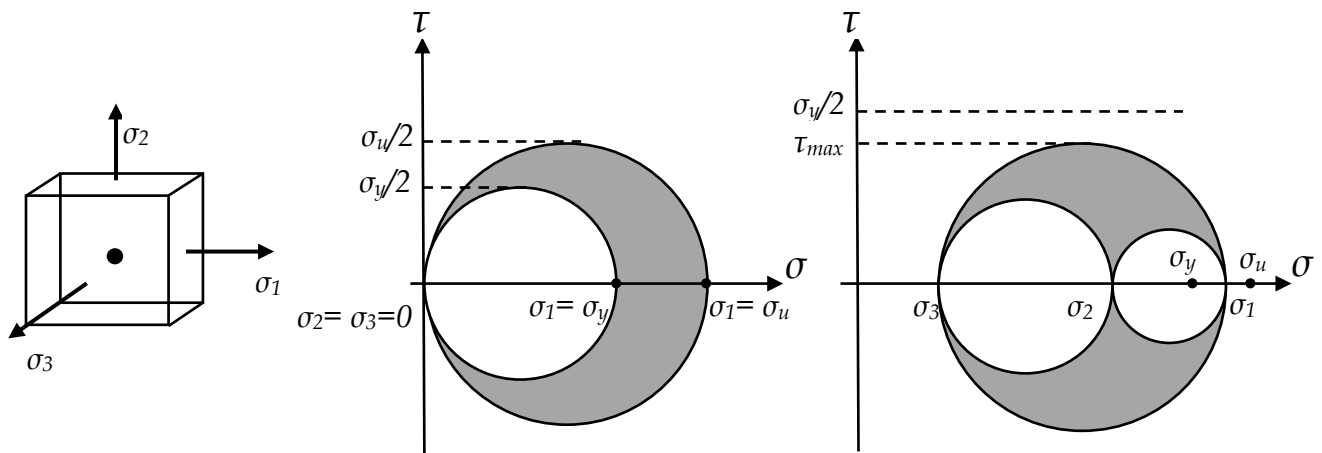


Figure 2.9: Effect of tri-axial restraints to the welds at the column face [Blodgett,1995; FEMA 355c, 2000]. (a) Material point showing the principal stress directions; (b) Mohr's circle representation of unrestrained ($\sigma_2 = \sigma_3 = 0$) state of stress, and (c) Mohr's Circle representation of restrained ($\sigma_2 \neq 0$; $\sigma_3 \neq 0$) state of stress. For yielding at the material point, the maximum shear stress τ_{max} must reach $\sigma_y/2$.

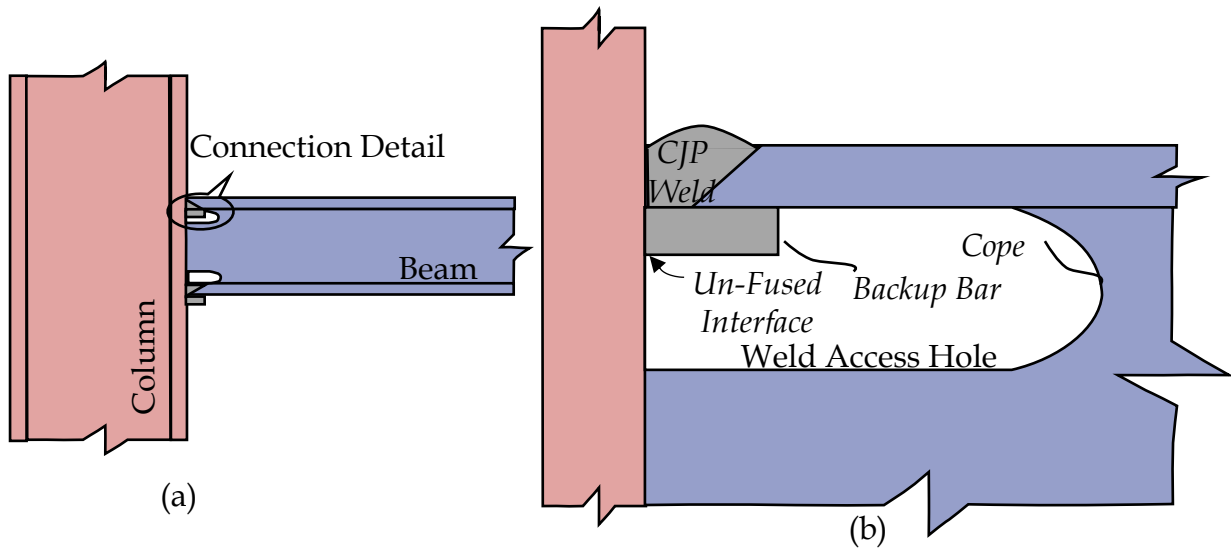


Figure 2.10: Beam flange to Column interface.

(a) Beam to column joint showing backup bars, web access holes and copes, and (b) Detail at the beam bottom flange to column interface; the un-fused interface adjoining backup bar provides a potential opening for crack initiation in the CJP weld.

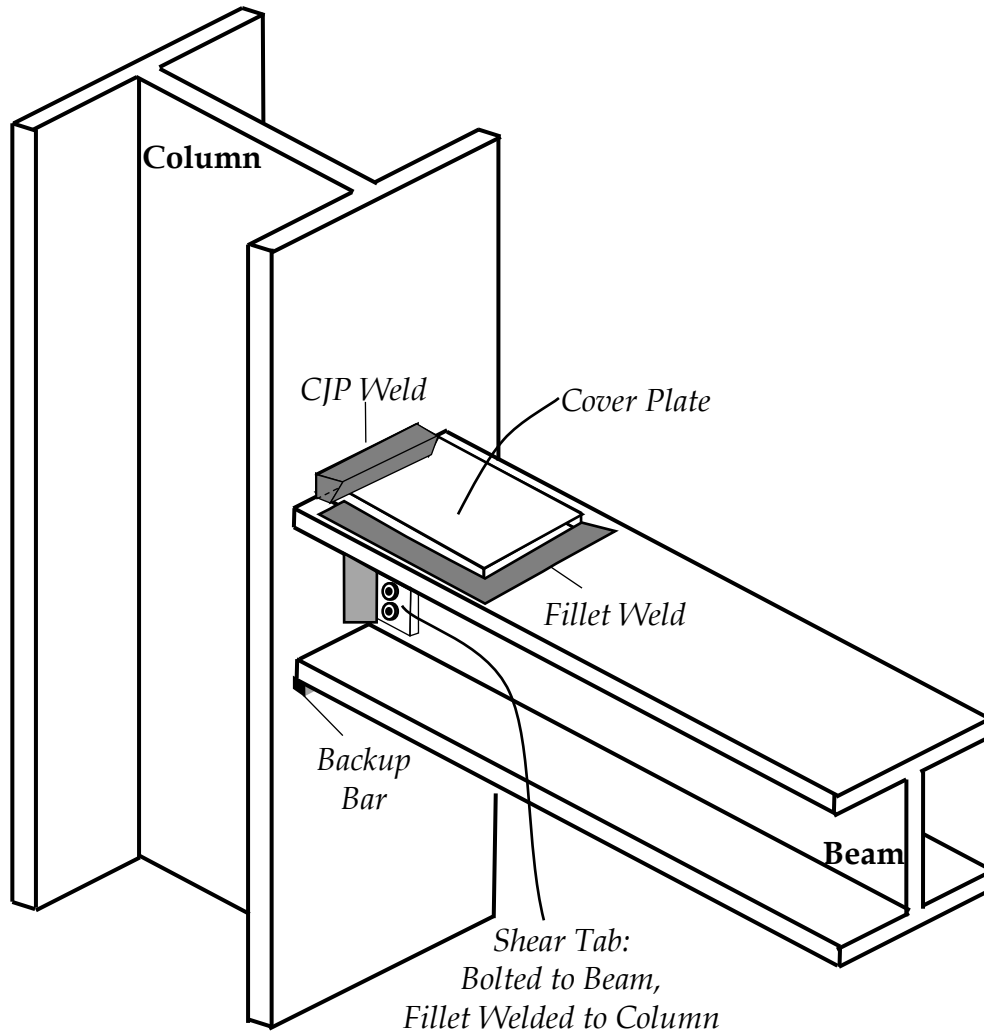


Figure 2.11: Beam to Column Joint with flange cover plates.

Cover plates are CJP welded to column, and beam web is connected to column through a shear tab.

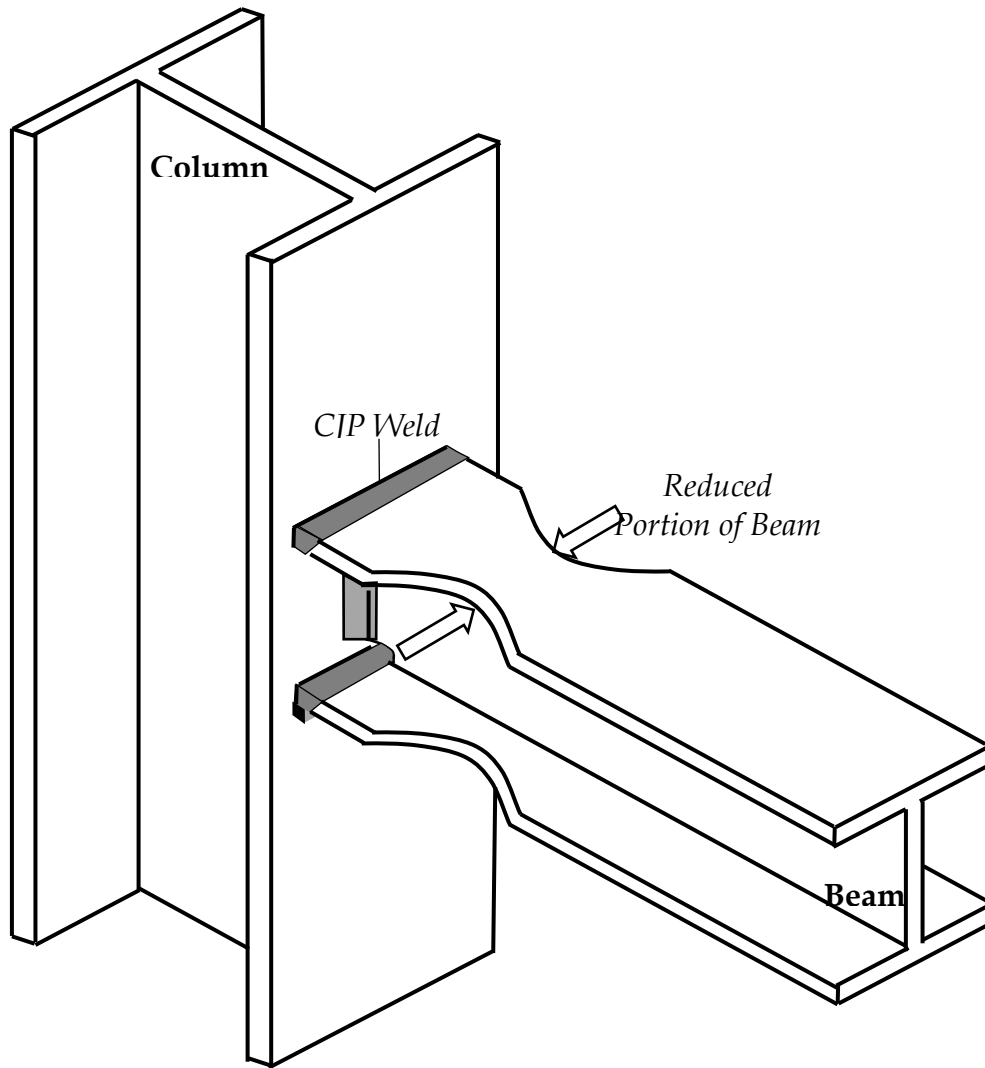


Figure 2.12: Beam to Column joint with RBS connection.

Reduction in beam flanges facilitates the formation of plastic hinges away from the column face [Engelhardt, et al., 1996; FEMA 350, 2000]

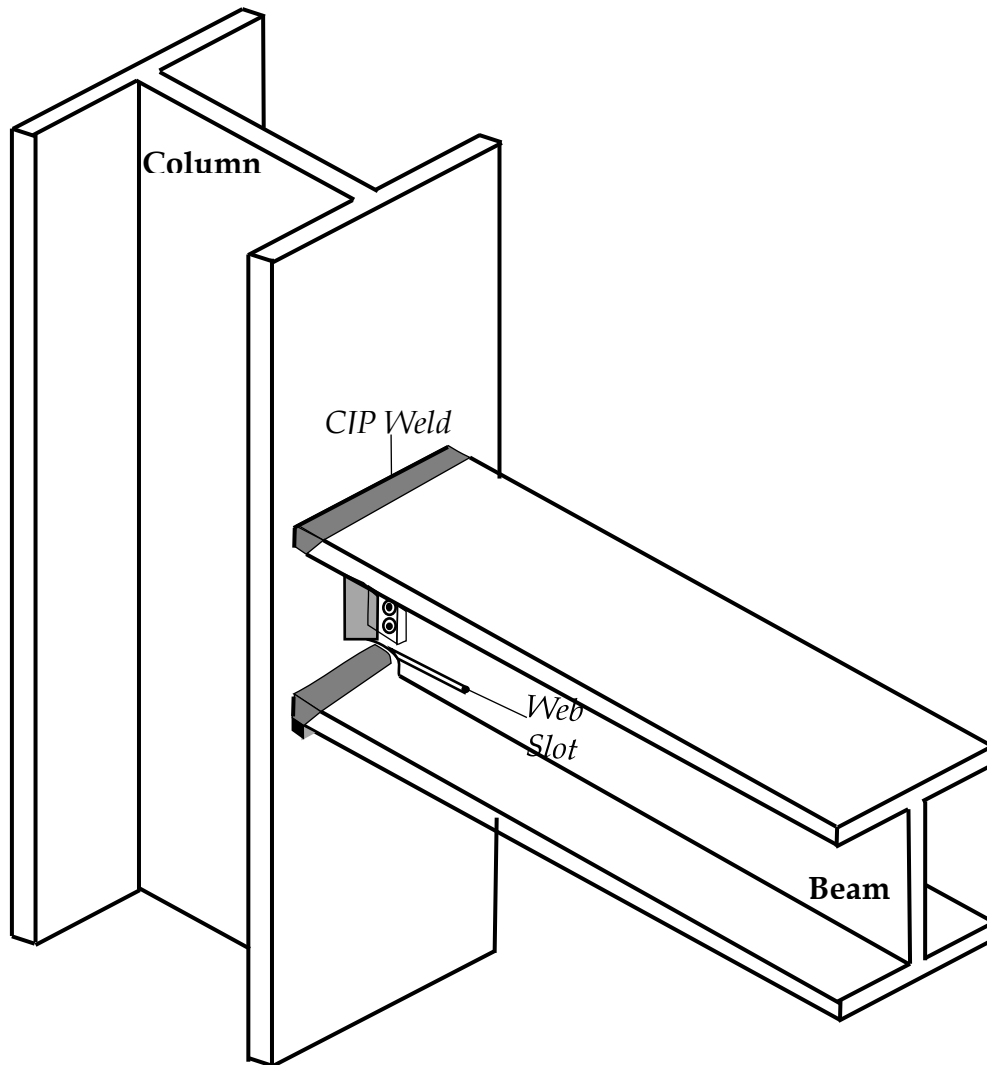


Figure 2.13: Beam to Column Joint with Slotted Beam Connection.

Web slot separates the flanges and the web allowing the web to transfer the forces independently [Richard, et al., 1997; FEMA 350, 2000]

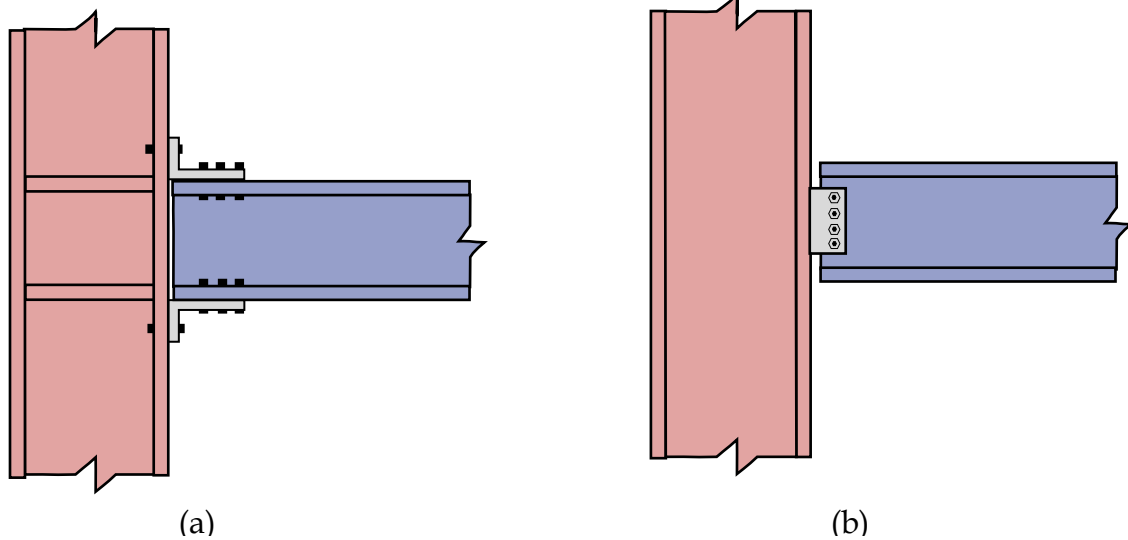


Figure 2.14: Non-seismic beam to column connections.

(a) Seat angle connection, and (b) single plate shear connection. All non-seismic connections are flexible or semi-rigid, and are designed for code specified dead and superimposed loads.

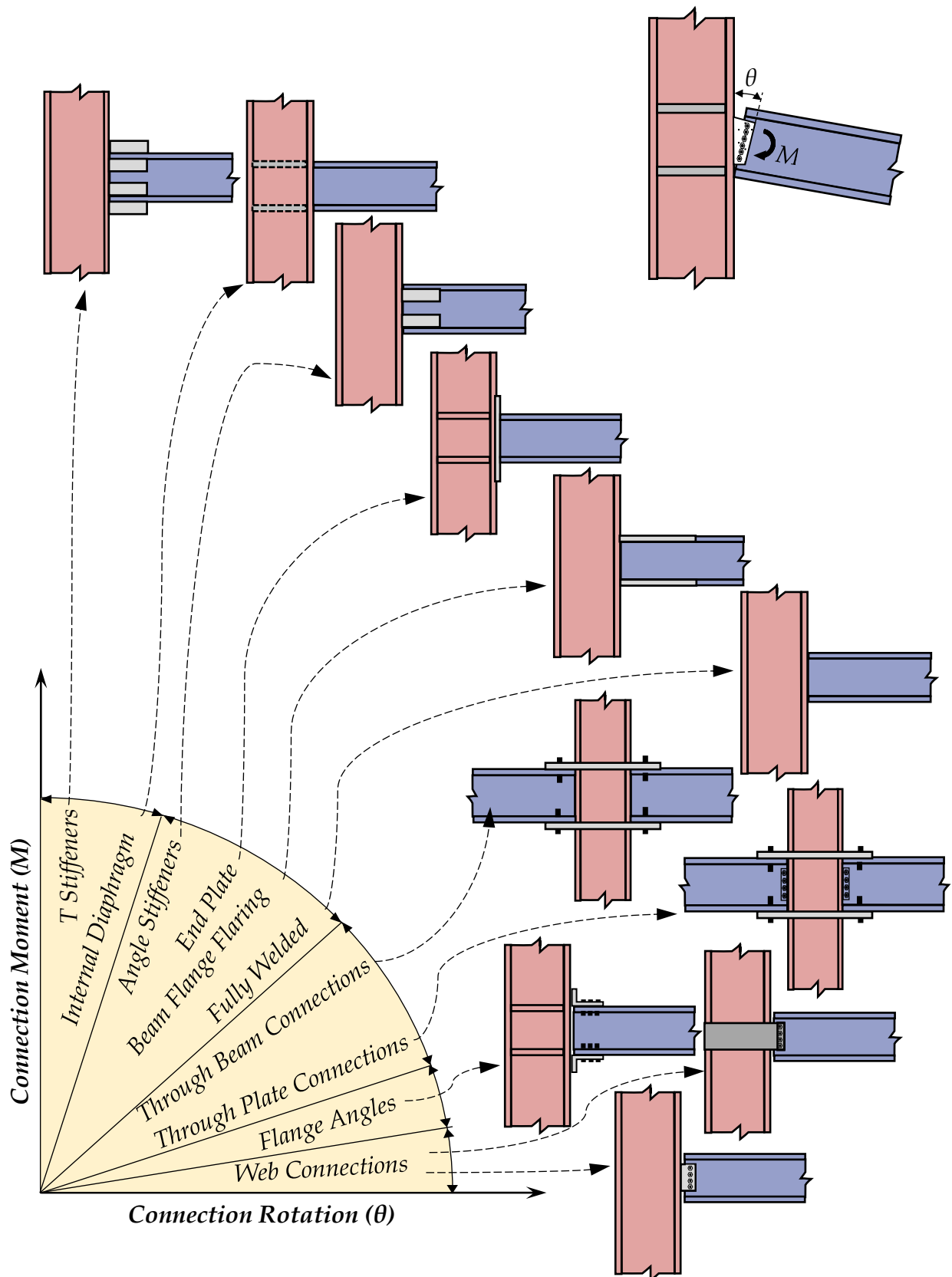


Figure 2.15: Connection Rigidity.

Connection flexibility reflected in the initial elastic portion of moment-rotation relationships of some typical connections [adapted from Mazzolani and Piluso, 1996]

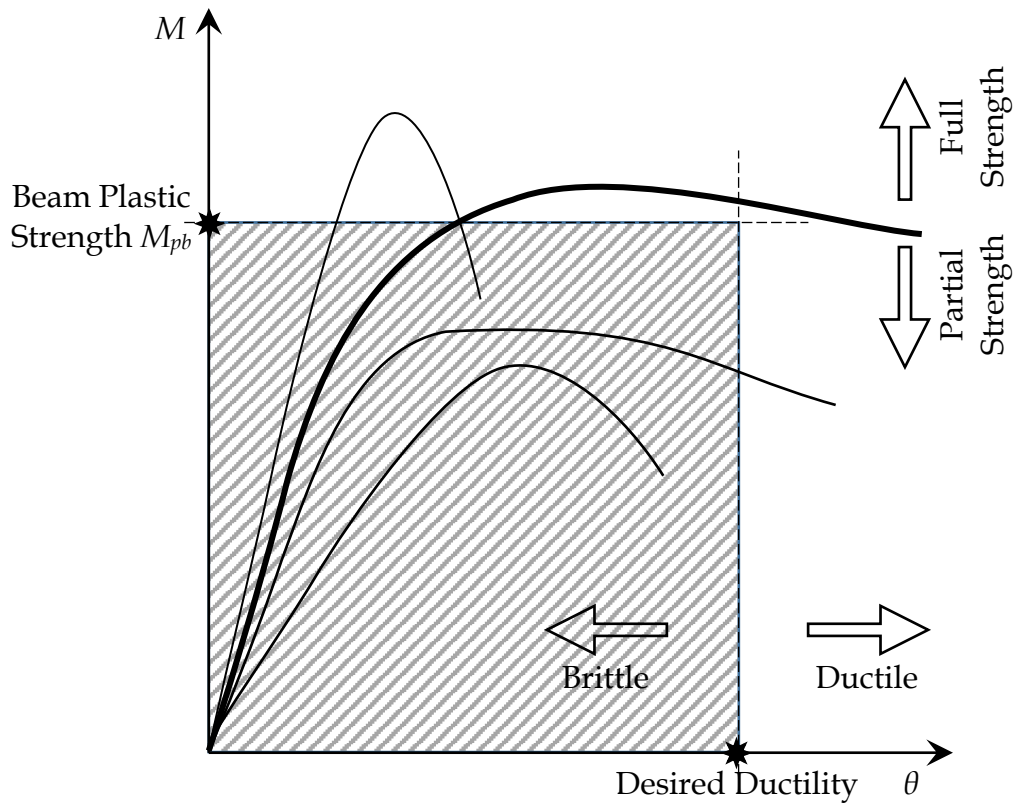


Figure 2.16: Typical Behaviour of Moment Resisting Connections [adapted from Mazzolani and Piluso, 1996]. For Seismic applications connections capable of full strength and adequate ductility are preferred.

Chapter 3

Effect of Column to Beam Strength Ratio on Inelastic Behavior of Strong Axis Beam to Column Joints

3.1 Overview

The Column to Beam Strength Ratio (CBSR) has been emphasized, across the research literature, as a vital parameter governing the behaviour of steel MRFs. Standards across the world prescribes CBSR value more than unity to achieve the Strong Column Weak Beam (SCWB) behaviour.

This chapter investigates the effect of CBSR on performance of interior beam to column joints (BCJs). The behaviour of strong axis interior BCJs, subjected to lateral loading, is studied through Nonlinear Finite Element Analyses. The study also examines the influence of continuity and doubler plates on joint behaviour.

3.2 Introduction

The current Strong Column Weak Beam (SCWB) design criterion prescribes a single acceptance limit of strength ratios for steel Moment Resisting Frames (MRFs). Research has shown that the required CBSR in steel MRFs vary with the factors such as the height of frames, joint location, seismic weight etc. [Choi et al., 2013]. AISC 341-10 stipulates that the ratio of sum of plastic flexural strengths of columns to the sum of plastic flexural strengths of beams connected at a joint, defined as column-to-beam-strength-ratio (CBSR), should be greater than unity. The SCWB criterion is based on the linear static analysis with the assumption that the inflection points of columns are located at column mid height, however, due to influence of nonlinear behavior, it is known that the real moment distribution of moment frames is different from that based on the linear static analysis and the column-hinge mechanism may be induced even if the SCWB condition is satisfied [Park & Pauley, 1975].

The flow of stresses in a direct BCJs happens from beams to columns through beam to column connections and JPZ region. Assuming that welds are capable of withstanding, and transferring the forces to column flanges, the JPZ region needs to

be adequately strong. As JPZ is a part of column, the yielding of JPZ can essentially be understood as the yielding of column, and should be avoided in case of moderate earthquakes. To ensure that JPZ region remains safe under moderate seismic excitations, a certain minimum thickness of column web is required. The thickness of column web doubler plates needs to be designed on the basis of CBSR of the joint. In order to prevent inelastic activity in columns, the JPZ region needs to be stronger than the beam. The thickness of column web, which is a property of column cross-section, depends on the CBSR of the joint. In cases where the JPZ region of beam to column joints are leaner than a particular (prescribed) thickness, column webs are to be reinforced with doubler plates. The purpose of column web doubler plates is to strengthen the JPZ region by increasing its shear area. A set of analyses are carried out with doubler plates of nominal thickness to identify their effects on the behaviour of strong axis interior BCJs.

Provision of continuity plates is mandatory according to the design codes of some countries, including Indian Standard. Apart from preventing the flexural yielding of column flanges, continuity plates ensures that sufficient lateral stiffness is maintained. They also stiffen the column web and distribute the forces to prevent local crippling when the beam undergoes inelastic deformation. The presence of continuity plates also reduces the concentration of stresses at beam to column joints.

The study investigates the effects of CBSR on the inelastic behaviour of BCJs. The effect of Joint Panel Zone reinforcements, namely, continuity and doubler plates, are also examined.

3.3 Modelling and Analysis

To investigate the effect of CBSR on the performance of a joint under lateral loading, a strong axis interior BCJ subassembly is modelled. The subassembly consists of column of height equal to the sum of distance between points of contraflexure above and below the joint. Beam length for subassembly is also taken as the distance between two points of contraflexures on either side of the column. The point of contraflexures are assumed at the mid-heights of members, and the subassembly is simply supported at column ends (Figure 3.1). Centerline

dimensions are considered and displacement loading is applied at beam ends. The height of columns in the subassemblages is 3.8m, which, in most cases, is the average storey height (Figure 3.2). The distance considered between column centerline and the point of application of load on beams is 3.0m, representing a typical span. Both material and geometric nonlinearities are considered in the analyses.

The members are of ASTM A36 grade steel with isotropic hardening model (yield stress of 250 MPa and ultimate stress of 415 MPa). Welds between beam and column of subassemblage are modelled as Complete Joint Penetration (CJP) welds. The properties of the welds are corresponding to ASTM E70 weld electrodes, having a bilinear stress strain relationship (yield strength of 345 MPa and ultimate tensile strength of 480 MPa at 20% elongation). Stress-strain relationships for A36 Grade steel and E70 electrodes used for analysis are shown in Figure 3.3. For both the materials, modulus of elasticity and Poisson's ratio are 200GPa and 0.260, respectively.

A classically isotropic plasticity model based on von Mises yield criteria and associated plastic flow is used to incorporate material nonlinearity.

The subassemblages are subjected to SAC's standard loading protocol (Figure 3.4), having multi-step reverse cyclic displacements at beam ends upto a drift of 4%. The displacement based nonlinear finite element analyses, using eight noded linear brick elements (C3D8R) with uniform mesh, are conducted using ABAQUS [HKS, 2013]. The CJP welds are modelled by carefully merging the common nodes between weld elements and parent material; von Mises stress contours have been considered for performance evaluation and comparison. The results are presented in the form of von-Mises and shear stress contours.

3.4 Numerical Study

A range of combinations of columns and beams have been selected on the basis of CBSRs. The deciding parameters for selecting a section as column or beam are, (a) plastic section moduli and (b) width of flange. Beam sections are such selected, that the width of beam flanges remains lesser than width of corresponding column flanges. A fair representation of a wide range of CBSRs is achieved through section selection. The class of selected section is determined using tables B4.1a and B4.1b of AISC 361-

10, and most of the sections selected are compact, while only a few classifies as non-compact.

CBSR values of the subassemblages selected varies from 1.2 to 3.89, most of the selected sections are 'compact' and are capable of developing plastic hinges across full depth, without significant loss of strength. The numerical study has been conducted for three joint configurations, namely, (a) direct joint, (b) joint with continuity plates, and (c) joint with continuity plates and doubler plates of minimum thickness (as recommended by AISC 360-10).

3.4.1 Direct Joints

Direct joints refer to strong axis beam to column joints without any reinforcements and stiffeners, i.e., the beams frames directly into the column flanges. For beam to column moment joints having direct connection between beams and column, CBSR is the only criteria on which design of joint depends.

3.4.2 Joints with Continuity Plates

Continuity Plates are, stiffeners in continuation of beam flanges, placed between the column flanges. It is a common provision to prevent bending of column flanges at beam column joints. For the purpose of present study, continuity plates of thickness equal to beam flange thickness has been provided.

3.4.3 Connections with Continuity and Doubler Plates

This joint configuration has continuity and doubler plates (column web reinforcements provided to strengthen the JPZ, and increasing the strength and stiffness of BCJs) of nominal thickness.

3.5 Results and Discussion

The von Mises stress contours, shear stress contours and variation in shear force with percentage drift are presented. The results for *direct joints*, *joints with continuity plates*, and *joints with continuity and doubler plates*, are shown in Figures 3.5 - 3.7.

Figures 3.5 (a) and (b) show the von Mises and Shear stress contours, respectively, for all subassemblages having *direct joints*. The results of finite element analyses show that for unreinforced joints (i.e. direct joint) having CBSR less than 3.89,

inelastic actions remains limited to the JPZ only. Also, for joints with CBSR less than 2.5, there is no observable yielding of beam flange. In case of joints having CBSR greater than 2.5, the participation of beams in energy dissipation is noticed only after significant yielding of JPZ. This can be attributed to the insufficient shear capacity of JPZ along with strain hardening.

Results of *joints with continuity plates* are depicted through Figure 3.6 (a) - von Mises stress contours and Figure 3.6 (b) - shear stress contours. From the results it is noticed that, the extent of beam flange yielding has increased for joints with CBSR greater than 2.5, however, there seem to be no contribution of continuity plates on the yield deformation of JPZs. The provision of continuity plates prevents the local buckling of column flanges thereby leading to enhanced participation of beams. However, for joints having CBSR lesser than 2.5, kinking of column flanges is observed, as inelastic actions remains localized at JPZ due to higher strength of beams framing into the joints. It can be concluded that provision of continuity plates prevents local buckling of column flanges, but also leads to concentration of stresses in column flange at the level of beam flanges.

Figures 3.7 (a) and (b) show the von Mises and Shear stress contours, respectively, for *joints with continuity and doubler plates*. The columns yielding is observed for CBSR less than 1.8, however, with further increase in CBSR the extent of inelasticity in columns reduces. Also, for joints having CBSR greater than 1.8, inelastic actions initiates in JPZ and progresses towards the beams, only after significant yielding of JPZ. It has been observed that the provision of doubler plates significantly increases the participation of beams in the energy dissipation phenomenon. This is primarily due to increased shear strength of JPZ. Further, the use of doubler plates delays the onset of yielding of JPZ region, but does not contribute much towards altering the order of yielding amongst different components.

The results of the finite element analysis of beam to column joint subassemblages have been used to develop the load-deformation hysteresis curve for each joint. The backbone curves are derived from the hysteresis curve by connecting the points having abscissa equal to the drift values of 0.375%, 1%, 2% and 4% and ordinate equal to the corresponding first reaction forces. Figure 3.5 shows the

hysteretic curves, and corresponding backbone curves for beam to column joint having CBSR 3.89. Shear force versus percentage drift backbone curves of beams, JPZs and columns for *direct joints*, *joints with continuity plates*, and *joints with continuity and doubler plates* are shown, through Figures 3.8 - 3.10, respectively. The shear force has been normalized with the corresponding member capacity. It is noted that for the considered range of CBSR the inelastic actions initiates in the JPZ, for all the three joint configurations.

3.6 Conclusions

Based on the results from the study following precise conclusions are drawn.

1. The joint panel zones inelasticity is the primary energy dissipation mechanism for joints having CBSR up to 3.9. Further, the inelastic actions in beams ends does not initiate upto a CBSR of 1.8. Also, a partial yielding of beam flanges is observed for joints having CBSR greater than 2.5.

2. The continuity plates are able to increase inelasticity in beam flanges, though their effect is not very significant. Thus, the role of continuity plates is to prevent local buckling of column flanges, and they do not have any significant contribution towards strengthening of a joint.

3. The column web doubler plates leads to de-localization of inelasticity from JPZ to the beam end region. This is attributed to increased shear capacity of the JPZ. However, it is also concluded that inelastic actions in JPZ can, at best, be delayed, and not prevented, by using column web doubler plates.

It can be concluded that the extent of inelastic yielding of beam end region depends on column to beam strength ratios. The results of Finite Element Analyses carried out in this chapter shows that even a Column to Beam Strength Ratio of about 4.0 is not sufficient to limit all the inelastic actions at the beam ends, upto a drift limit of 4% (0.04 rad).

Table 3.1: Properties of selected Column and Beam Sections.

S. No.	Column Sections	M_{pC} (kNm)	b_{cf} (mm)	Beam Sections	M_{pB} (kNm)	b_{bf} (mm)	M_{pC}/M_{pB}	$t_{DP,min}$ (mm)
1.	W27X235	3142	361	W16X100	807	264	3.89	11
2.	W24X176	2079	328	W18X71	593	194	3.51	11
3.	W24X229	2748	333	W21X93	908	214	3.03	12
4.	W27X178	2309	358	W21X93	908	214	2.54	13
5.	W24X176	2079	328	W18X97	857	282	2.43	11
6.	W18X192	1818	292	W21X93	908	214	2.00	10
7.	W18X119	1078	287	W10X112	605	264	1.78	7
8.	W18X119	1078	287	W21X68	636	210	1.69	10
9.	W18X130	1179	284	W21X83	793	212	1.49	10
10.	W16X100	808	264	W24X62	619	179	1.31	11
11.	W21X83	787	212	W24X62	619	179	1.27	12
12.	W18X130	1179	284	W27X84	986	254	1.20	12

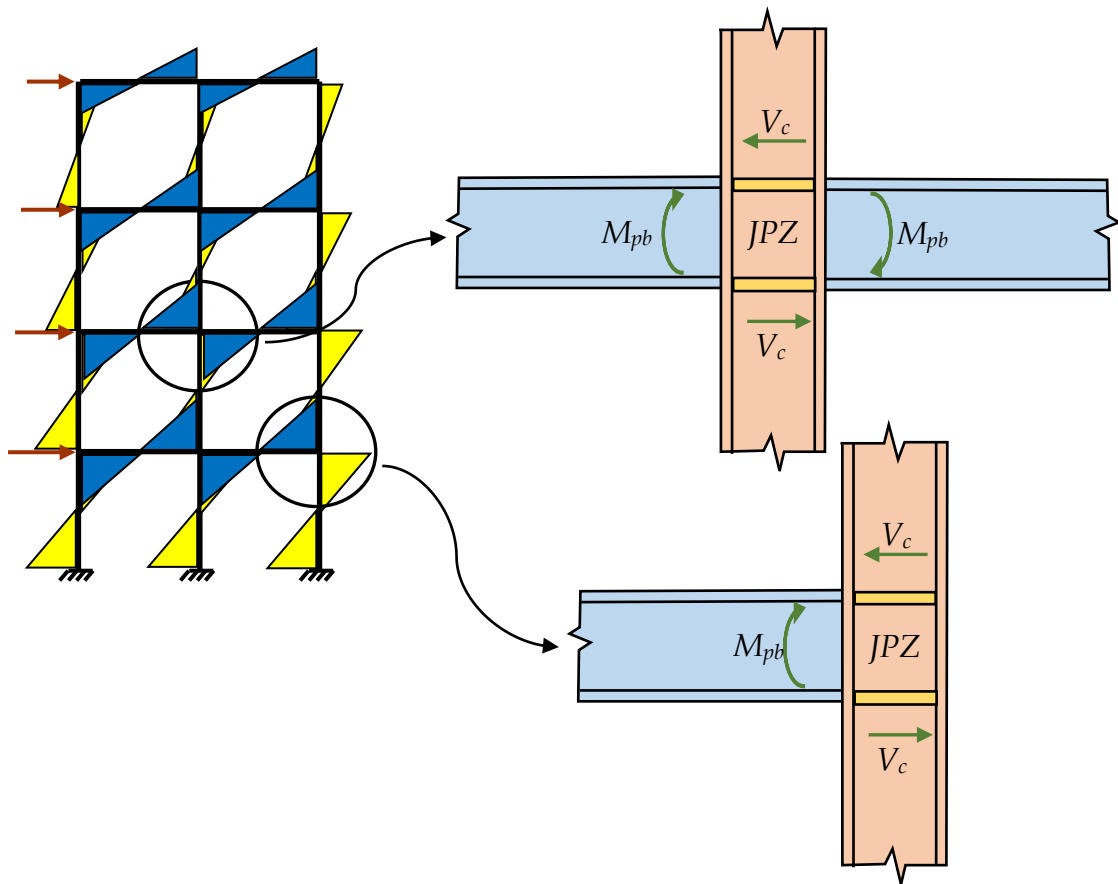


Figure 3.1: Interior and Exterior Beam Column Joints in a MRF. Depicting the forces under lateral load conditions.

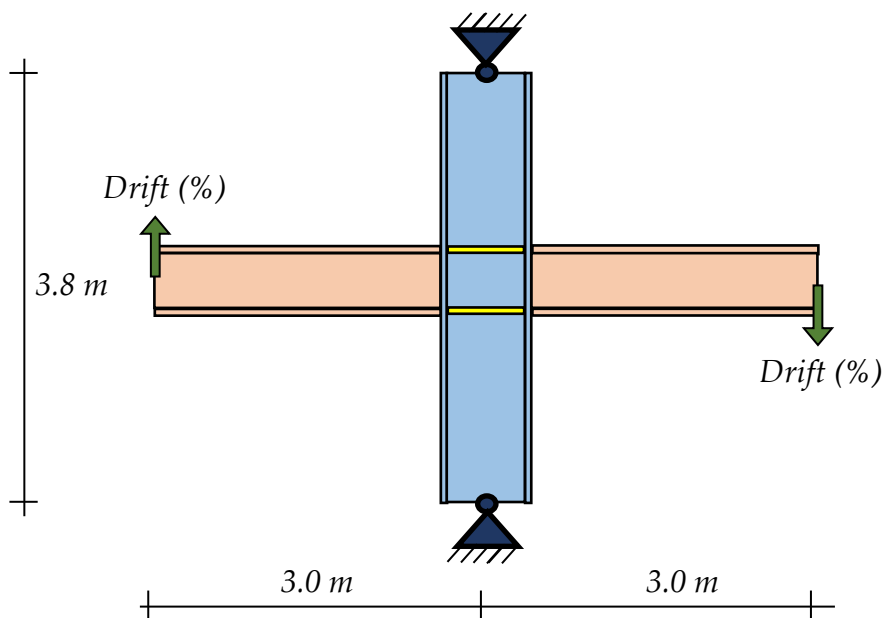


Figure 3.2: Beam-Column Joint Subassembly. Height of column and Length of beam are taken 3.8 m and 3.0 m, respectively, representing typical storey height and beam spans.

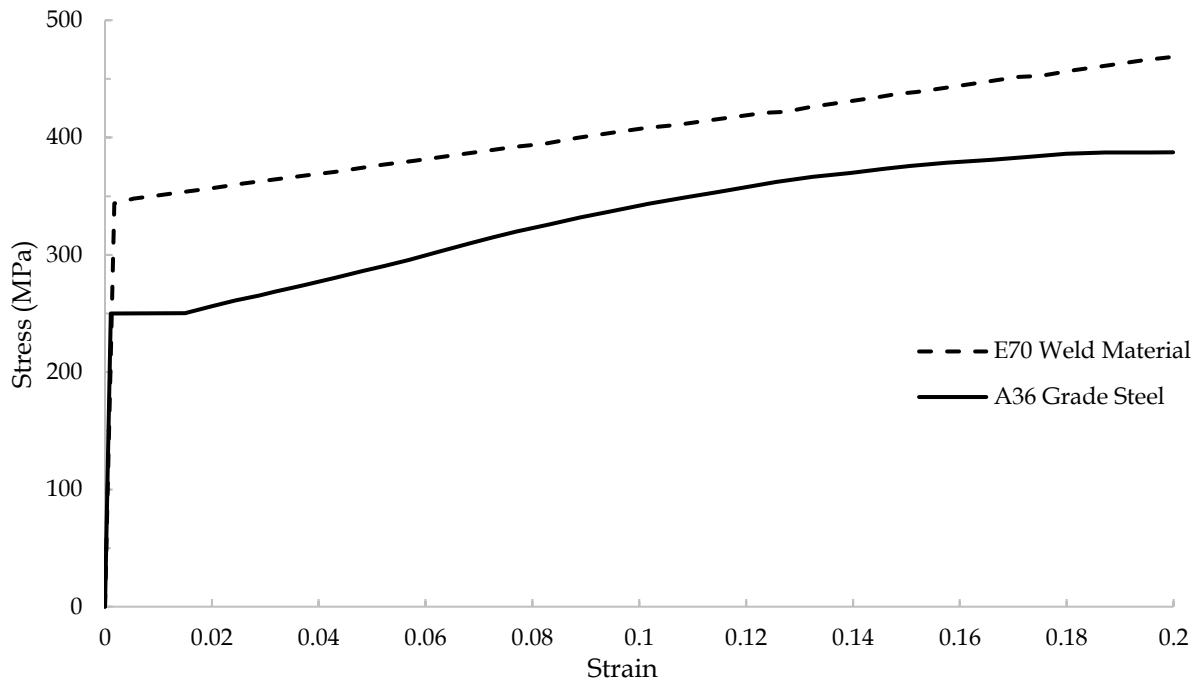


Figure 3.3: Stress Strain Curves for A36 Steel and E70 welds as modelled.

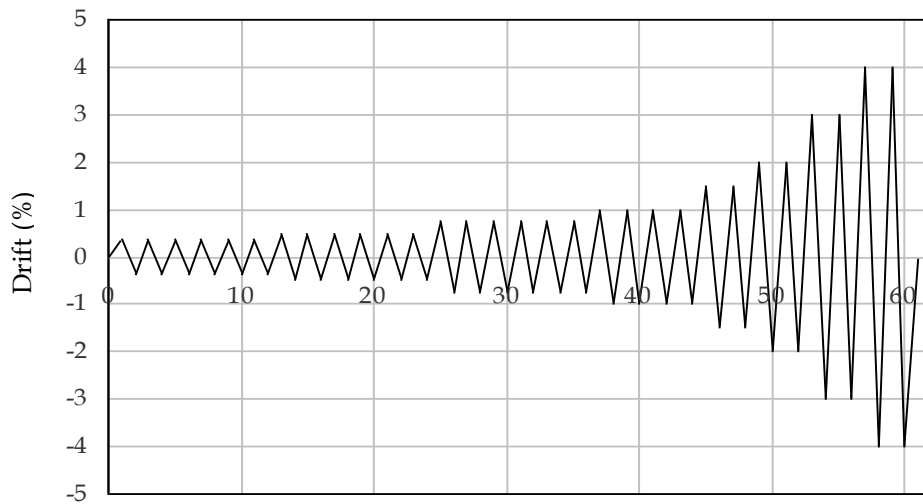


Figure 3.4: SAC's Standard Loading Protocol [ANSI/AISC 341-10]

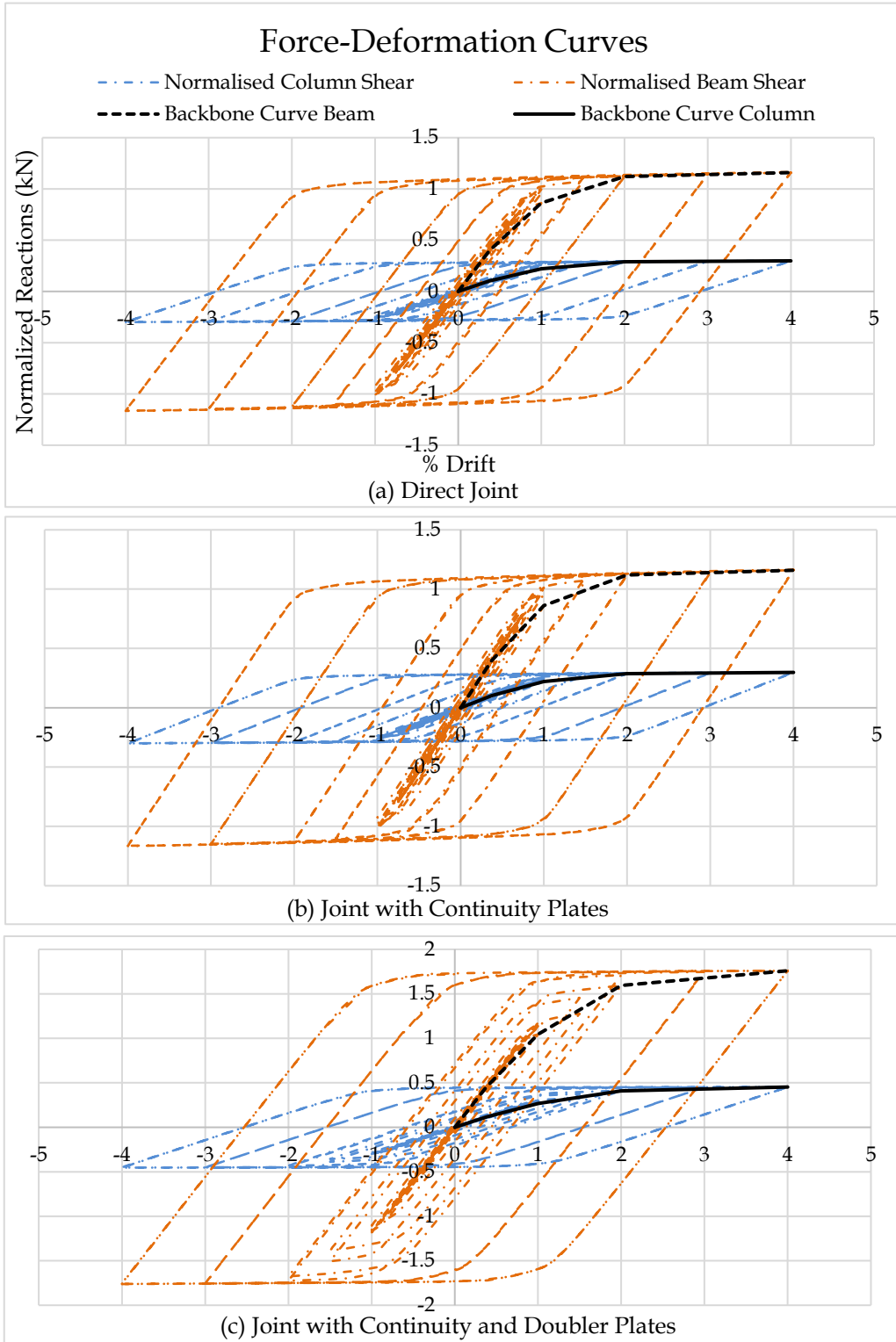
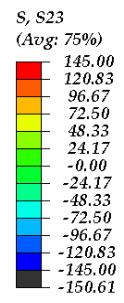
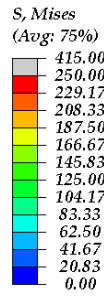
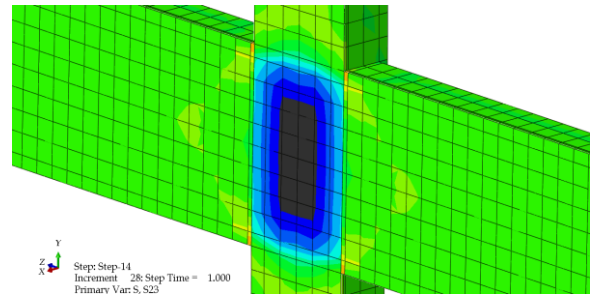
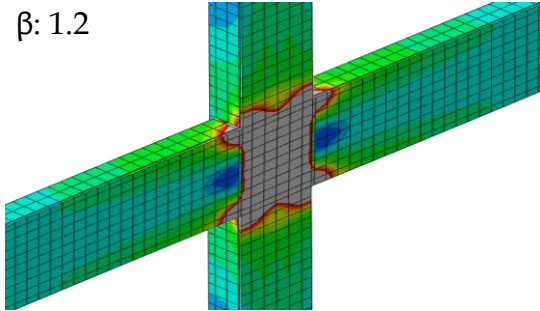


Figure 3.5: Hysteretic Curves and Backbone Curves for CBSR of 3.89.

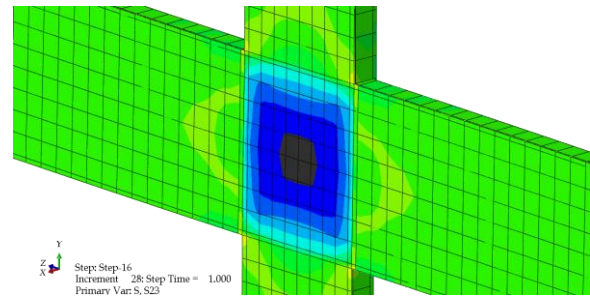
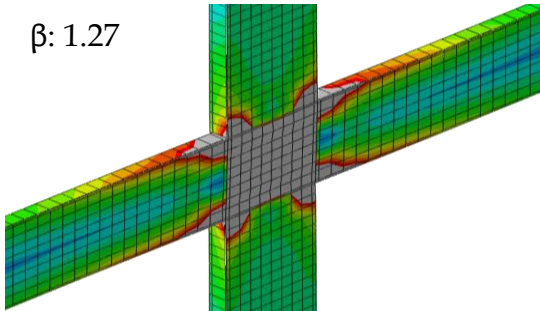
The backbone curves are obtained by connecting origin with points having abscissa as 0.375%, 1%, 2% and 4% and the corresponding forces as ordinates.



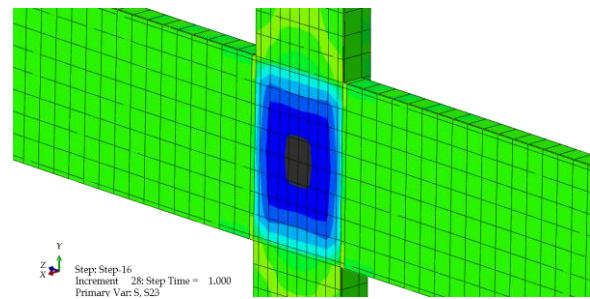
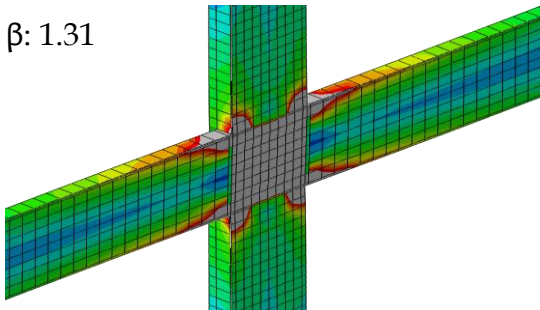
β : 1.2



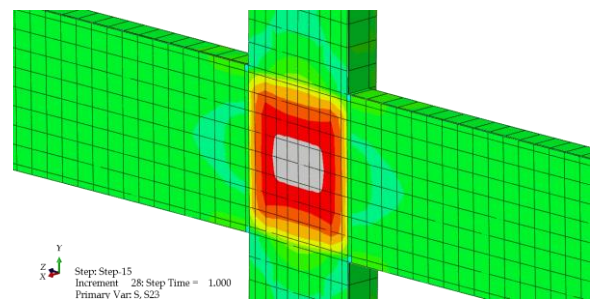
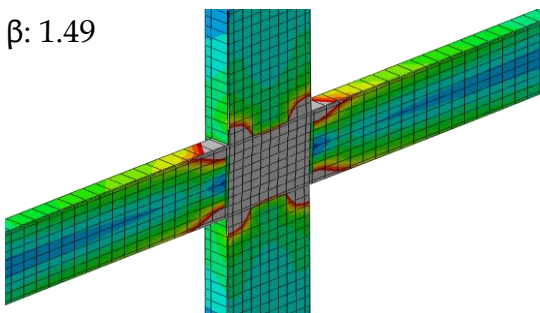
β : 1.27



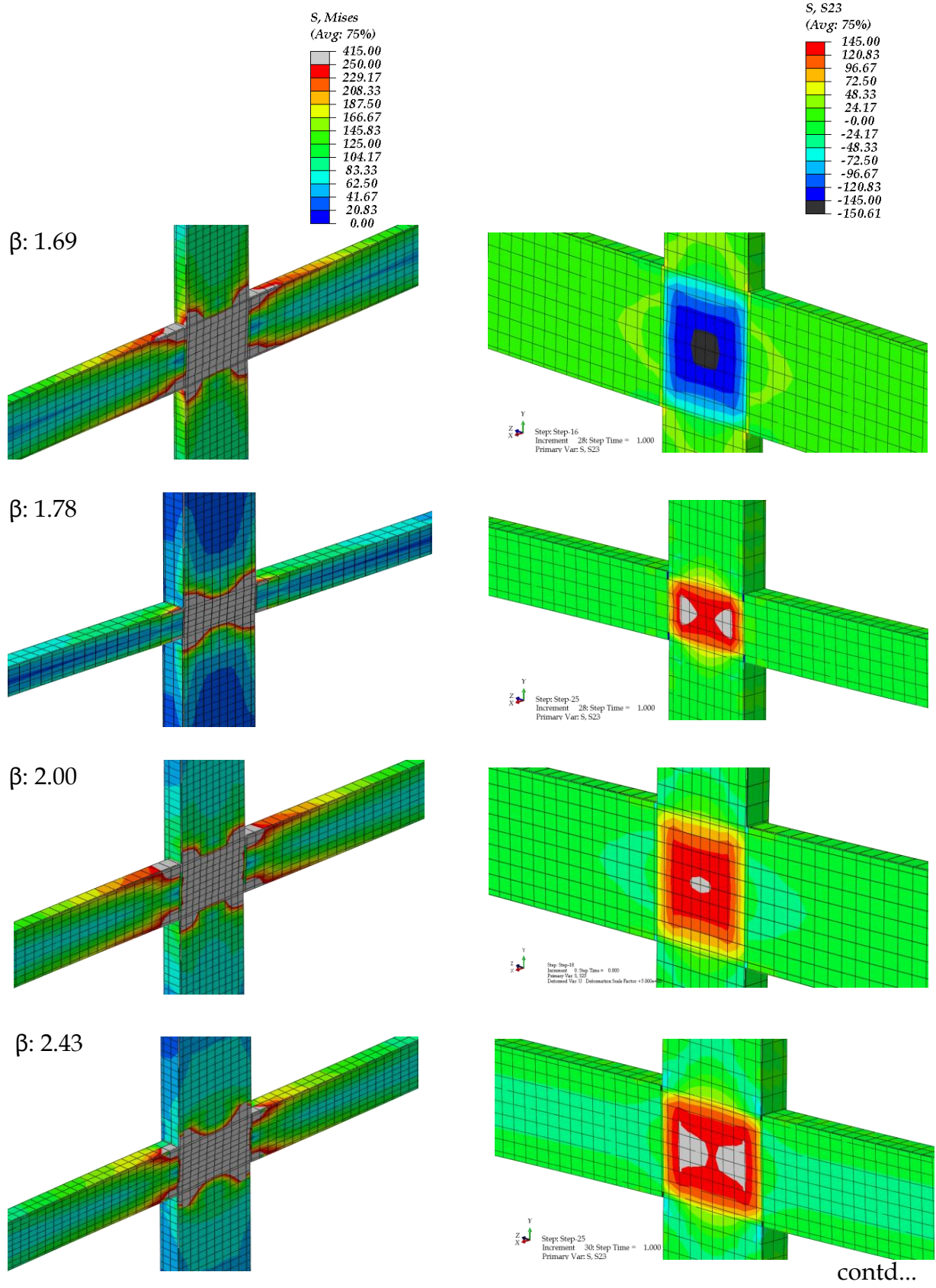
β : 1.31



β : 1.49



contd...



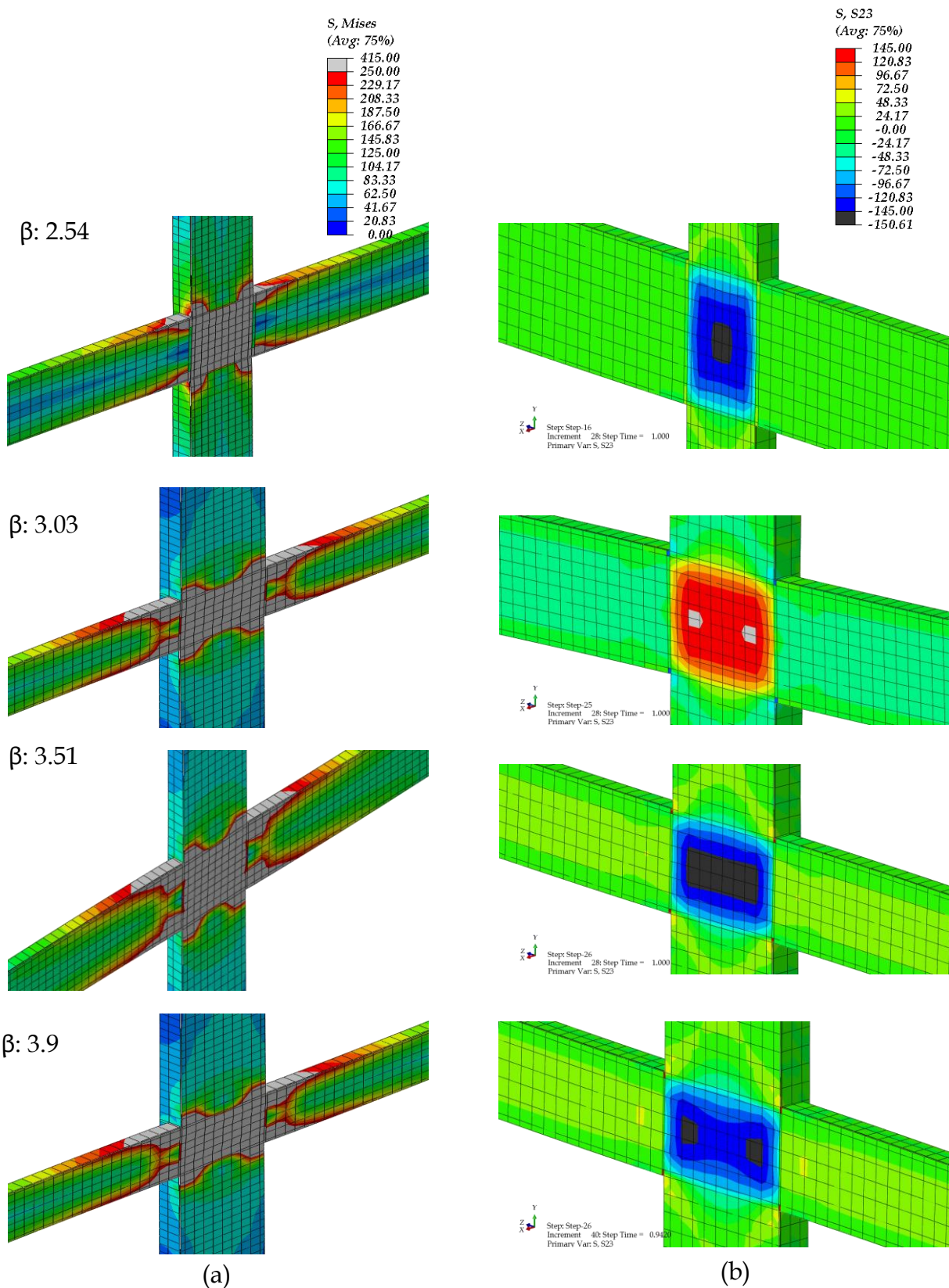
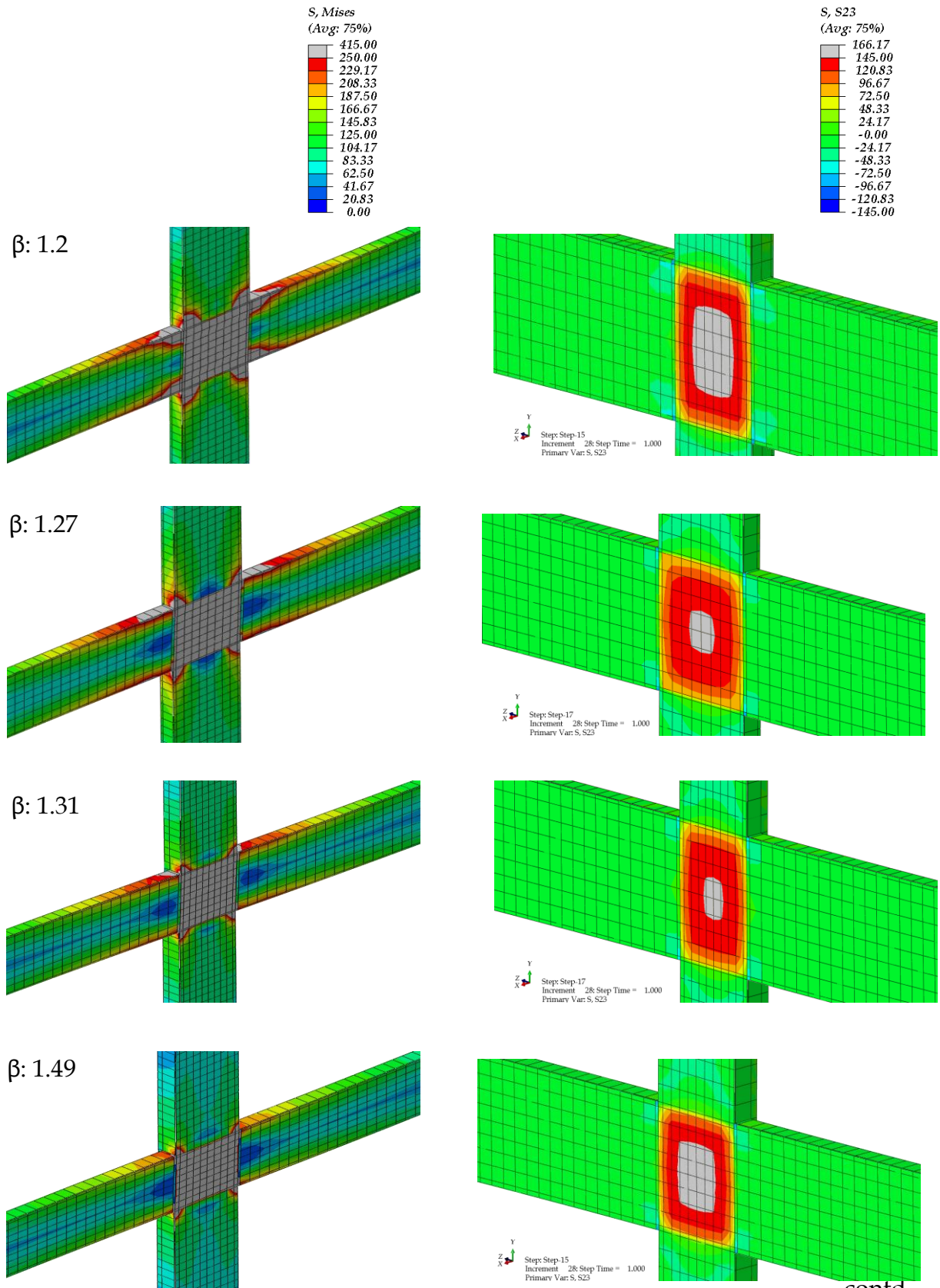
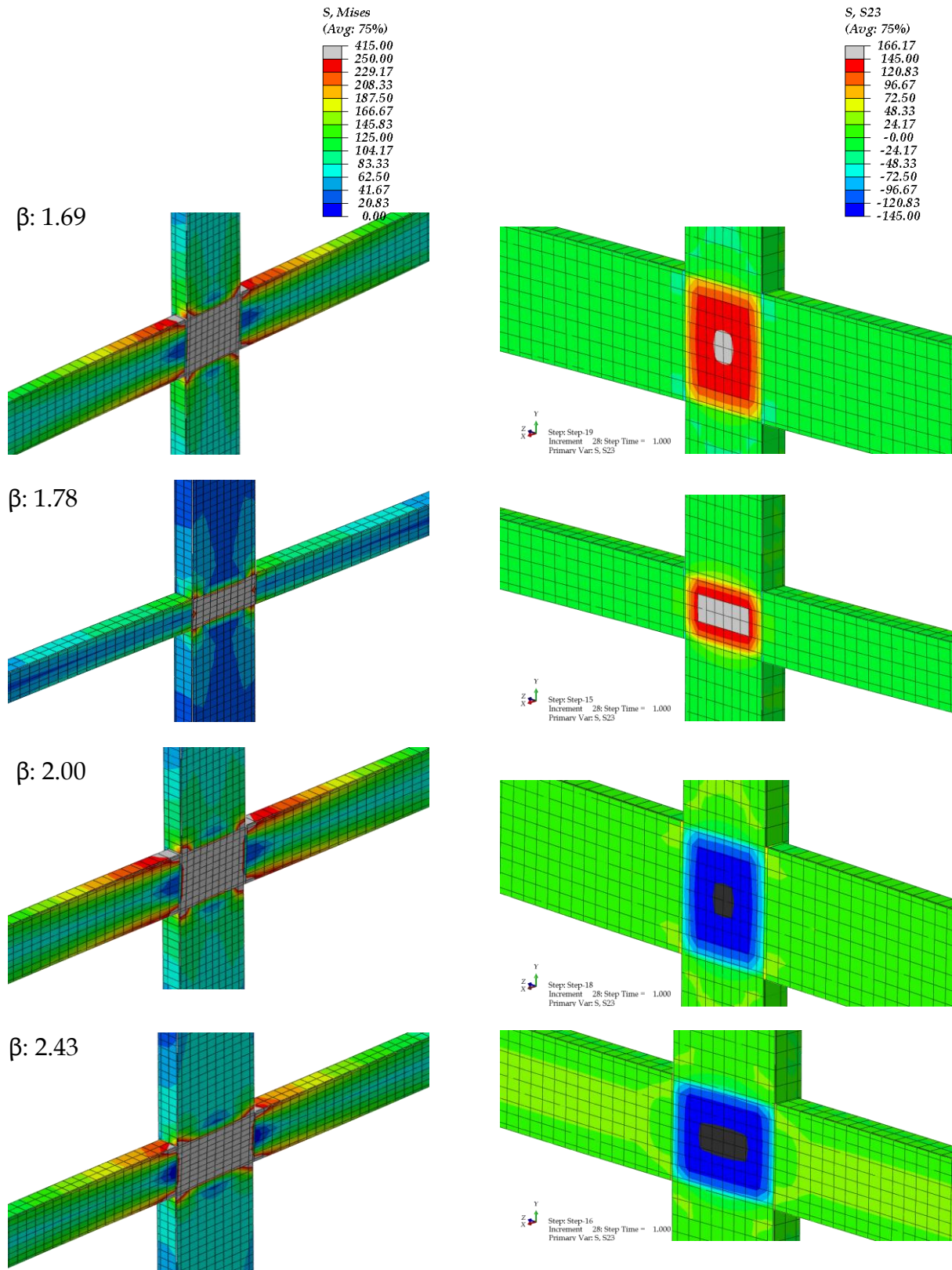


Figure 3.6: (a) von Mises Stress contours at final step and (b) Shear Stress contours at initiation of yielding, for direct joints. For joints having low CBSR, the inelasticity remains localized, at the JPZ region only. An increase in Column to Beam Strength Ratio results in mobilization of inelasticity into beams.



contd...



contd...

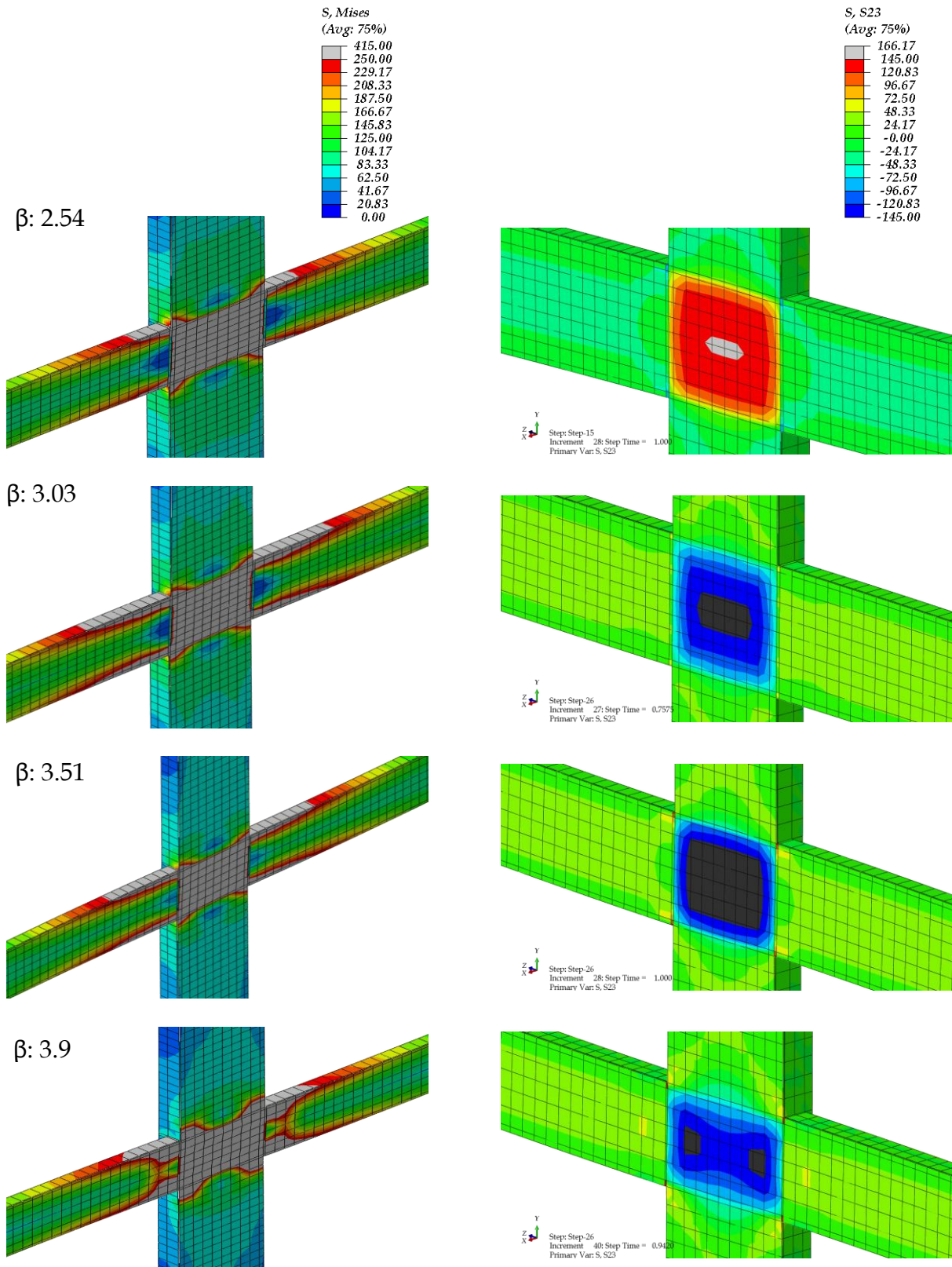
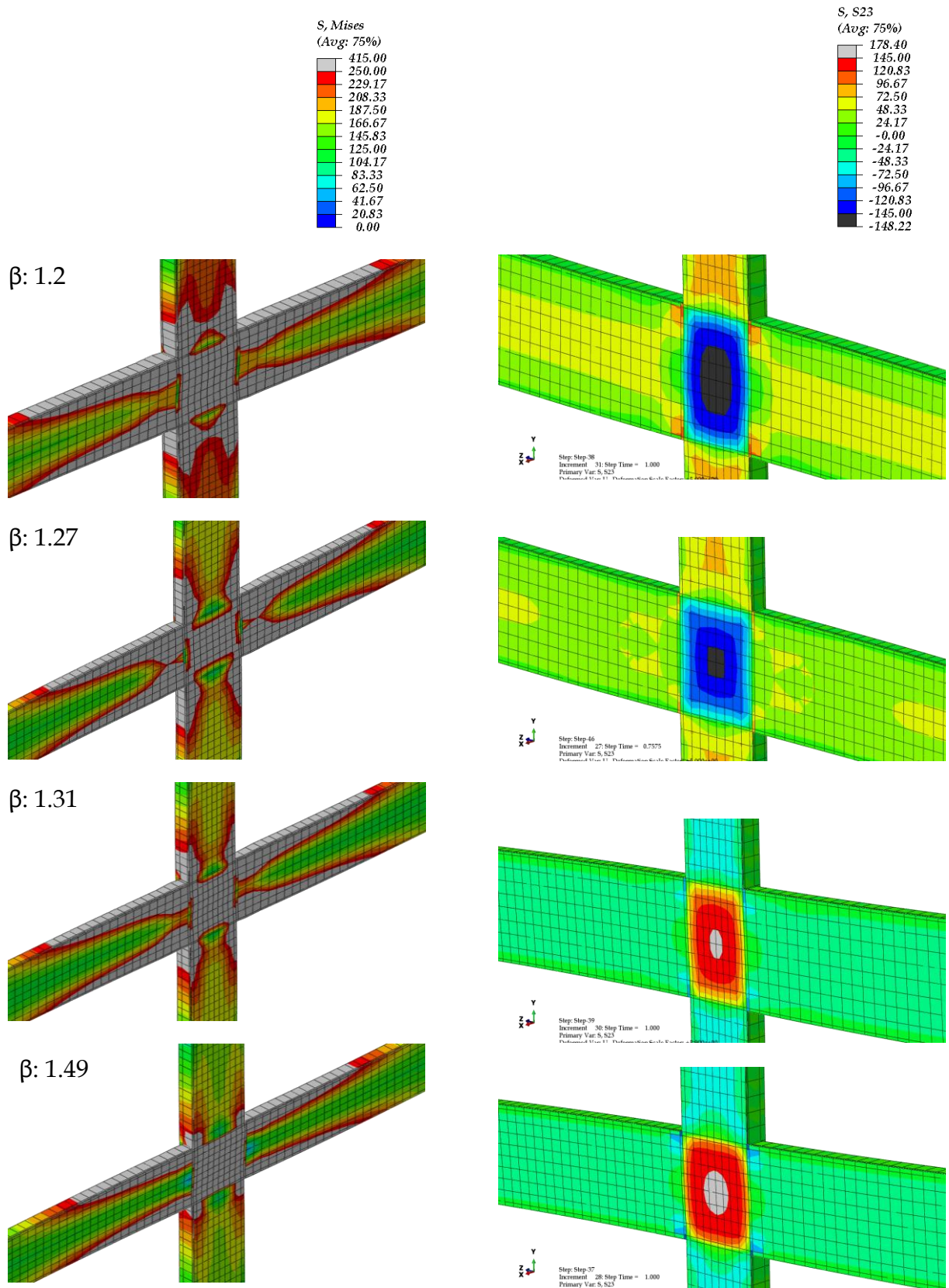
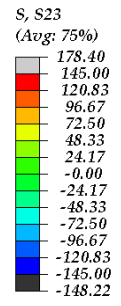
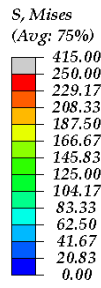


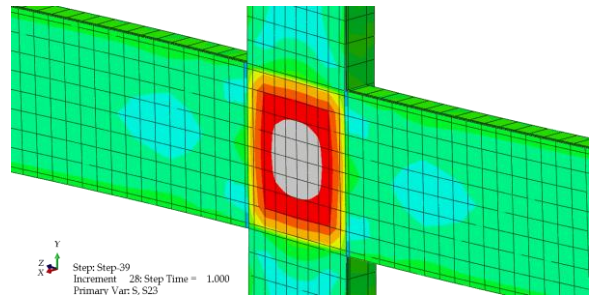
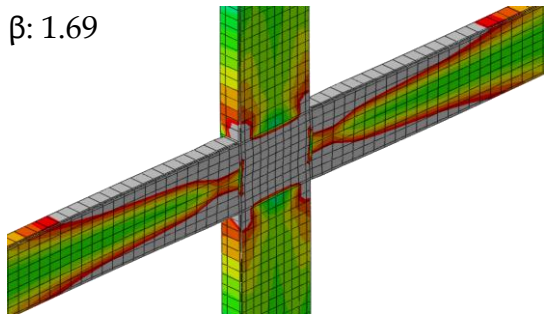
Figure 3.7: (a) von Mises Stress contours at final step and (b) Shear Stress contours at initiation of yielding, with Continuity Plates. The contribution of Continuity Plates towards enhancing the strength and stiffness of joint is marginal.



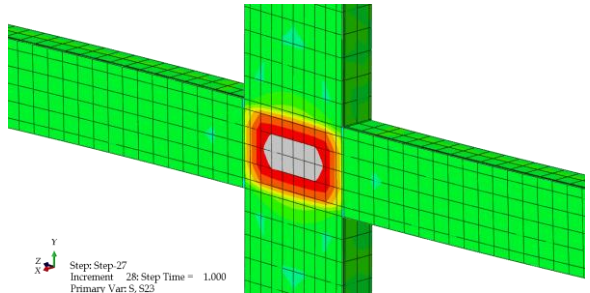
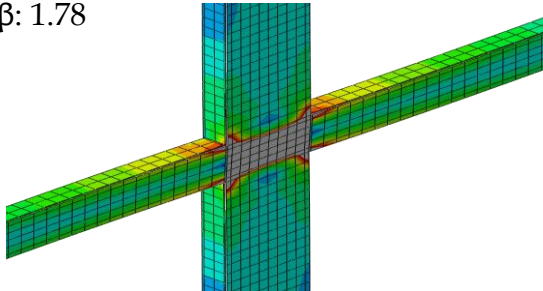
contd...



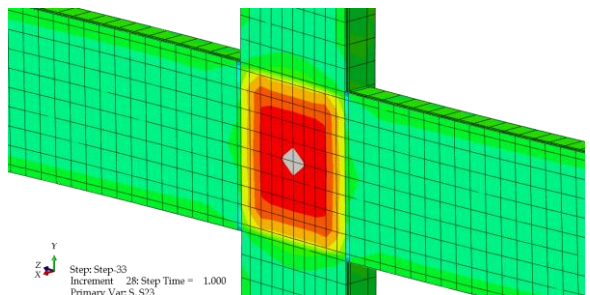
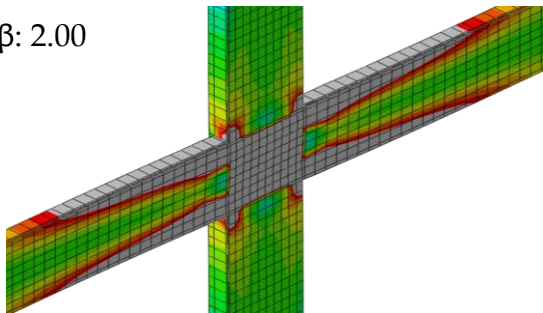
β : 1.69



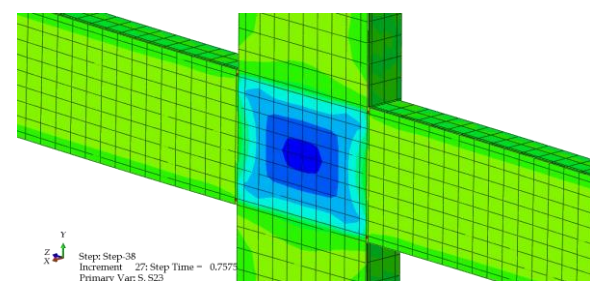
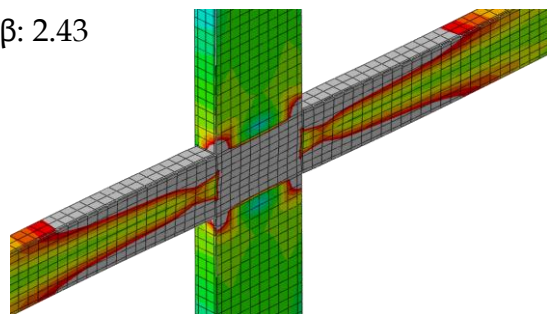
β : 1.78



β : 2.00



β : 2.43



contd...

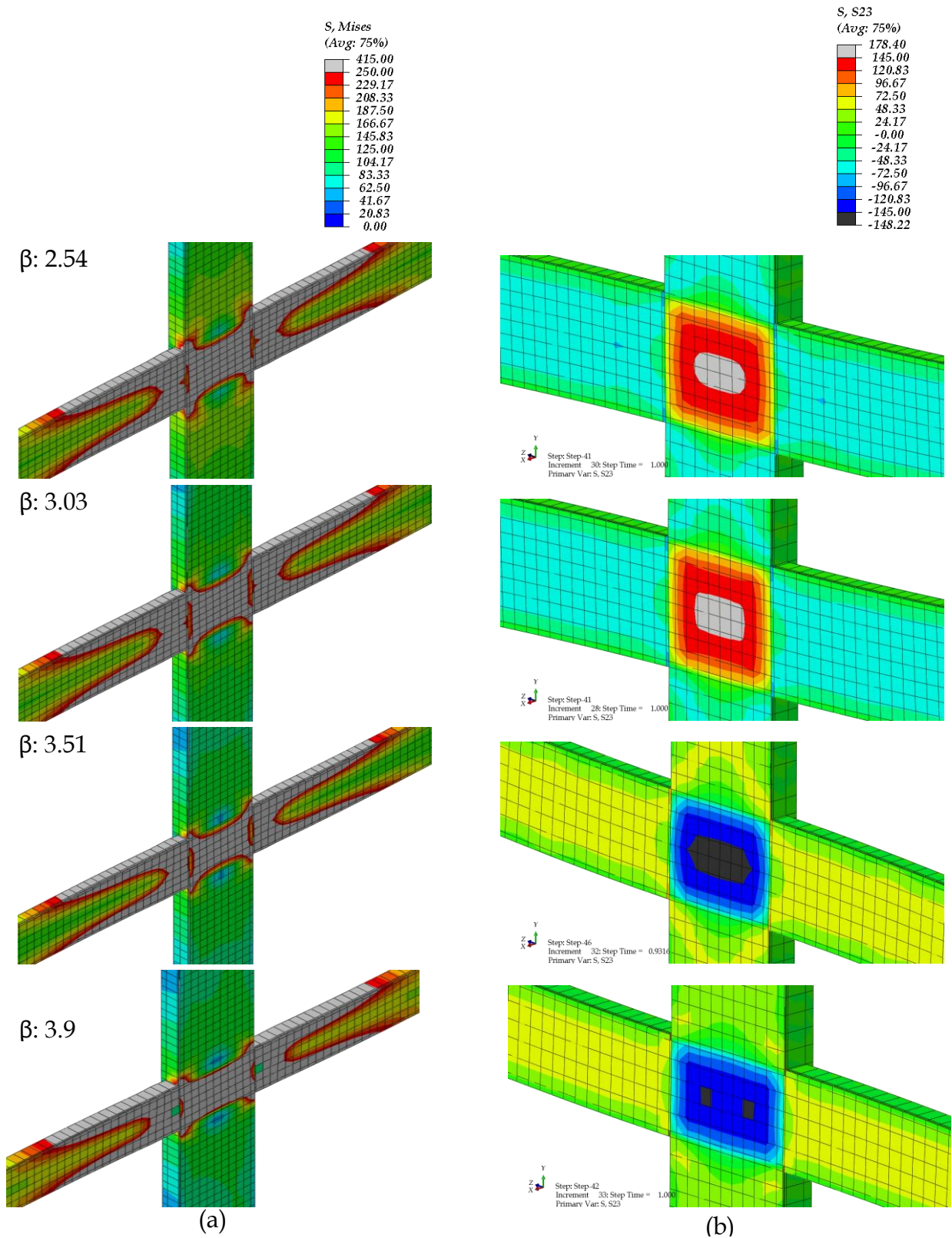


Figure 3.8: ((a) von Mises Stress contours at final step and (b) Shear Stress contours at initiation of yielding, with Doubler and Continuity Plates. Connections having Doubler Plates are able to dissipate much greater inelastic energy. However, the provision of Doubler plates does not ensures that inelasticity remains confined to beam ends.

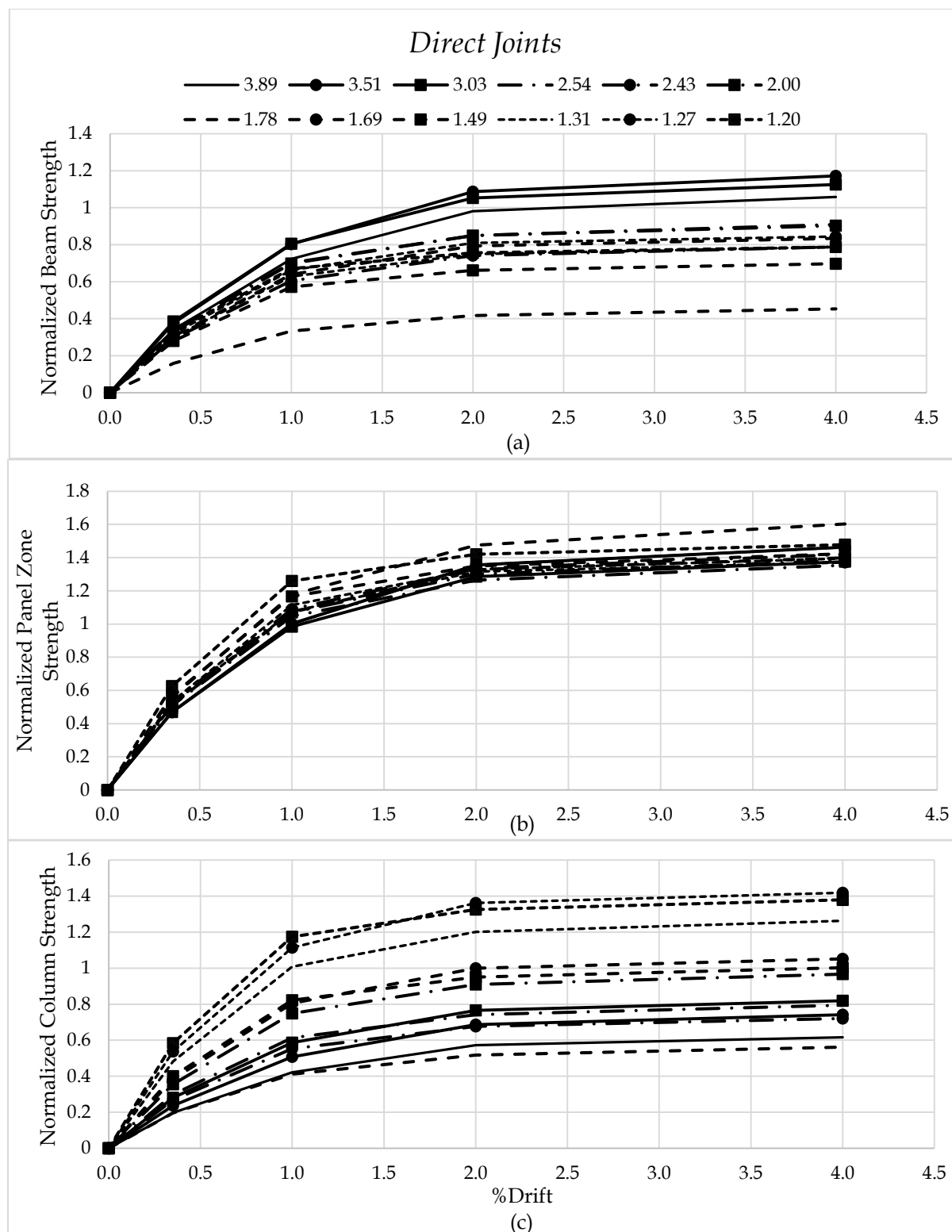


Figure 3.9: Normalized Force Deformation Behaviour of Prequalified Beam to Column Joint Subassemblages (Normalized by the Capacity of individual member). The connections having CBSR>3.0 have inelasticity in beams, while JPZ have yielded significantly in all cases.

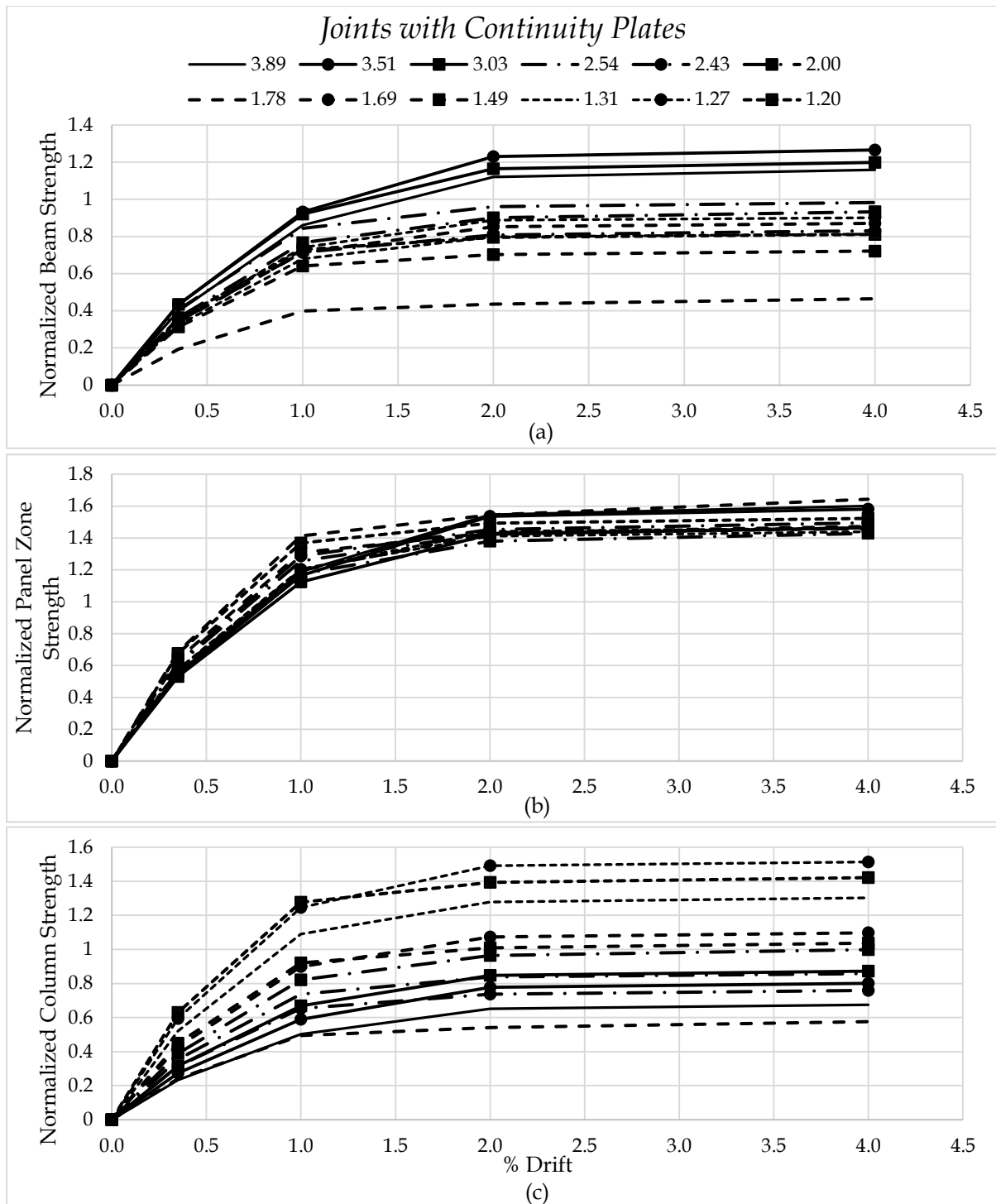


Figure 3.10: Normalized Force Deformation Behaviour of Prequalified Beam to Column Joint Subassemblages with Continuity Plates (Normalized by the Capacity of individual member). Provision of continuity plates leads to a marginal increase in stiffness of Joints..

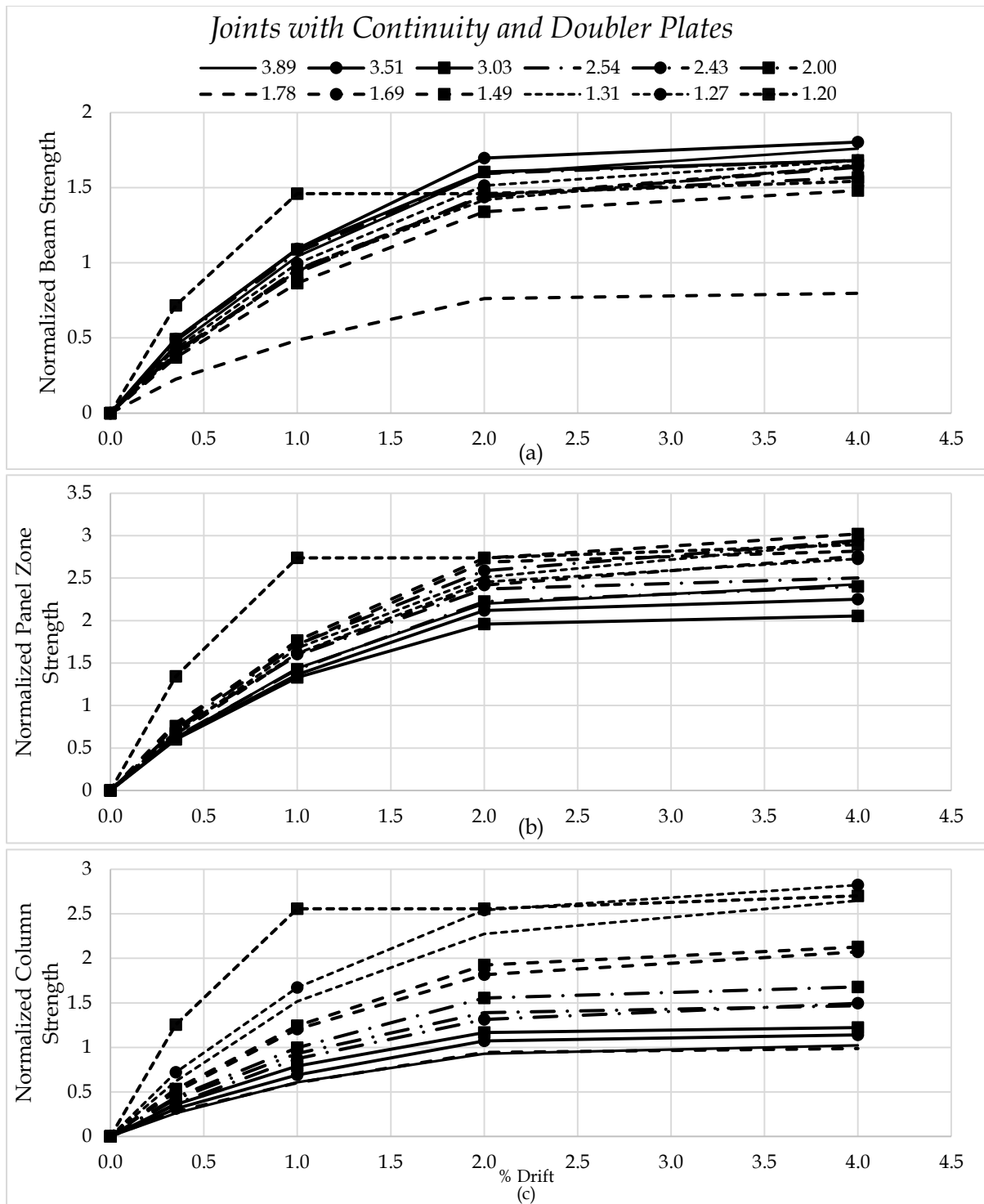


Figure 3.11: Normalized Force Deformation Behaviour of Prequalified Beam to Column Joint Subassemblages with Doubler and Continuity Plates (Normalized by the Capacity of individual member). The provision of Doubler plates forces inelastic actions in beams and columns, but does not prevent significant inelastic shear yielding of Joint Panel Zones.

Chapter 4

Mechanics based Monotonic Load Deformation Curves of Beam to Column Joints

4.1 Overview

Steel Moment Resisting Frames (MRFs), when subjected to strong earthquake shaking, are expected to dissipate the seismic input energy through inelastic action without collapse. Therefore, inelasticity in different components of beam to column joints is inevitable under severe earthquake ground motion. Conventionally, to determine the distribution and extent of inelasticity in components of beam to column joints nonlinear finite element analysis is to be carried out. The analyses process is computationally exhaustive and time consuming.

In this study a simple mechanics based analytical closed form method has been proposed to predict the nonlinear force-deformation behaviour of beam to column joint subassemblages. The proposed model is verified through Finite Element Analyses. A wide range of CBSR (1.2 to 11) has been tried to investigate behaviour of joints; and from the results it was noted that to limit inelasticity within beam ends a very high value of CBSR, of the order of eight and above, is needed.

4.2 Introduction

The concept of *capacity design* envisages a hierarchy of strength of members such that energy dissipation capacity of the system is utilized, to the maximum, without collapse or local instability. In the context of steel MRFs, the strength hierarchy (in the increasing order of strength) shall be- *Beam, Joint Panel Zone, Beam to Column Connections, Column, Column Base Connection and Foundation*. This translates in to Strong Column Weak Beam (SCWB) design approach, that is, the yielding of beams shall precede the yielding of columns. Furthermore, the Joint Panel Zone needs to be identified as a separate entity in the strength hierarchy.

In this chapter, a computationally elegant and efficient mechanics based hand calculation method is developed to predict the yielding sequence and force

deformation behaviour of joints. The method can be used to predict the drifts at which inelastic actions initiate and propagate, for both interior and exterior moment joints. Using the *Proposed Method* the sequence of yielding of the components of a beam to column joint can be estimated, once the size and geometry of sections to be used as beams and columns is decided. The *proposed method* also provides fair estimation of the drifts at which each of the component of a moment joint yields. This makes the *proposed method* comparatively less cumbersome than the classically used Finite Element Analysis.

To verify the accuracy of the proposed method, nonlinear finite element analyses of twenty five strong column weak beam interior and exterior joint subassemblages have been carried out. The analyses also gives the tentative minimum value of Column to Beam Strength Ratio (CBSR) to prevent yielding of Joint Panel Zone, up to a drift limit of at-least 4%. Also, assuming the connections to remain elastic, three probable modes of inelastic actions, namely, Beam Flange Yielding, Beam Plastic Hinging and Panel Zone Shear Yielding have been selected (shown in Figure 4.1). The method is able to predict the sequence of occurrence of the modes of yielding for a given beam column joint.

4.3 Mechanics Based Method for Prediction of Force Deformation Behaviour

Assuming rigid and unyielding connections, in a strong axis, strong column weak beam interior/ exterior joint, three possible modes of yielding are,

- (i) *Flexural Yielding of Beam Flanges,*
- (ii) *Shear Yielding of Joint Panel Zone and*
- (iii) *Formation of Plastic Hinges in Beam.*

The sequence of yielding depends on relative strength of the components, and the yield mode having least capacity shall be the first to occur. The formation of plastic hinge in beam will be preceded by yielding of beam flanges, however, shear yielding of Joint Panel Zone is independent of the other two modes. Assuming that the columns

are strong enough to not undergo any inelastic actions, there are three possible scenarios for yielding of a beam to column joint. These can be

The capacity of each of the components can be evaluated as,

Beam Flange Yield Strength,

$$F_{y,bf} = f_{yb} \cdot b_{bf} \cdot t_{bf} \quad (3.1)$$

where, f_{yb} is the yield strength of beam material, b_{bf} is width of beam flange and t_{bf} is thickness of beam flange.

Panel Zone Yield Strength,

$$V_{y,pz} = \left(\frac{f_{yc}}{\sqrt{3}} \right) \cdot d_c \cdot t_{pz} \quad (3.2)$$

where, f_{yc} is the yield strength of column material, d_c is depth of column section and t_{pz} is the thickness of JPZ region, which is, thickness of column web (t_{cw}) and doubler plate (t_{dp} , if provided).

Beam End Force to develop Beam Plastic Hinge

$$F_{p,b} = \frac{M_{pb}}{d_b - t_{bf}} \quad (3.3)$$

where, M_{pb} is plastic moment carrying capacity of beam section and d_b is depth of beam section.

For beam to column moment joints the inelastic yielding of beam flanges will occur before inelastic yielding of JPZ, only when $F_{y,bf} < \frac{V_{y,pz}}{2}$ (interior joint) and $F_{y,bf} < V_{y,pz}$ (exterior joint). Further, for beam to develop plastic hinge before the yielding of JPZ is initiated, $F_{p,b} < \frac{V_{y,pz}}{2}$ (interior joint) and $F_{p,b} < V_{y,pz}$ (exterior joint).

For the known yield sequence, e.g. Panel Zone Yielding (PZY), Beam Flange Yielding (BFY), and Beam Plastic Hinging (BPH), the drift corresponding to each mode can be computed as below.

For JPZ to yield, which in this case will be the first mode of yielding, the deformation at beam end should be such that it imposes a demand of $V_{y,pz}$ in the JPZ, for which a force of $V_{y,1}$ needs to be applied at beam ends, which is given by

$$V_{y,1} = \frac{V_{y,pz}(d_b - t_{bf})}{2 \times (L_b - d_c/2)} \quad (3.4)$$

where L_b is the length of beam. The resultant moment transferred to the columns due to application of force $V_{y,1}$ at beam end is

$$M_{c,1} = 2 \cdot V_{y,1} \cdot \left(\frac{L_b}{2} \right). \quad (3.5)$$

The rotation due to moment $M_{c,1}$ at column face is

$$\theta_{c,1} = \frac{M_{c,1}(L_c/2)}{3E_c I_c} \quad (3.6)$$

where L_c is the length of column, and E_c and I_c are properties of material and cross-section called, modulus of elasticity and moment of inertia respectively. Also, due to application of force $V_{y,1}$ at beam ends, the JPZ of the interior joint is subjected to a force of

$$V_{pz,1} = 2 \cdot V_{y,1} \cdot \frac{(L_b - d_c)/2}{d_b - t_{bf}} \quad (3.7)$$

which in-turn causes a distortion.

$$\gamma_{pz,1} = \frac{V_{pz,1}}{G \cdot d_c \cdot t_{pz}}. \quad (3.8)$$

Thus, the overall drift at beam end is obtained as the sum of drifts due to rotation of beams $\Delta_{b,1}$, rotation of columns $\Delta_{c,1}$ and rotation of JPZ $\Delta_{pz,1}$, which is obtained as

$$\Delta_{b,1} = \frac{V_{y,1}}{3E_b I_b} \left((L_b - d_c)/2 \right)^3 \quad (3.9)$$

$$\Delta_{c,1} = \theta_{c,1} \cdot \frac{L_b}{2} \quad (3.10)$$

$$\Delta_{pz,1} = \gamma_{pz,1} \cdot (L_b - d_c)/2 \quad (3.11)$$

Therefore, $\Delta_{total,1} = \Delta_{b,1} + \Delta_{c,1} + \Delta_{pz,1}$ and thus, the beam end drift at first yield is

$$\frac{\Delta_{total}}{L_b/2} \times 100 \quad (3.12)$$

For the second and third yield modes, the yield forces are to be obtained on the basis of capacity of next stronger member. The drift at which the next yield will occur can be calculated by considering post yield stiffness of already yielded members, in similar manner. The force deformation behaviour indicating the post yield stiffness of Joint Panel Zone and Beams, adopted for the present study, have been shown in Figures 4.2 and 4.3 respectively. This method, to obtain force deformation characteristics of a strong axis beam to column joint subassemblage can be used for both interior as well as exterior joints. An illustrative worked out example to predict the force deformation behaviour has been presented in Annexure A.

4.4 FEA Validation of proposed method

The effectiveness of proposed method, in predicting the force deformation behaviour, has been validated through Finite Element Analyses using ABAQUS Software package [ABAQUS, 2010].

The joints considered for this study are in compliance with the strong column weak beam design philosophy. A total of 50 beam to column joint subassemblages, 25 external and 25 internal are considered; selected sections with CBSR are given in *Table 4.1*.

A single step monotonic drift upto 4%, in about 125 fixed increments, is applied at the beam ends, and the reactions at the simply supported ends of the column are monitored. Force deformation behaviour of the joints are obtained and compared with those predicted by the proposed method.

The von Mises and Shear Stress contours for beam to column joints subassemblages are shown in Figures 4.3 and 4.4 for exterior and interior joints, respectively. The von-Mises stresses are shown at 4%, while shear stresses are shown at initiation of yield.

Figures 4.5 and 4.6 show a comparison of proposed method and FEA in terms of force deformation relationships for exterior and interior joints, respectively. The

figures depicts a close correspondence between the response of beam to column joints obtained using the *proposed method* and FEA. The *proposed method* is able to predict the force deformation behaviour of both interior and exterior joints fairly accurately with relatively lesser computational efforts.

4.5 Conclusions

1. The proposed mechanics based hand calculation method provides a tri-linear force deformation behavior of beam to column joint subassemblages.
2. The method is able to predict the sequence of three modes of yielding, namely, Beam Flange Yielding, Panel Zone Yielding and Formation of Plastic Hinges in beams; and the corresponding drifts.
3. The comparison of results obtained from the method with FEA shows that the method is able to predict the force deformation behaviour with reasonable accuracy.
4. The results of finite element analyses are in agreement with the predicted force deformation behavior of beam column joint subassemblages, for both interior and exterior joints.
5. The proposed method is computationally elegant and efficient and able to predict yield drift for three components of beam column subassemblage without resorting to detailed FEA. The method can be used for design of strong and unyielding joint panel zone.
6. The results of FEA analyses indicate that, minimum value of CBSR to prevent inelastic actions in JPZ is as high as eight, for both exterior and interior joints. This substantiates the major finding of chapter three, which shows that a CBSR of even 4.0 is not sufficient to prevent inelastic actions in JPZ region.

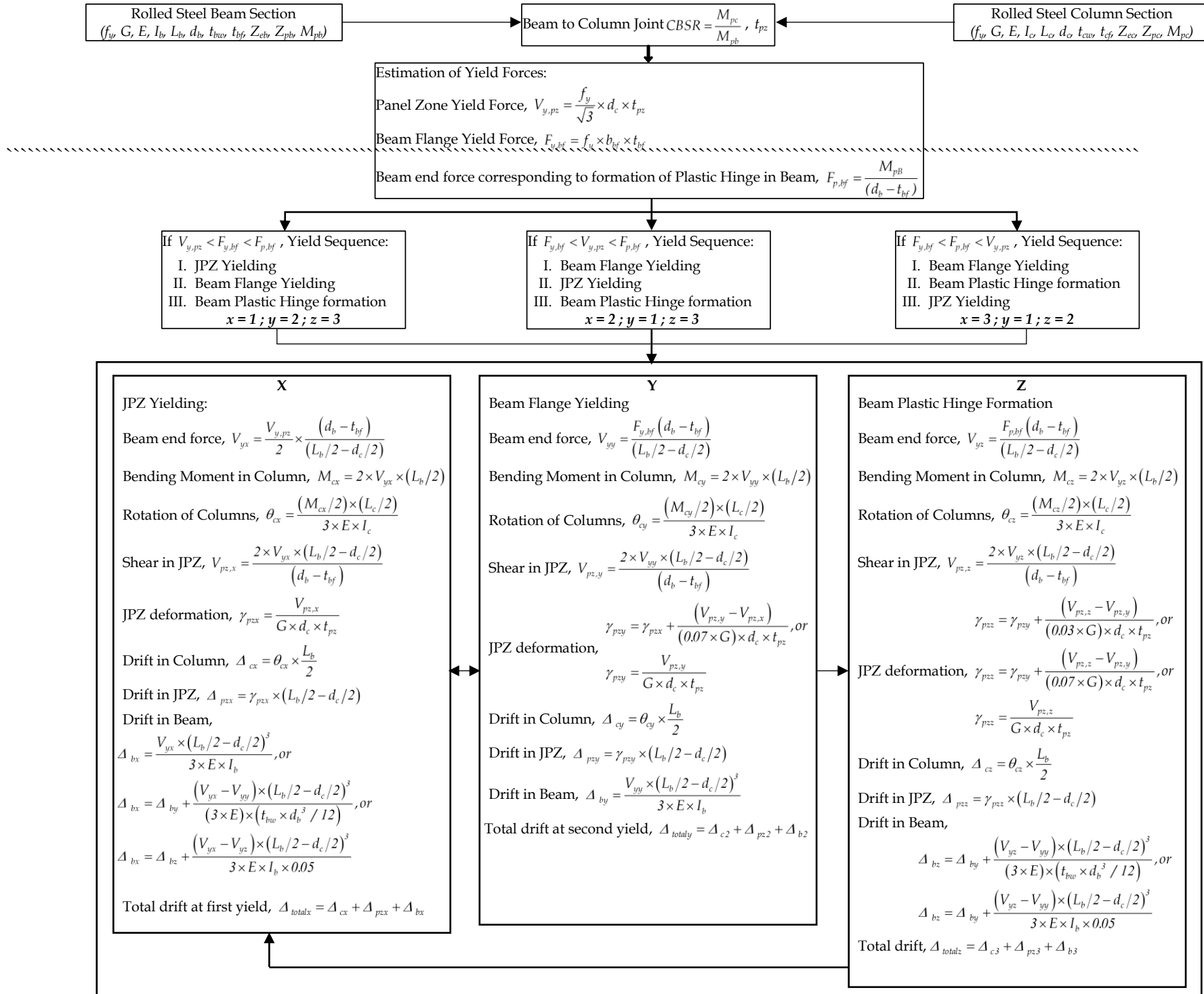
Table 4.1: List of Column and Beam sections used to model the subassemblages. 25 Interior Beam to Column Joint Subassemblages and 25 Exterior Beam to Column Joint Subassemblages are modelled to demonstrate the effectiveness of proposed hand calculation method.

S.No.	Column	M_{PC} (kNm)	Beam	M_{PB} (kNm)	t_{PZ} (mm)	CBSR	
						Interior	Exterior
1.	W18×130	1,176	W27×84	986	17	1.19	2.38
2.	W21×83	787	W24×62	619	13	1.27	2.54
3.	W16×100	808	W24×62	619	15	1.31	2.62
4.	W18×130	1,176	W21×83	787	17	1.49	2.98
5.	W18×119	1,079	W21×68	636	17	1.70	3.40
6.	W14×176	1,296	W21×73	708	21	1.83	3.66
7.	W18×192	1,800	W21×93	909	24	1.98	3.96
8.	W24×176	2,078	W18×97	858	19	2.42	4.84
9.	W27×178	2,285	W21×93	909	18	2.51	5.02
10.	W24×229	2,747	W21×93	909	24	3.02	6.04
11.	W24×176	2,078	W18×71	606	19	3.43	6.86
12.	W27×235	3,148	W16×100	808	23	3.89	7.78
13.	W40×503	9,394	W18×234	2,276	39	4.13	8.26
14.	W33×318	5,157	W24×103	1,141	26	4.52	9.04
15.	W36×487	8,626	W21×166	1,779	38	4.85	9.70
16.	W27×539	7,746	W27×129	1,587	50	4.88	9.76
17.	W40×431	7,931	W18×158	1,467	34	5.41	10.82
18.	W36×529	9,484	W30×124	1,675	41	5.66	11.32
19.	W40×593	11,201	W24×162	1,914	45	5.85	11.70
20.	W36×652	11,928	W33×130	1,911	50	6.24	12.48
21.	W36×487	8,626	W27×102	1,229	38	7.02	14.04
22.	W27×539	7,746	W21×101	1,024	50	7.57	15.14
23.	W40×503	9,394	W30×90	1,114	39	8.43	16.86
24.	W36×529	9,484	W27×84	986	41	9.62	19.24
25.	W40×593	11,201	W24×94	1,019	45	10.99	21.98

Table 4.2: Yield Drifts as obtained through **Proposed Method** and **FEA** for both Interior and Exterior Joints

S. N.	Interior							Exterior						
	CBSR	Drift at Yield (mm)						CBSR	Drift at Yield (mm)					
		Panel Zone		Beam Flange		Beam Plastic Hinge			Panel Zone		Beam Flange		Beam Plastic Hinge	
FEA	Proposed	FEA	Proposed	FEA	Proposed	FEA	Proposed	FEA	Proposed	FEA	Proposed	FEA	Proposed	
1.	1.19	19.308	13.40	31.807	68.588	-	220.839	2.38	20.38	21.405	14.38	14.993	46.82	47.121
2.	1.27	21.027	15.014	35.77	40.523	-	186.752	2.54	26.38	29.585	13.18	13.726	32.38	33.290
3.	1.31	20.346	15.209	40.74	51.115	-	212.733	2.62	25.15	27.655	11.95	14.925	38.35	41.966
4.	1.49	20.123	13.544	40.913	81.749	-	212.461	2.98	26.35	21.470	16.75	17.471	49.15	51.726
5.	1.70	20.420	15.01	36.658	56.342	-	173.077	3.40	28.75	17.63	14.35	16.224	33.55	36.492
6.	1.83	16.746	14.602	76.74	73.391	-	201.558	3.66	26.35	26.219	14.35	17.643	46.11	47.331
7.	1.98	21.274	14.848	33.437	49.802	-	153.566	3.96	40.75	41.479	14.35	15.501	28.75	31.754
8.	2.42	19.296	13.229	29.158	73.071	-	160.254	4.84	25.18	27.230	15.58	17.491	46.78	40.093
9.	2.51	17.083	13.123	35.721	43.958	-	141.366	5.02	26.01	28.639	12.81	13.734	46.41	43.462
10.	3.02	21.845	15.123	28.322	24.935	-	107.566	6.04	47.83	109.525	11.83	13.120	26.23	27.987
11.	3.43	22.579	16.172	31.95	29.167	-	111.925	6.86	32.35	121.367	13.15	14.904	40.75	32.002
12.	3.89	21.55	15.356	31.146	44.091	-	109.347	7.78	41.95	100.710	14.35	16.769	32.35	33.334
13.	4.13	21.546	12.568	27.171	36.561	-	85.713	8.26	88.78	85.187	12.17	13.110	45.58	22.796
14.	4.52	25.214	12.632	20.946	19.205	-	34.011	9.04	-	175.760	10.71	10.061	28.52	22.000
15.	4.85	66.577	14.228	22.177	14.755	92.977	60.933	9.70	-	159.781	11.78	11.4469	23.78	22.576
16.	4.88	25.425	10.889	26.625	22.321	106.8	71.783	9.76	-	301.624	8.93	8.877	24.64	19.640
17.	5.41	25.183	14.998	26.383	17.346	-	63.154	10.82	-	173.094	11.98	12.654	31.22	24.321
18.	5.66	76.673	71.374	22.576	8.783	88.613	19.021	11.32	-	277.739	5.88	7.154	21.87	16.729
19.	5.85	51.216	43.805	20.016	11.294	84.816	21.923	11.70	-	184.885	8.33	9.074	25.13	20.028
20.	6.24	-	105.451	22.629	7.468	93.429	16.860	12.48	-	331.978	5.49	6.148	22.33	14.943
21.	7.02	92.608	106.408	19.408	9.170	83.008	20.295	14.04	-	363.766	6.13	7.720	25.01	18.292
22.	7.57	-	149.202	23.025	12.464	77.025	26.499	15.14	-	499.096	9.67	10.810	28.87	24.428
23.	8.43	-	174.533	17.21	7.081	73.005	17.477	16.86	-	485.592	7.15	6.099	31.05	15.972
24.	9.62	-	200.173	18.387	8.021	82.455	19.37	19.24	-	554.194	5.95	7.016	37.41	17.898
25.	10.99	-	222.082	18.420	8.881	88.620	20.117	21.98	-	495.030	8.16	8.128	34.62	19.173

Flowchart depicting the steps involved in Proposed Method for Interior Joints



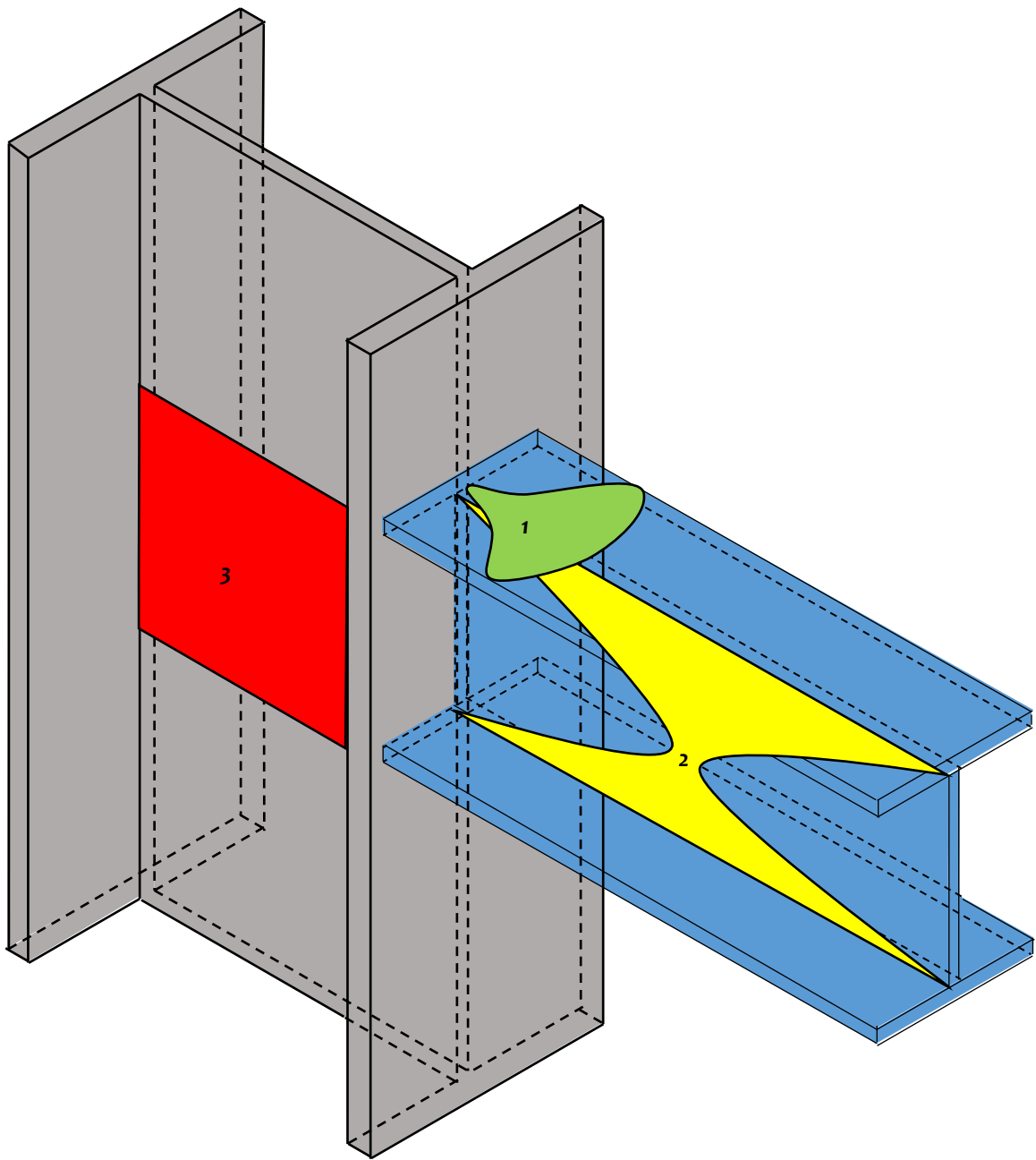


Figure 4.1: A schematic of an exterior beam to column joint depicting the three probable yield locations. The preferred order of inelastic yielding, as per capacity design, is (1) Beam Flange Yielding, (2) Beam Plastic Hinges and (3) Panel Zone Shear Yielding.

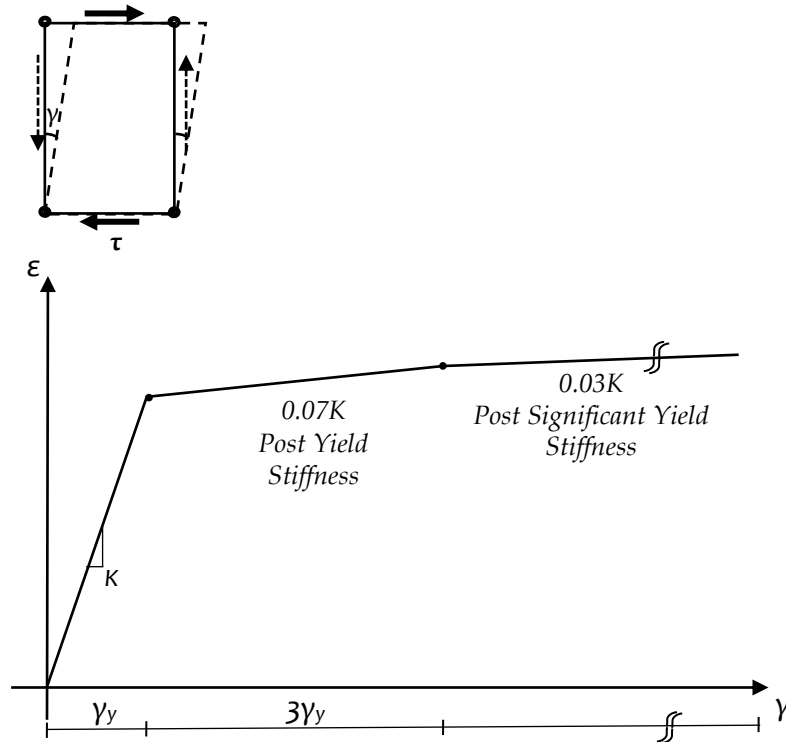


Figure 4.2: Adopted Force Deformation Behaviour of Joint Panel Zone Region.

Literature suggests that the post yield stiffness is approximately 7% of initial stiffness upto a rotation of $4\gamma_y$, and is 3% beyond the rotation of $4\gamma_y$.

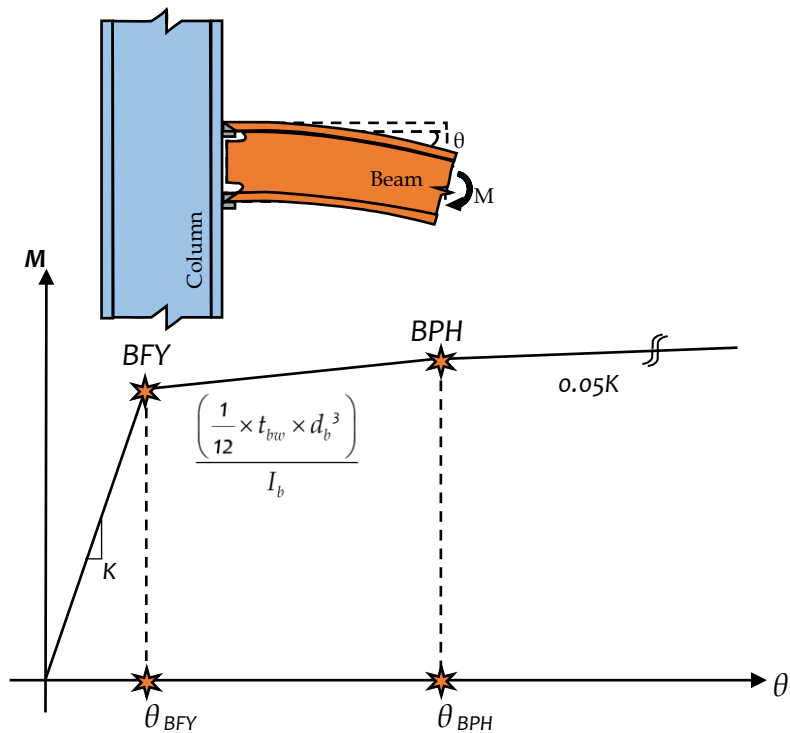
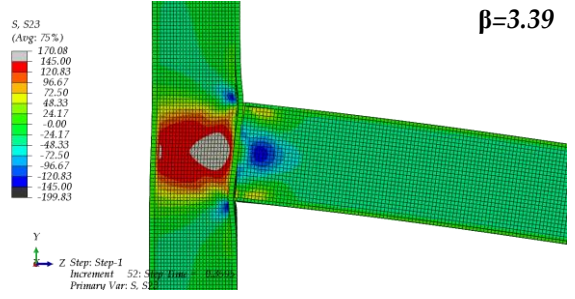
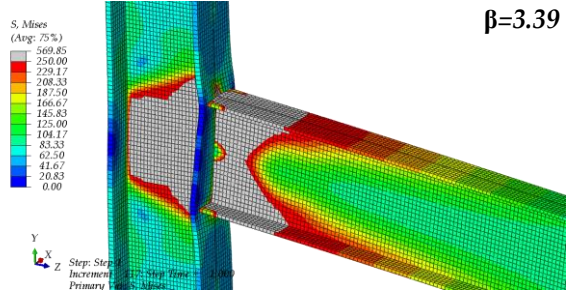
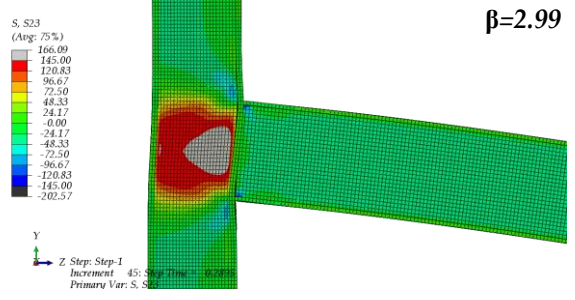
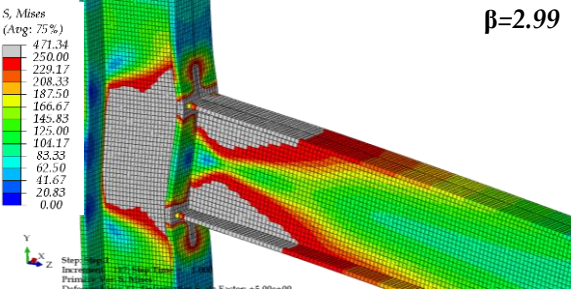
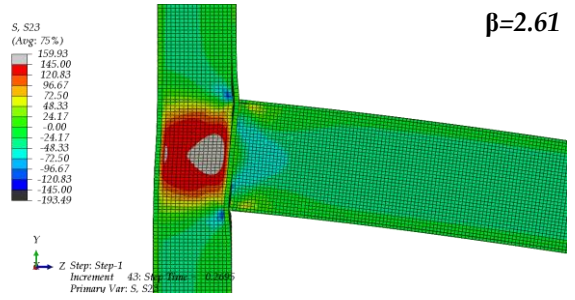
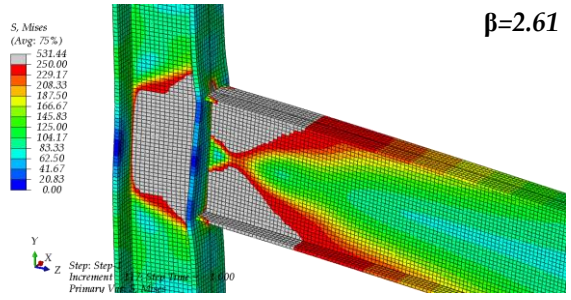
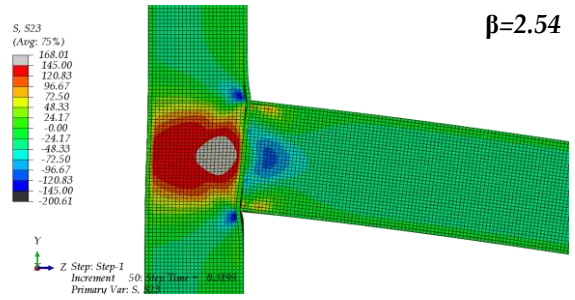
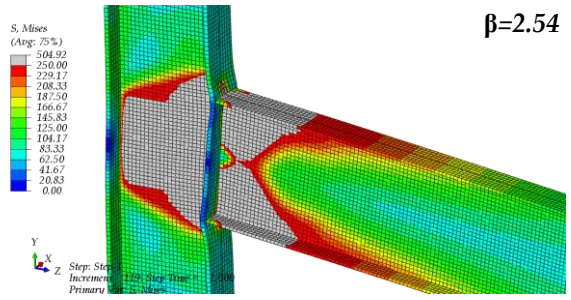
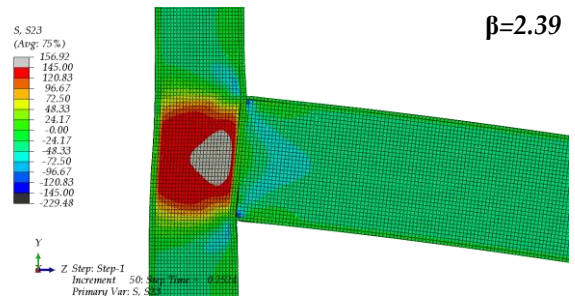
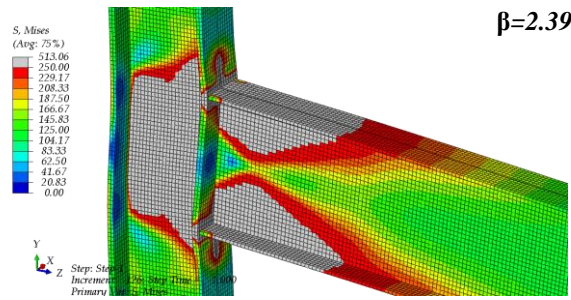


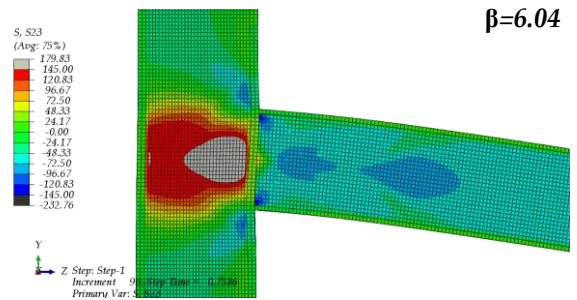
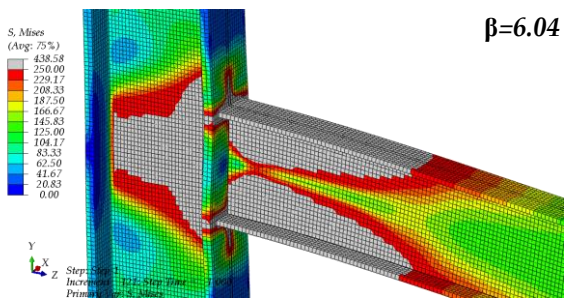
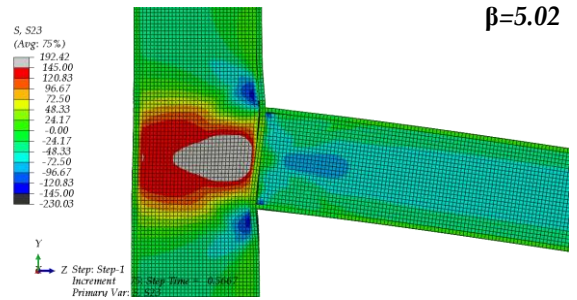
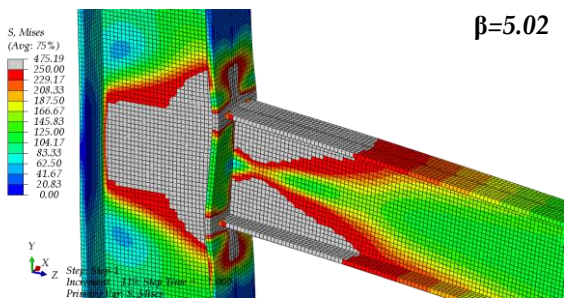
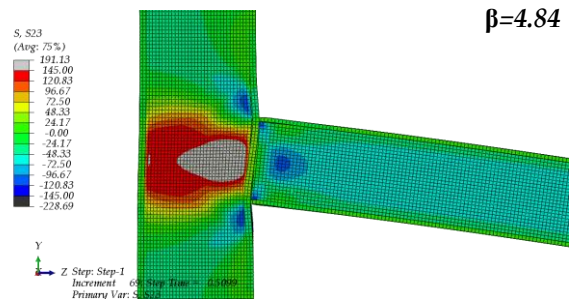
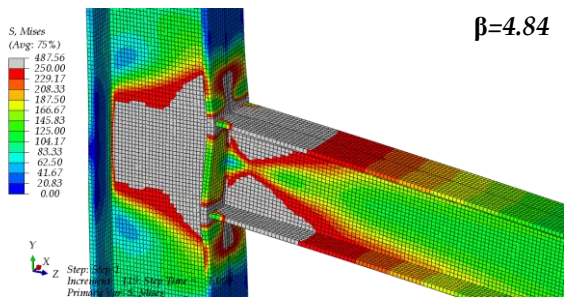
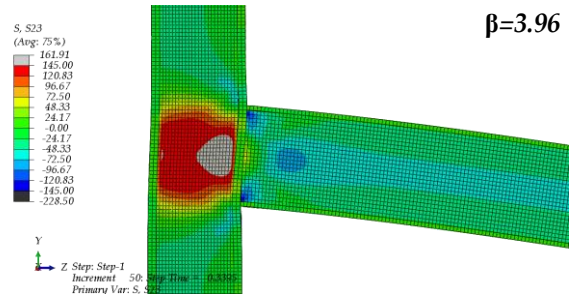
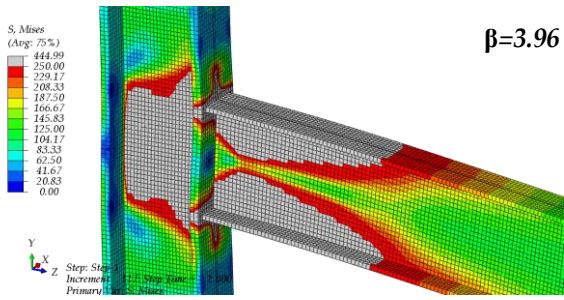
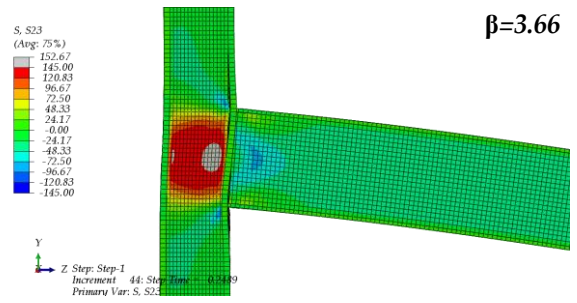
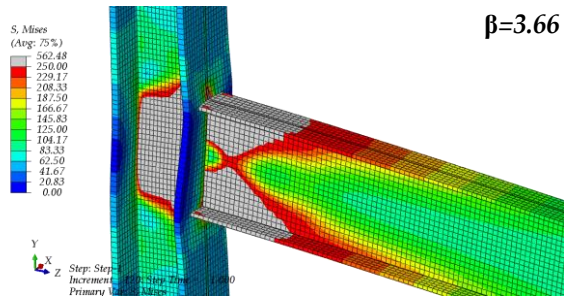
Figure 4.3: Adopted Force Deformation Behaviour of Beams.

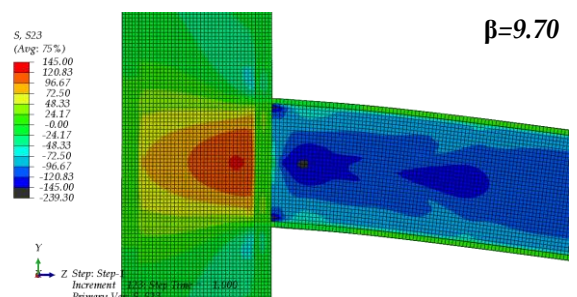
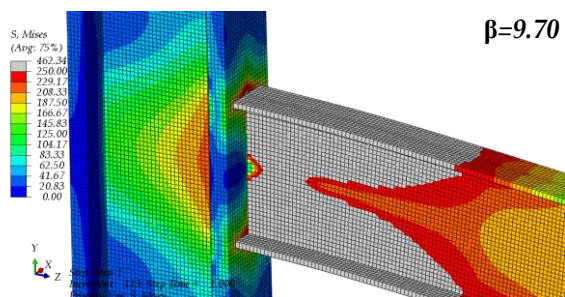
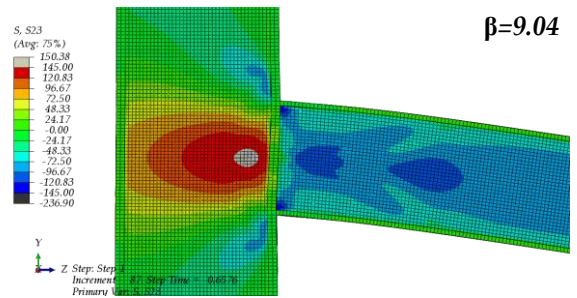
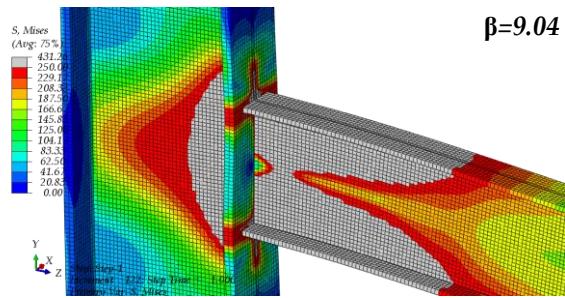
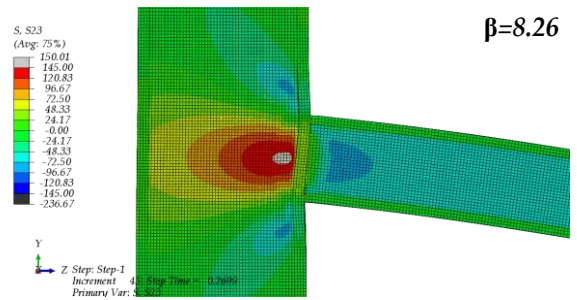
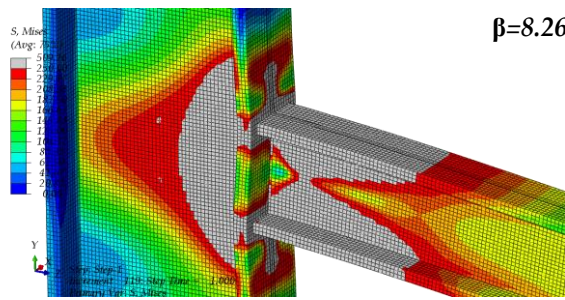
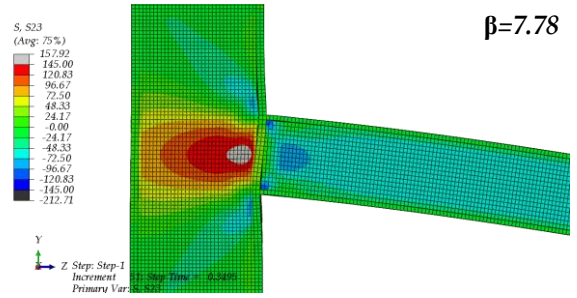
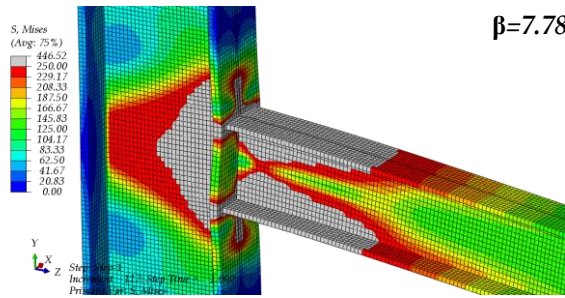
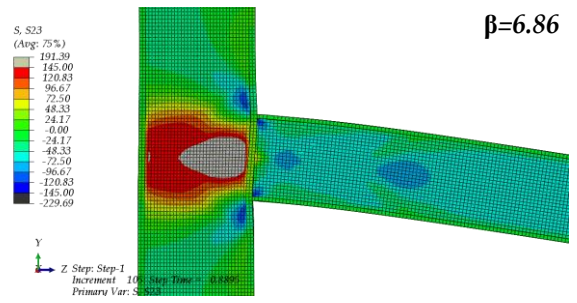
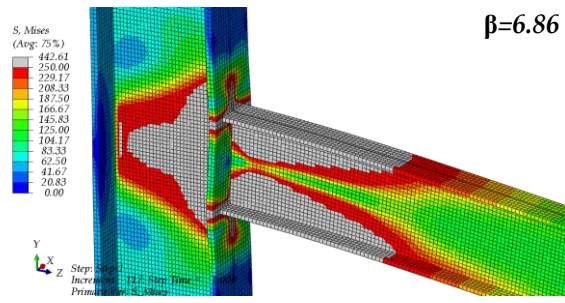
The stiffness of beam post Beam Flange Yielding (BFY) is estimated by multiplying the initial beam stiffness by a factor, given in Equation 4.14. The stiffness after formation of Beam Plastic Hinges (BPH) is assumed to be 5% of the initial elastic stiffness.

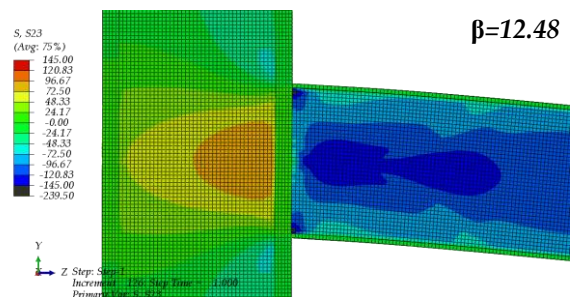
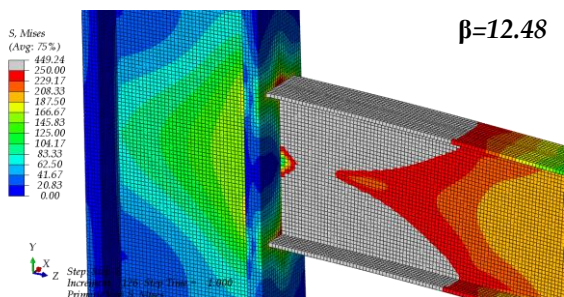
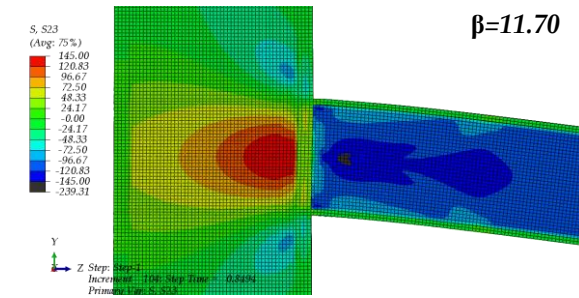
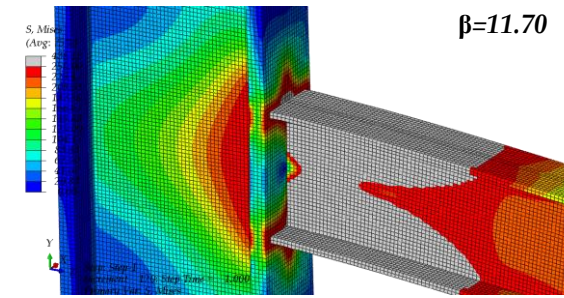
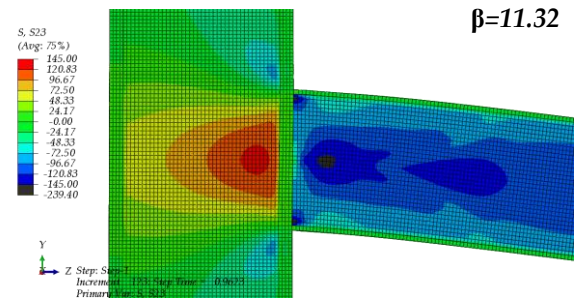
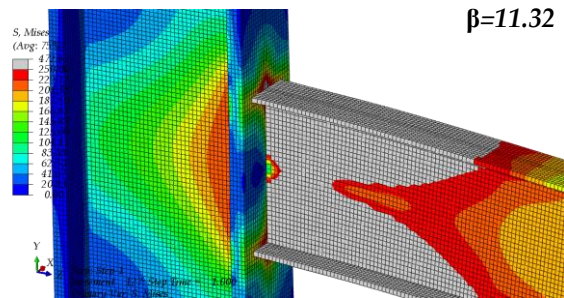
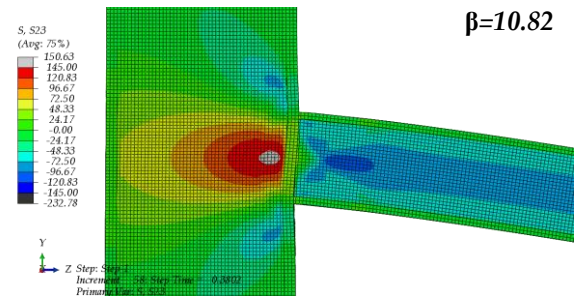
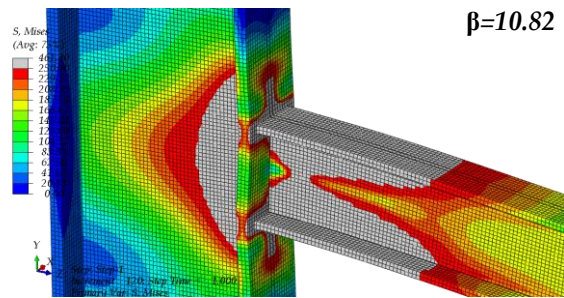
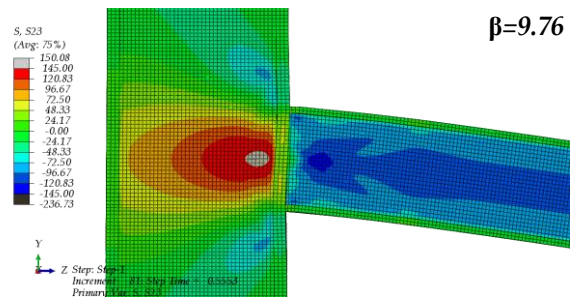
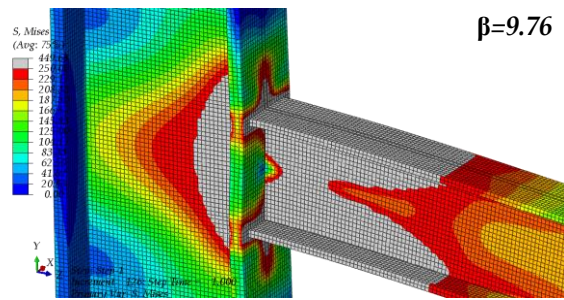
Chapter 4: Mechanics based Monotonic Load Deformation Curves of Beam to Column Joints



Chapter 4: Mechanics based Monotonic Load Deformation Curves of Beam to Column Joints







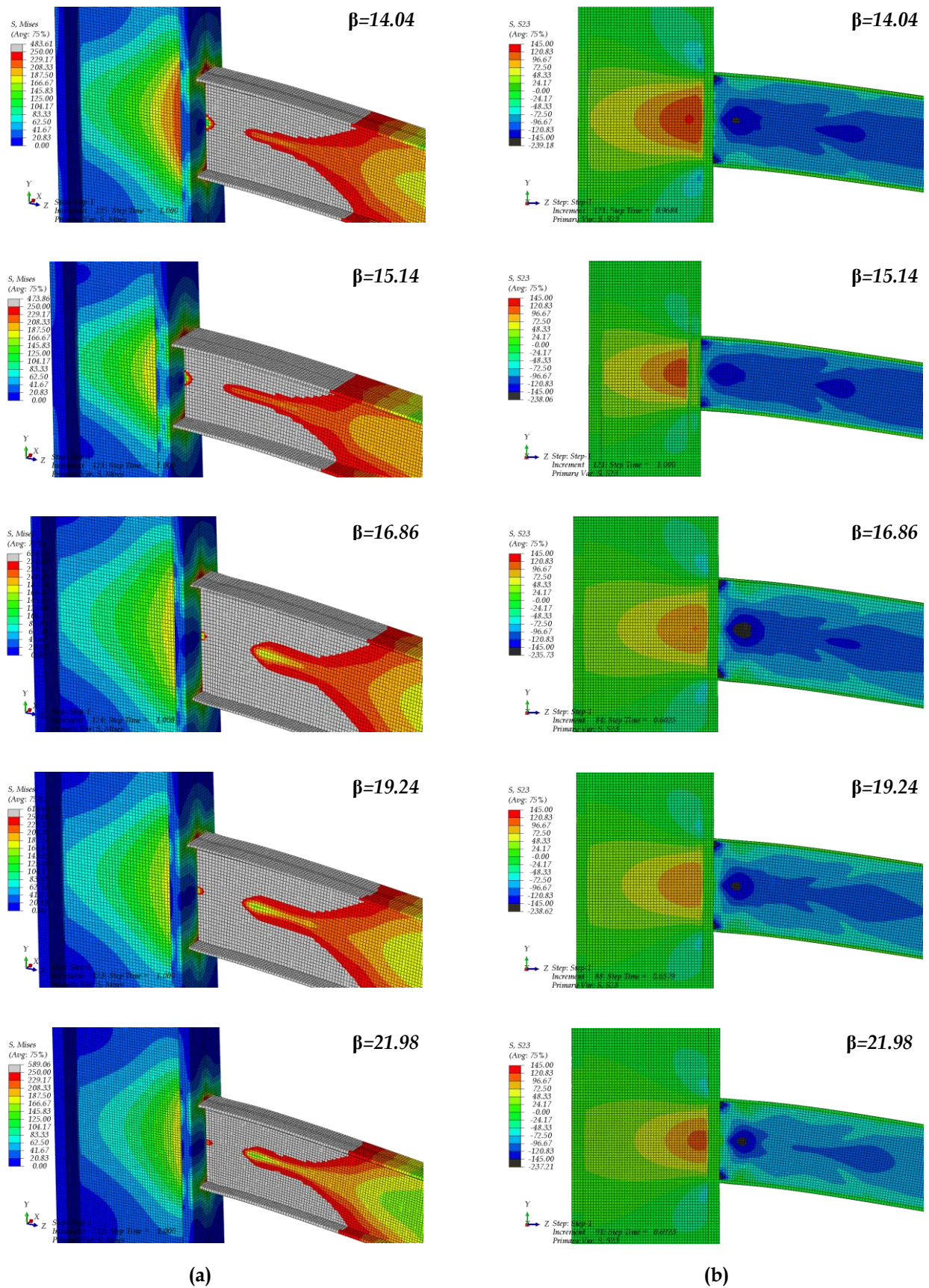
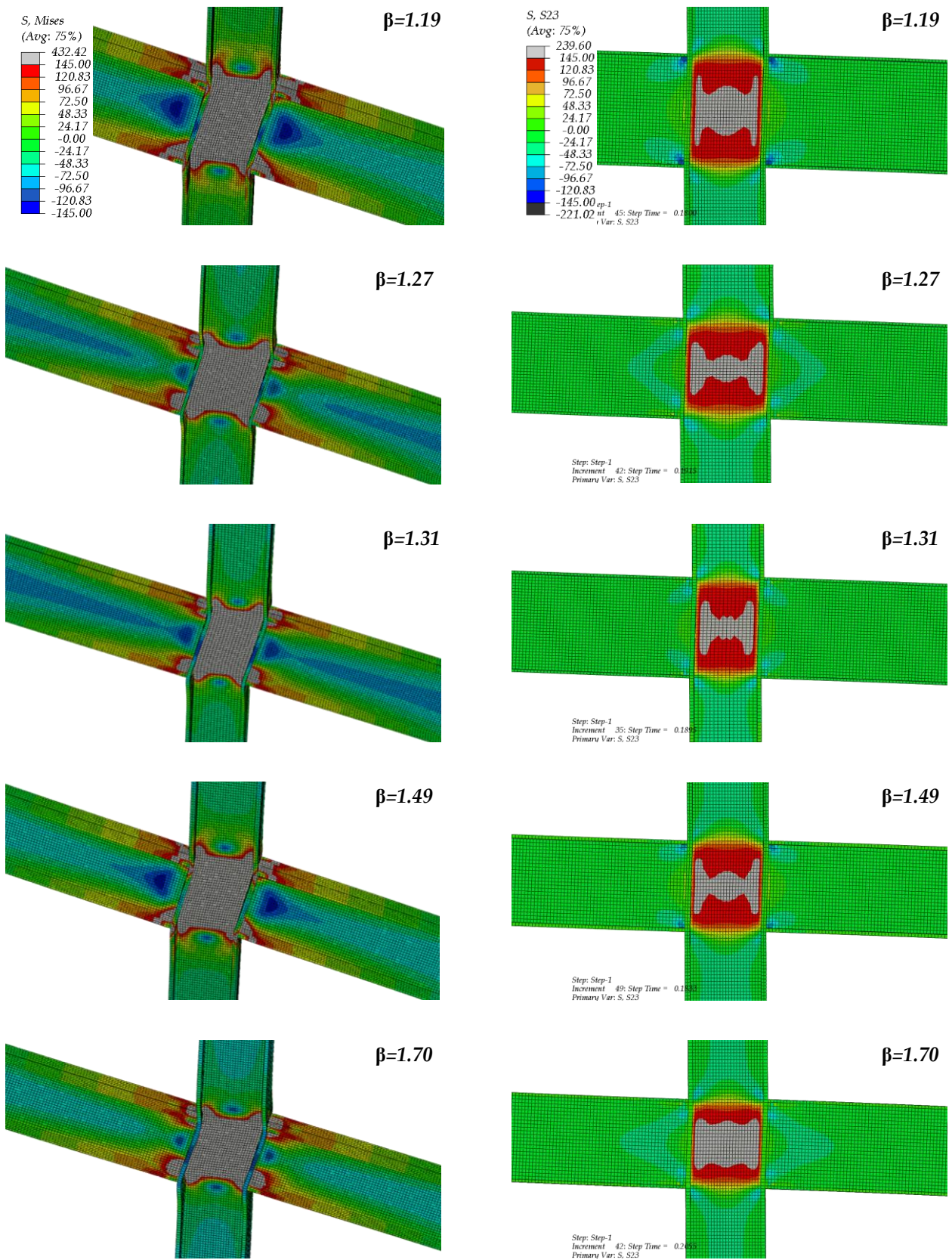
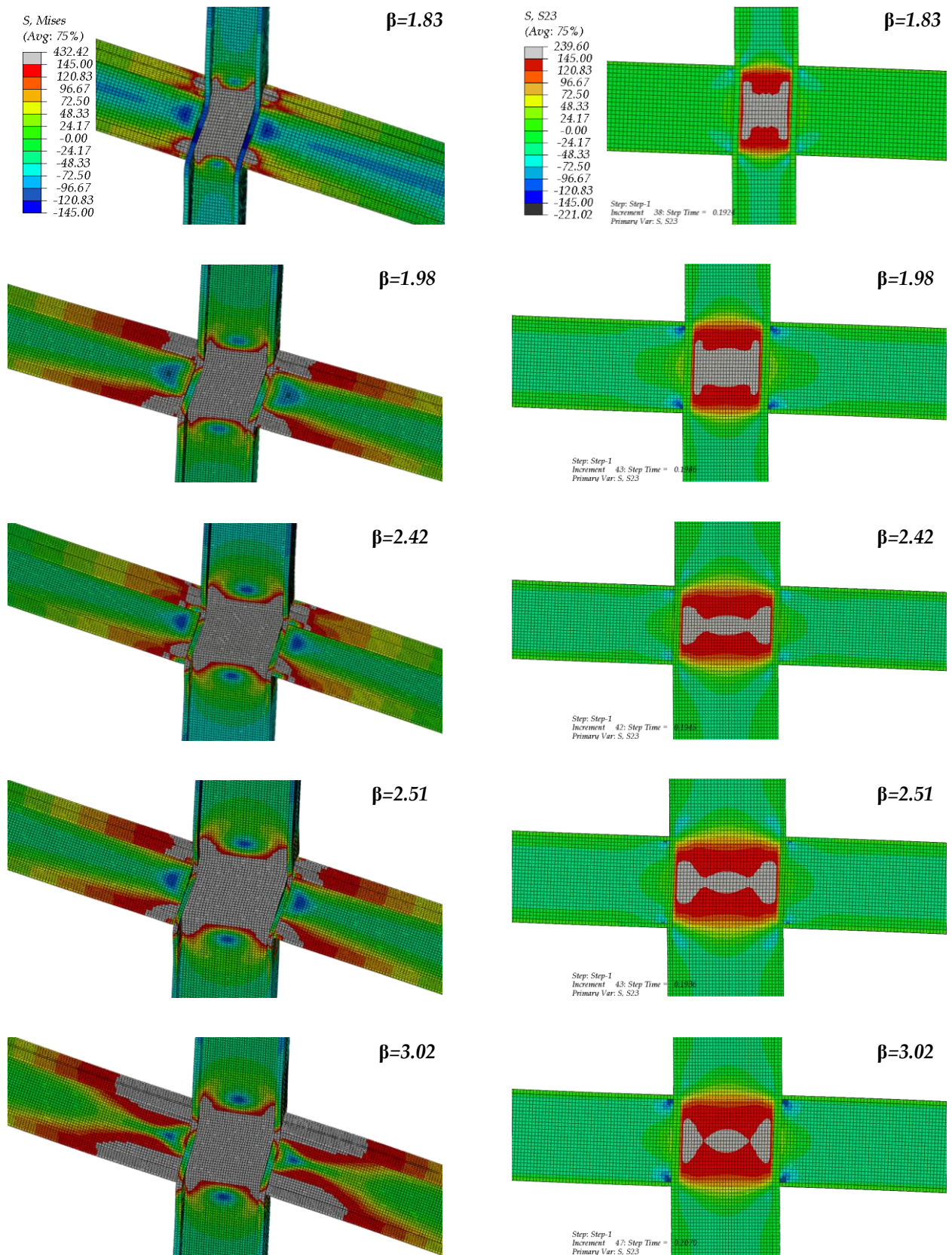
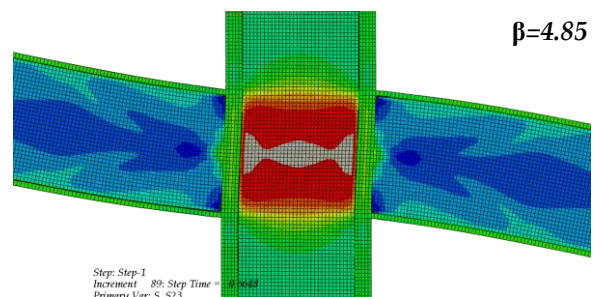
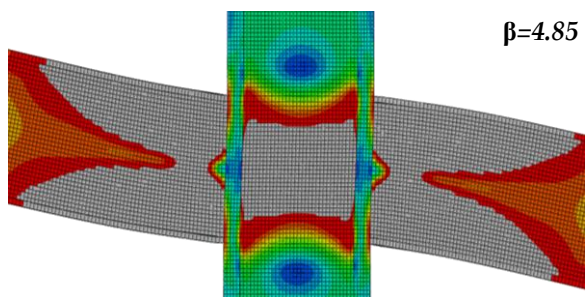
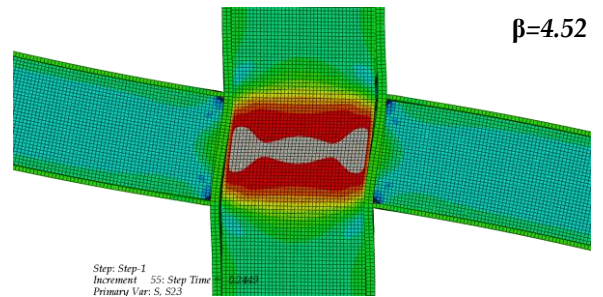
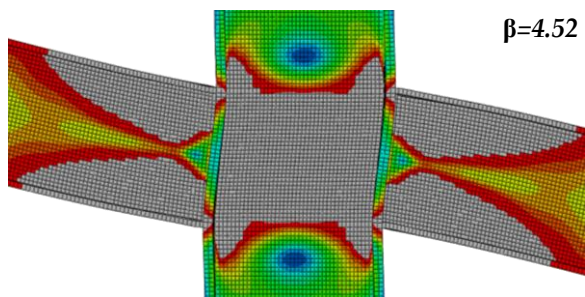
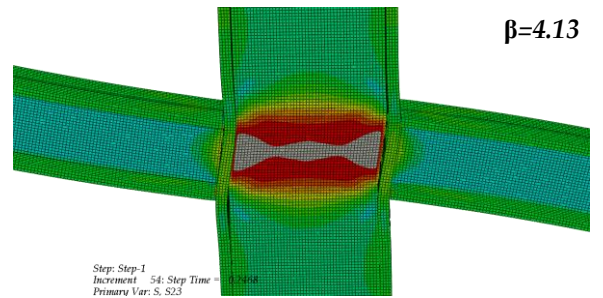
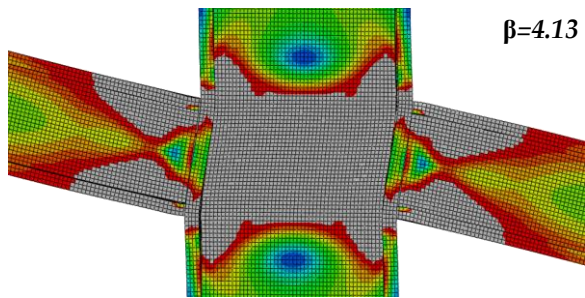
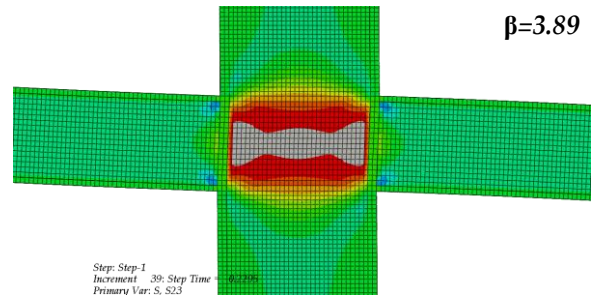
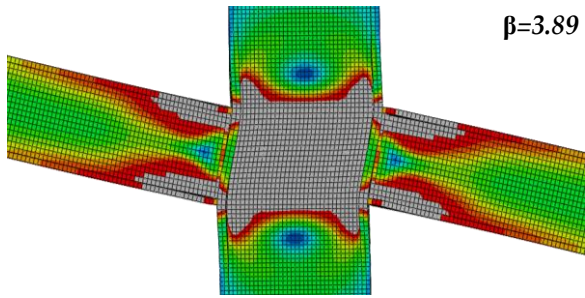
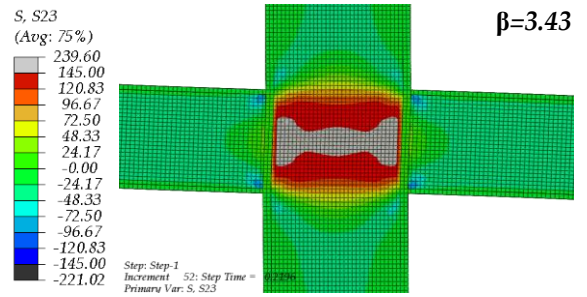
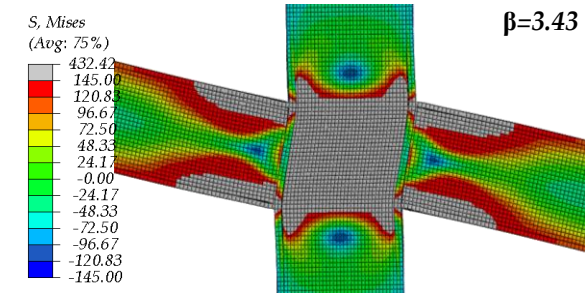
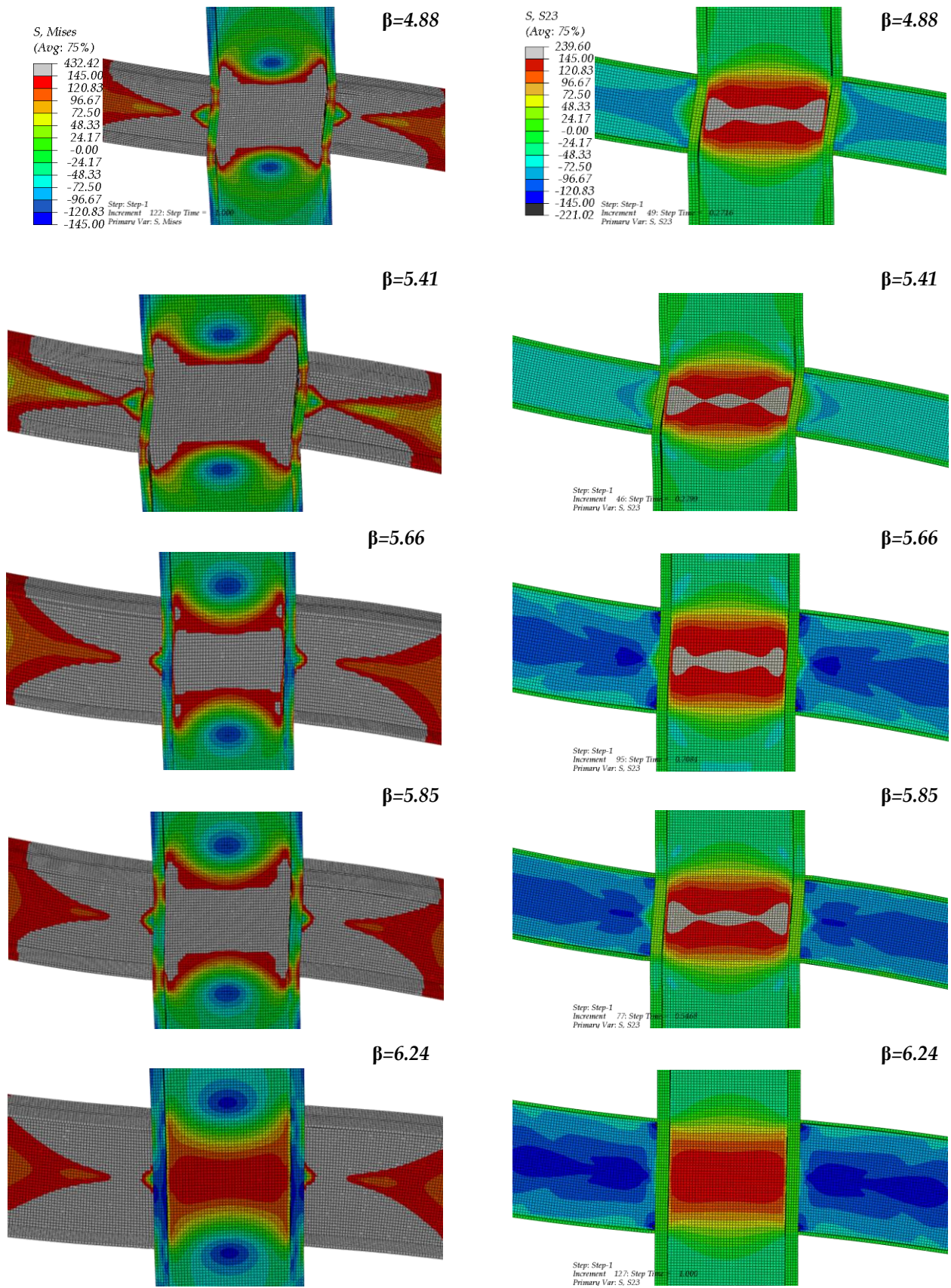


Figure 4.4: (a) von Mises stress contour at 4 % drift (b) Shear stress contours at initiation of yield for exterior joints. Joints with CBR less than eight, undergoes significant yielding of JPZ









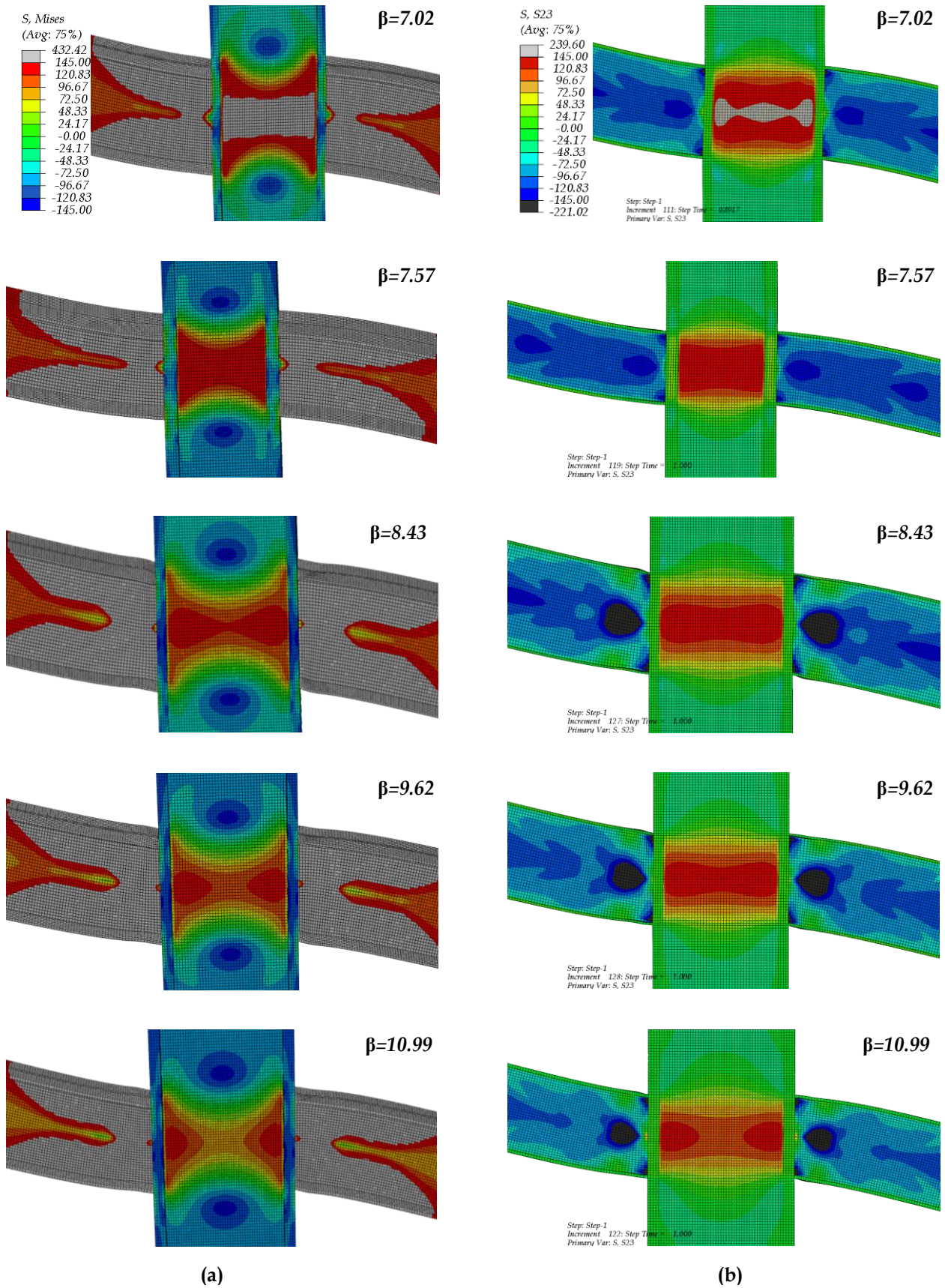
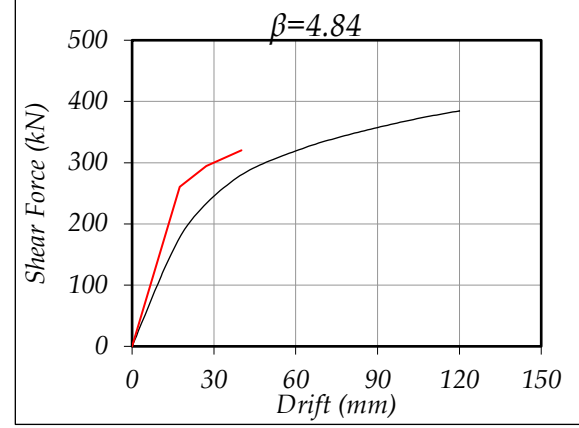
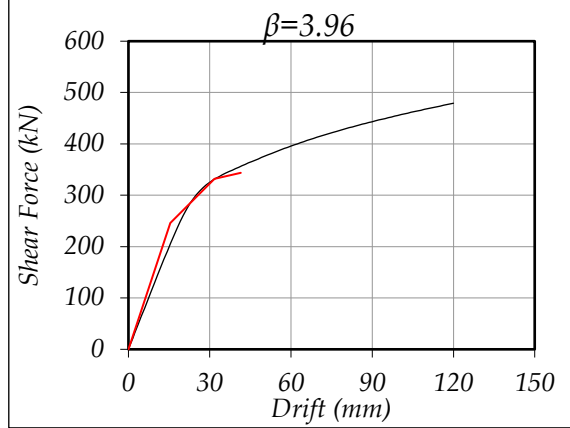
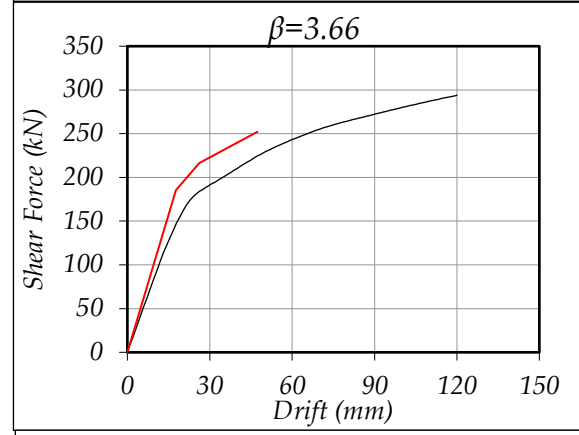
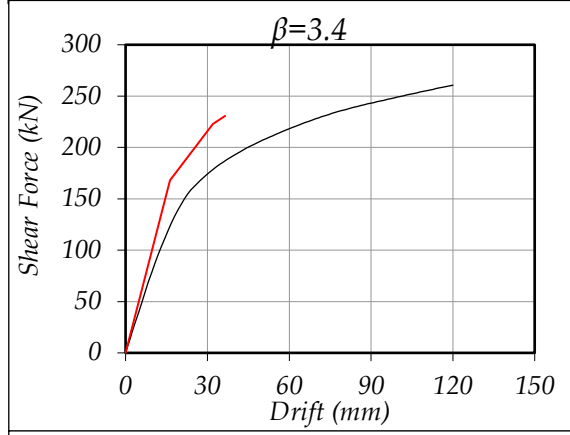
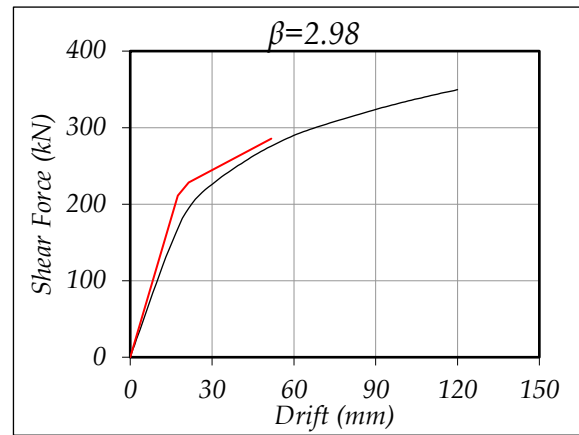
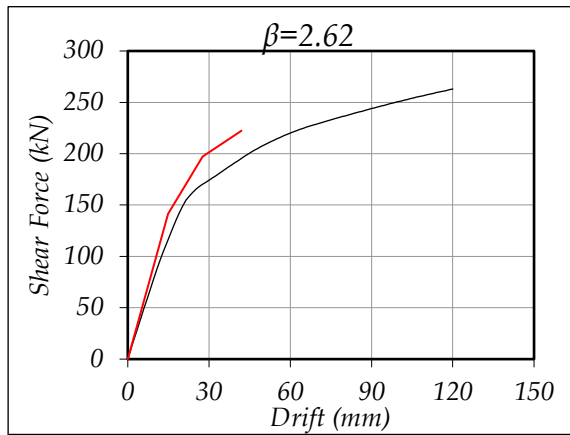
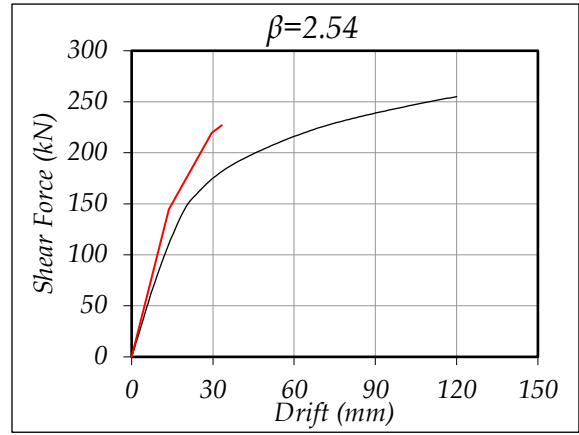
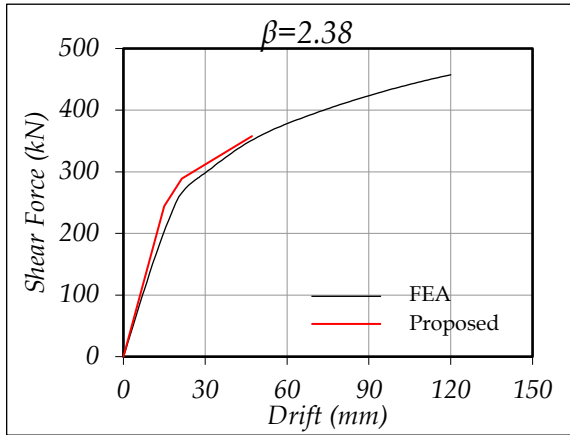
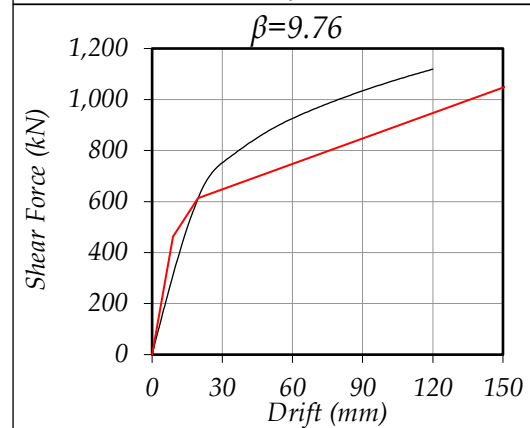
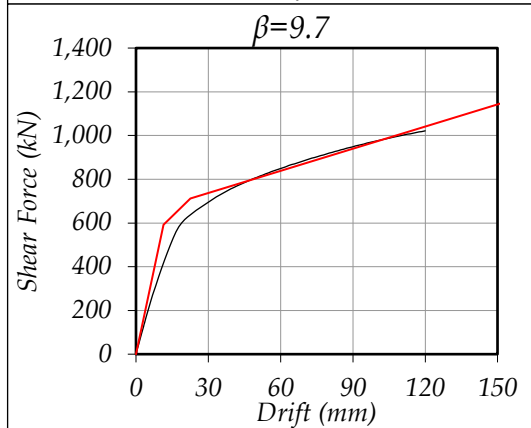
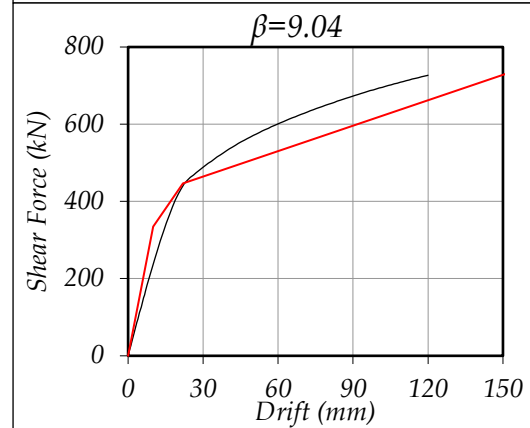
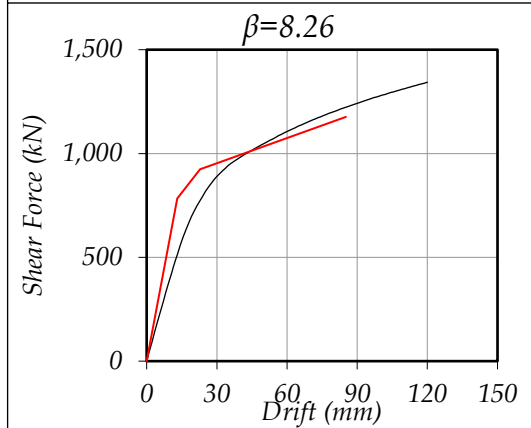
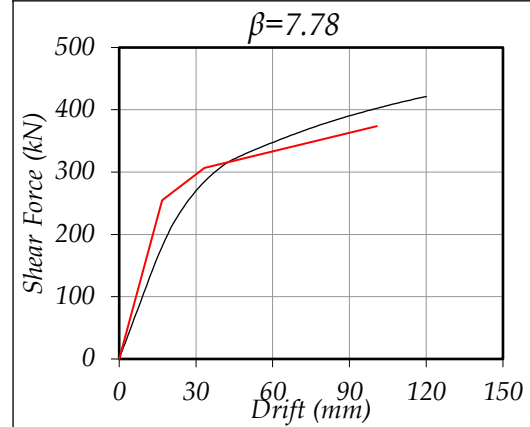
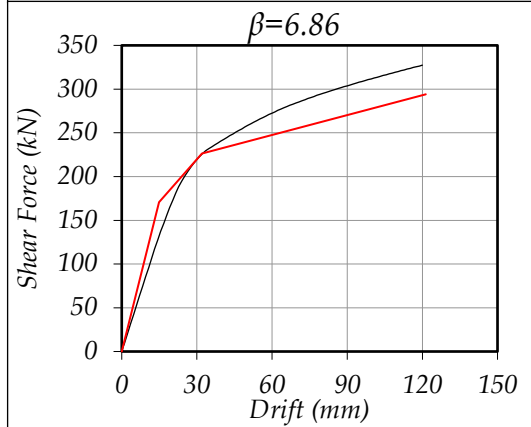
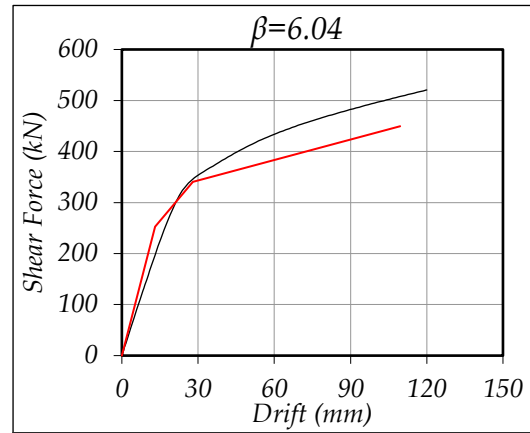
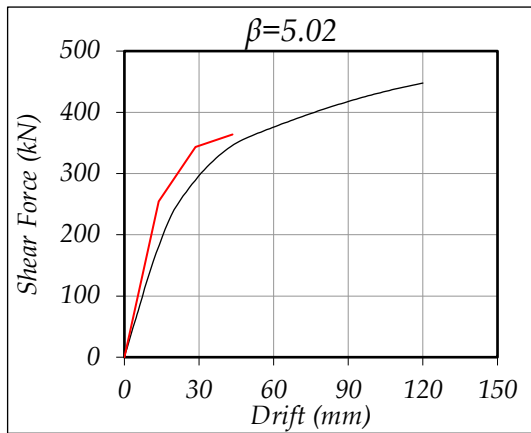
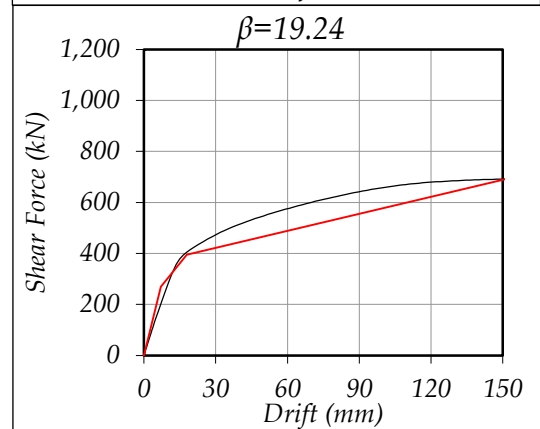
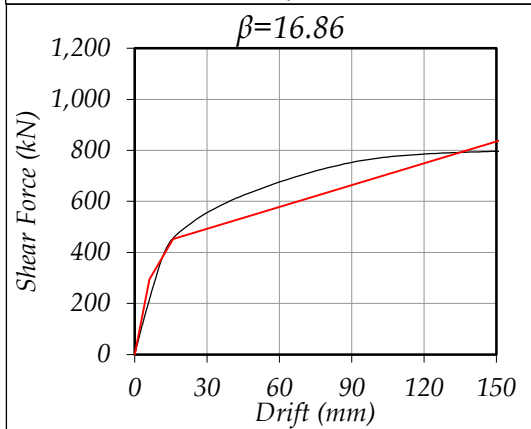
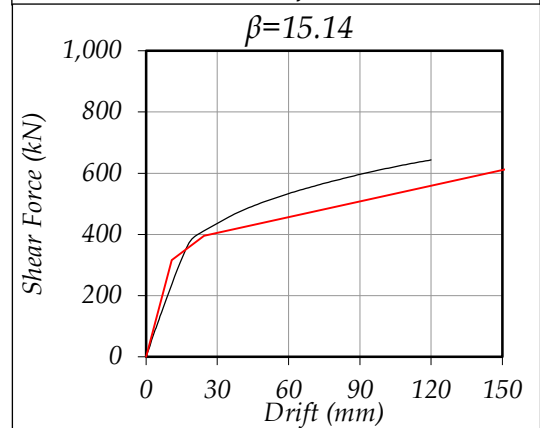
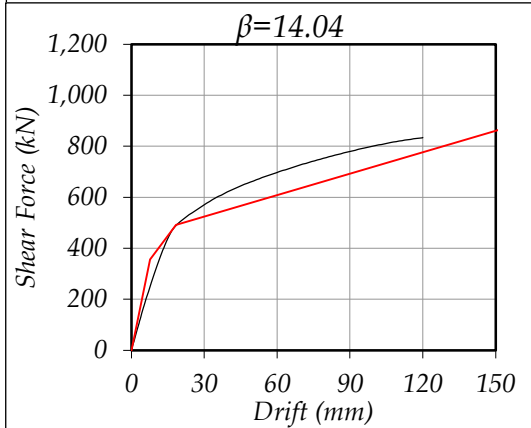
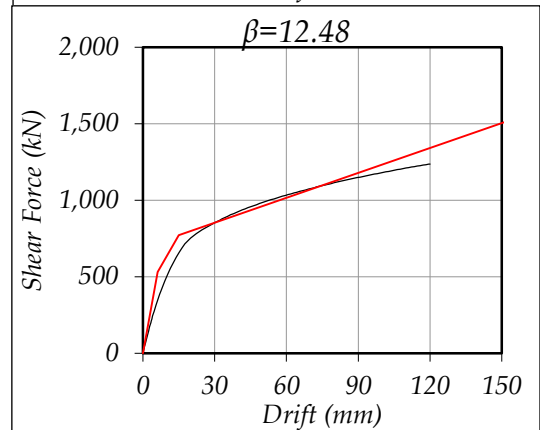
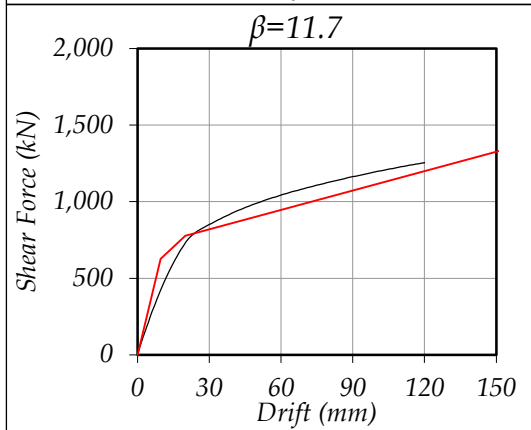
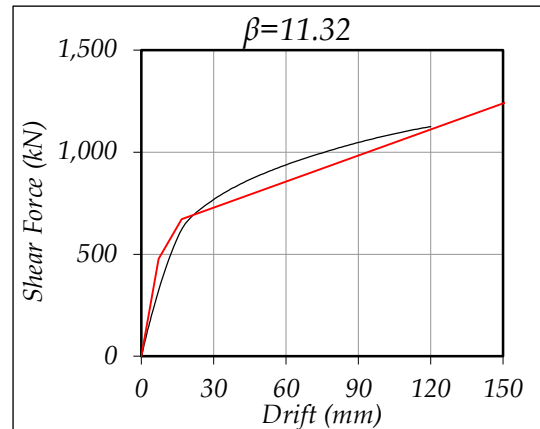
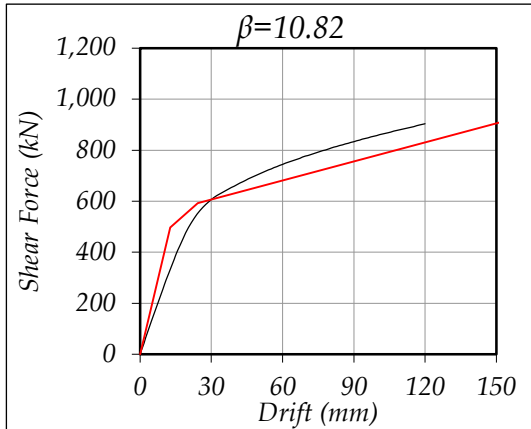


Figure 4.5: (a) von Mises stress contour at 4 % drift (b) Shear stress contours at initiation of yield for interior joints. Joints with CBSR greater than eight sustains no yielding of JPZ region.







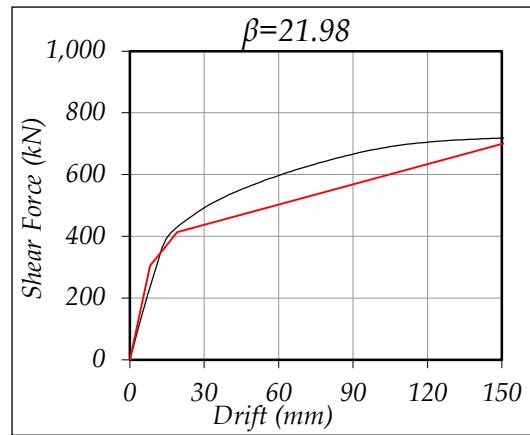
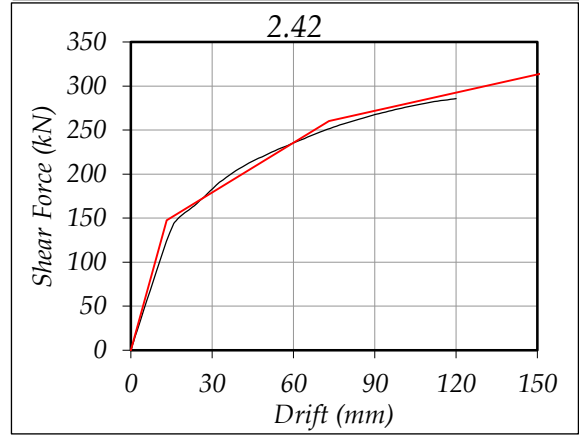
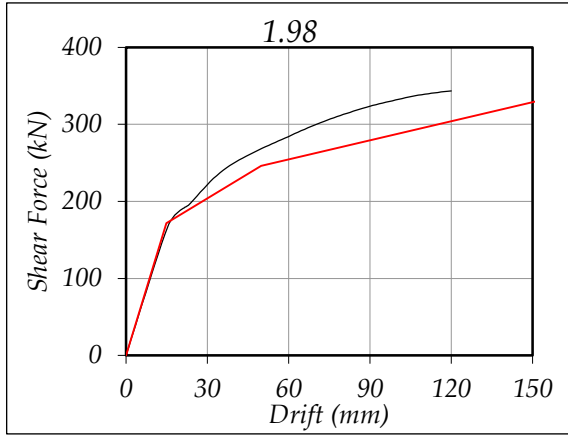
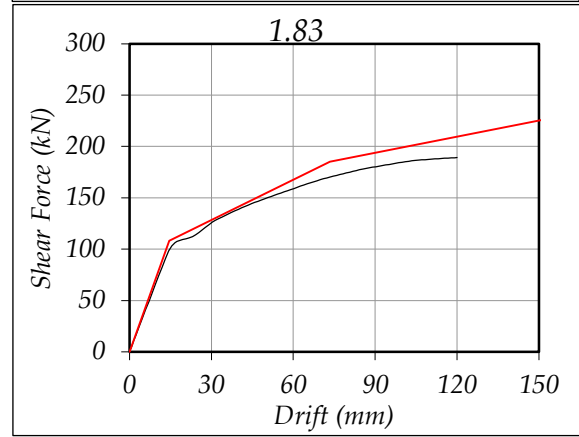
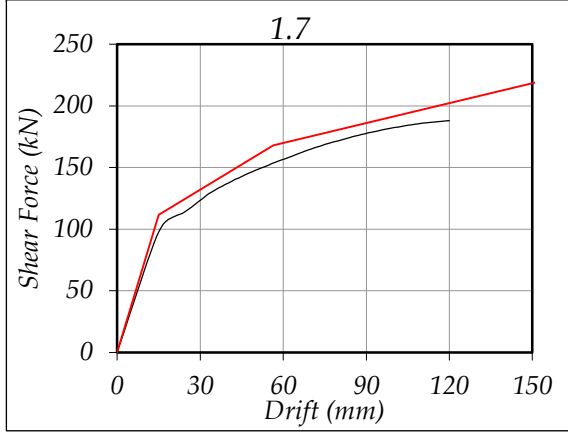
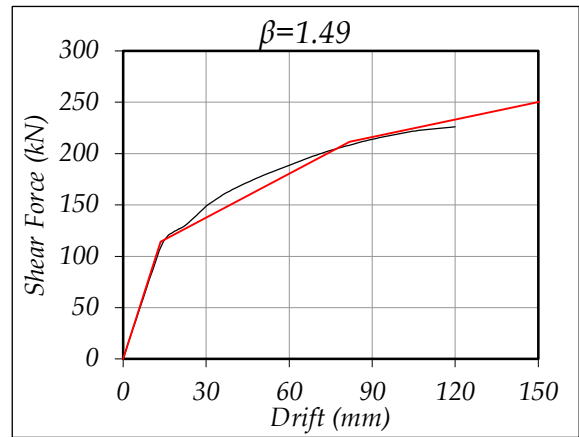
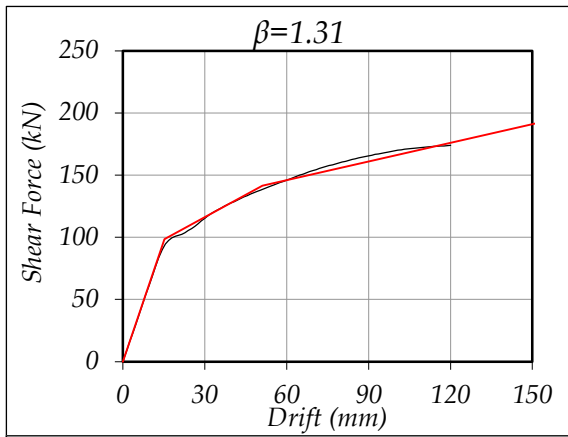
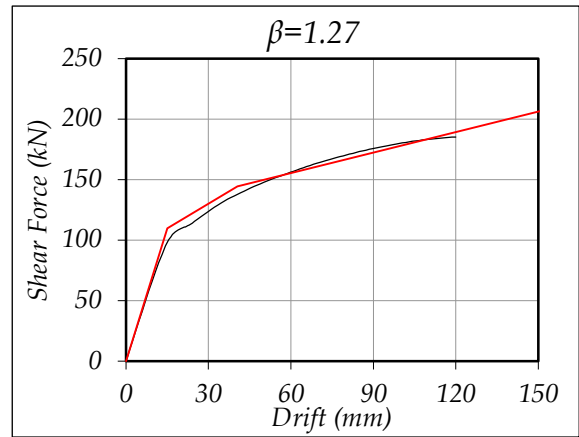
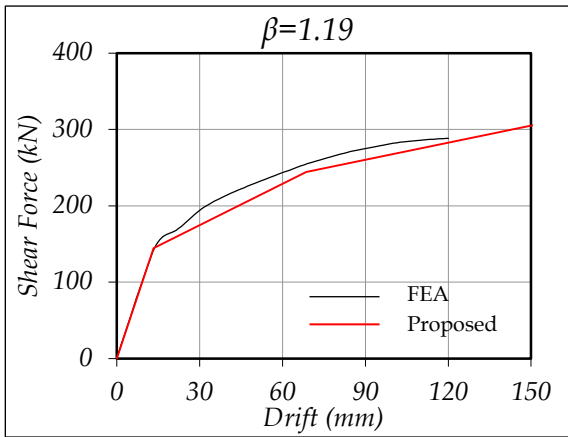
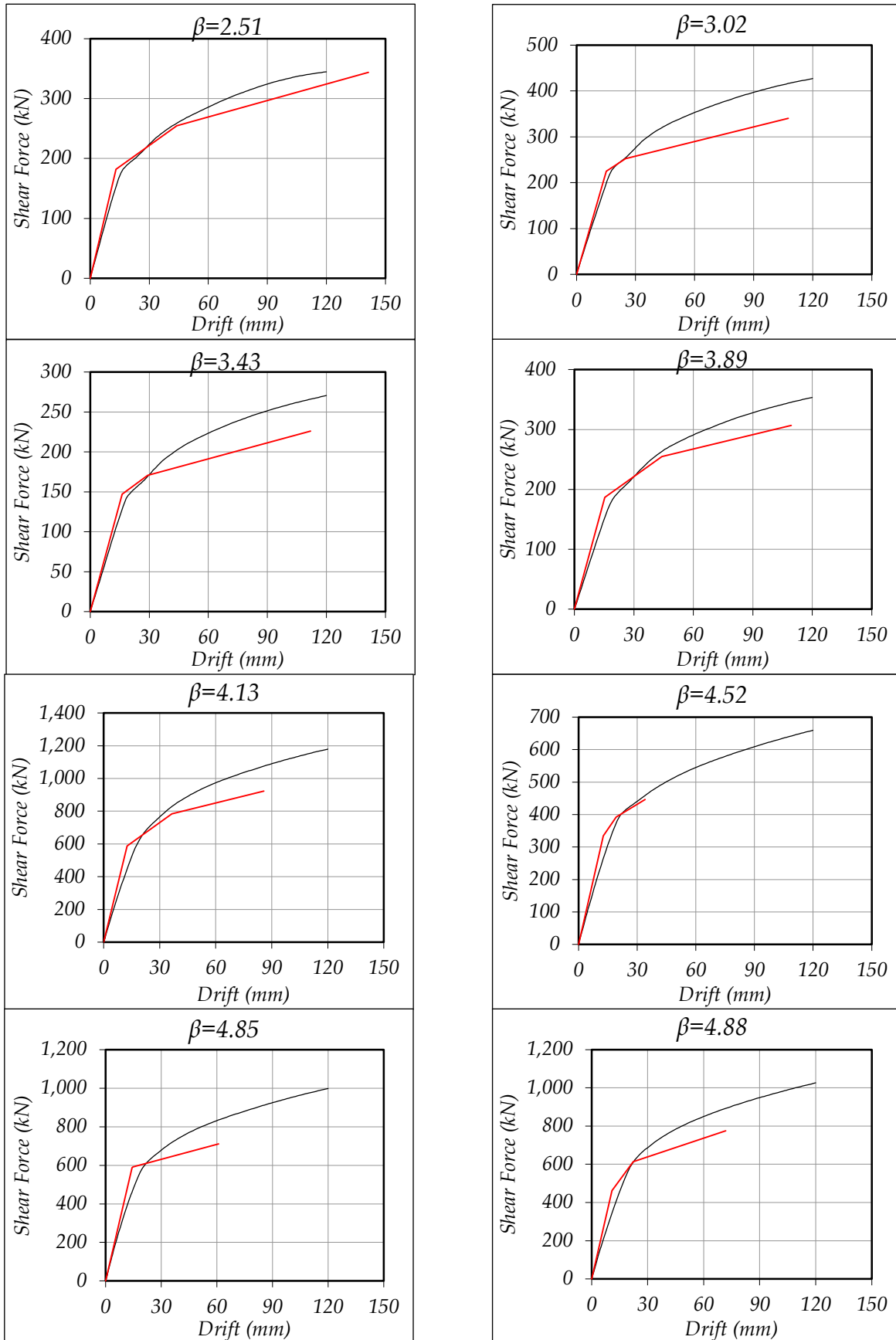
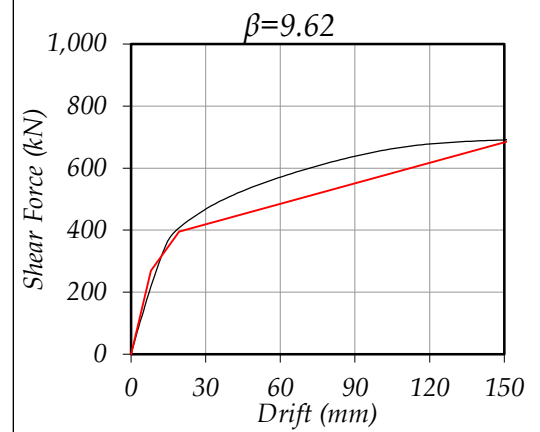
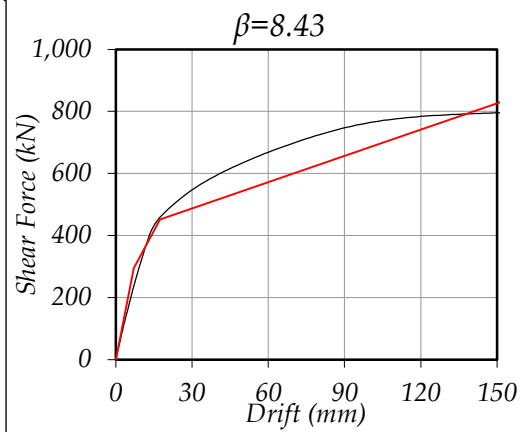
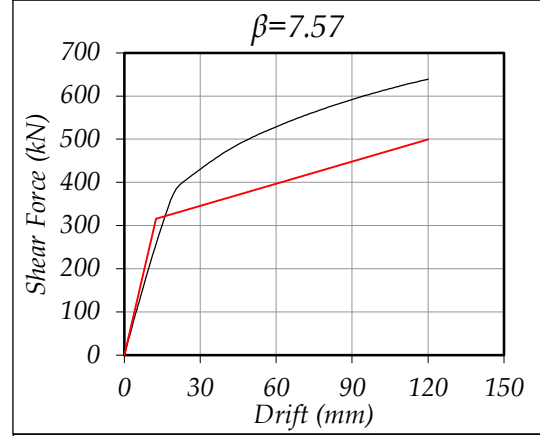
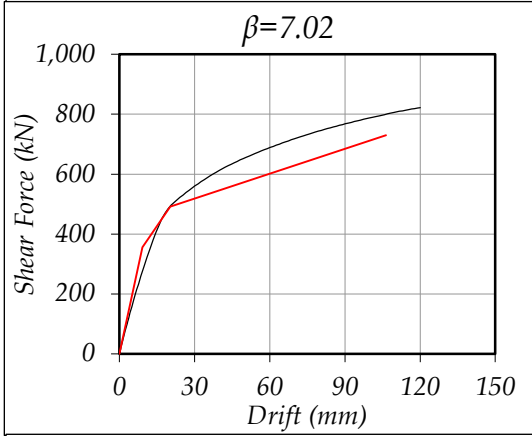
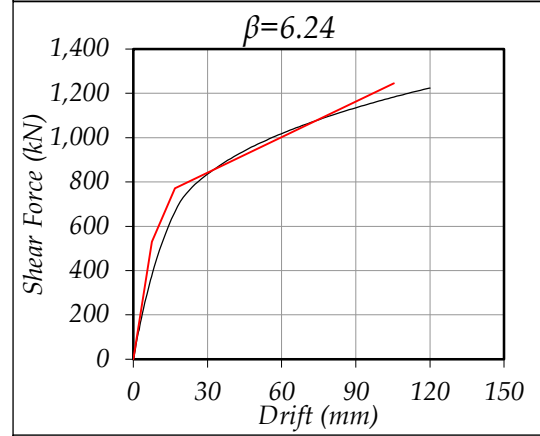
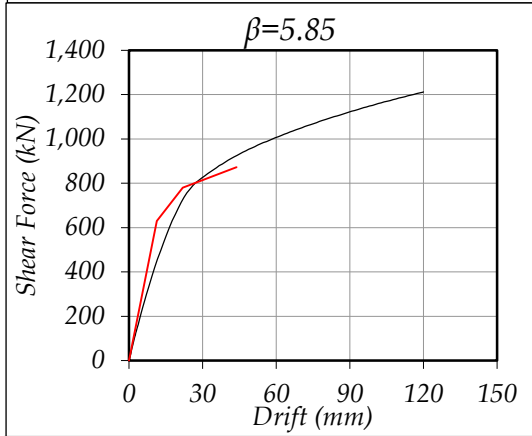
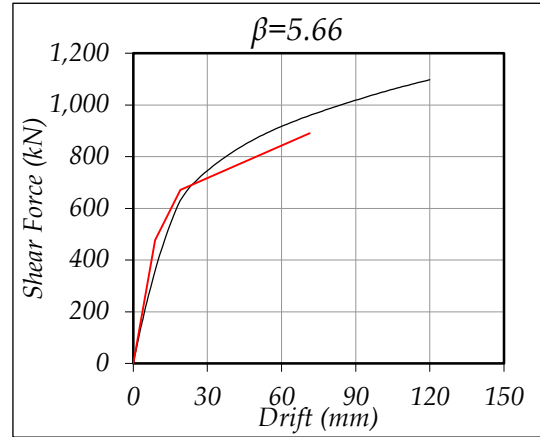
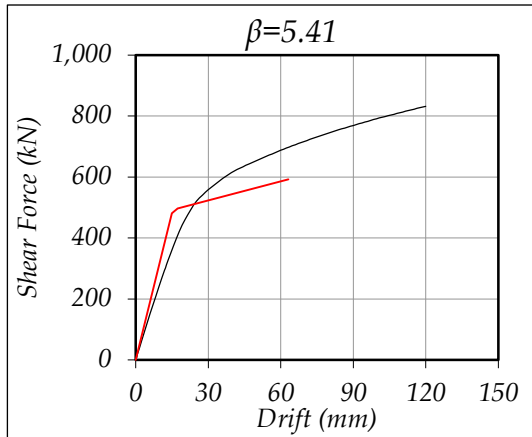


Figure 4.6: Column Shear Force versus Beam End Drift relationships for Exterior Beam to Column Joints. The graph shows that the proposed method is able to predict the force deformation behaviour with reasonable accuracy.







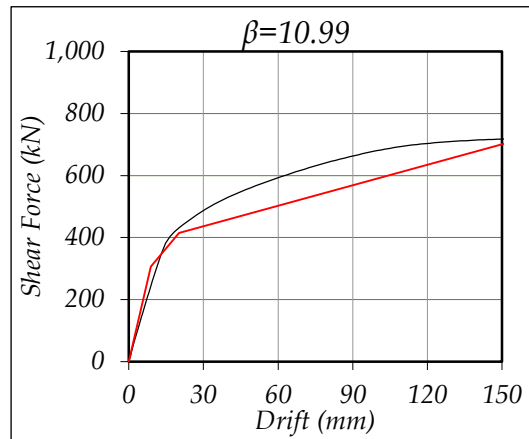


Figure 4.7: Column Shear Force versus Beam End Drift relationships for Interior Beam to Column Joints. The graph shows that the proposed method is able to predict the force deformation behaviour with reasonable accuracy.

Chapter 5

Nonlinear Dynamic Analysis of Benchmark Steel Moment Resisting Frame

5.1 Overview

Nonlinear dynamic time history analysis (THA) is, by far, the most exact method to compute the earthquake response of a structure. In this chapter THA of two benchmark frames have been carried out, using the force deformation curves obtained from the proposed method, and also using FEMA 356 hinge properties. The results of the THA have been compared with the published results [Tsai and Popov. 1988].

To obtain the proposed hinge properties for benchmark frames, the force deformation curves have been idealized as bilinear curves (refer Appendix A, Step IX). Results from the Non-Linear Dynamic Analysis, using proposed hinges are compared with those obtained using FEMA hinge properties. The responses are in close correspondence, which validates the efficacy of the proposed method.

5.2 Introduction

Moment frames, when subjected to earthquake ground motions, are designed to undergo inelastic action at predetermined locations in a pre-decided order, in order to attain wide and stable hysteretic behaviour. Beam to column joints in a steel MRF are the highly vulnerable to damage. The desired behaviour is usually attained by proportioning the members such that inelastic yielding remains limited at the beam ends. However, research have established that the JPZ sustains inelasticity, even before beams develop plastic hinges, and the same has been noted in results of numerical study presented in Chapter 4. The panel zone may be reinforced or unreinforced, and depending on the design it may yield due to the large moment transferred through the joint. To realistically estimate the seismic response of a structure each component needs to be explicitly modelled. This includes modelling of, uniformly elastic beams and columns, the rigid end offsets for beam and column ends, and JPZ as a separate structural entity.

The nonlinear behaviour of frames depends on the properties of hinges assigned to individual members. FEMA 356 recommends that, hinge properties shall be estimated on the basis of material, geometric and cross-sectional properties, along with location of plastic hinges.

In this chapter, THA have been carried out for two distinct cases of hinge properties, i.e., (i) FEMA 356 prescribed hinge definitions (hereafter referred to as *FEMA hinges*), and (ii) Hinge properties based on force deformation behaviour obtained using proposed method (hereafter referred to as *proposed hinges*). The analyses have been carried out using SAP 2000 [CSi Berkeley]. The two benchmark moment frames considered for this study are shown in Figure 5.1 and 5.2. Both the buildings comprises of standard AISC rolled steel sections, of ASTM A36 grade steel.

The seismic response of MRFs, apart from the ground motion characteristics, depends upon the nonlinear behaviour of the joints. Therefore, modelling of nonlinear properties is critical in capturing the true behaviour. Conventionally, at a beam to column joint, the nonlinear properties are defined at beam ends, column ends and Joint Panel Zone, i.e., five points of nonlinearities. The proposed method for prediction of nonlinear behaviour of joints, takes into consideration, inelastic actions in the beams as well as in JPZ. As a result, the number of points having nonlinearities, at a beam to column joint are reduced from five to three.

5.3 Numerical Study of Benchmark Moment Frames

The numerical details of two benchmark frames as reported by Popov and Tsai, 1988 are given as under. The benchmark buildings are two office buildings of six and twenty storied having peripheral MRFs, constructed in California, Berkeley. In both the frames, the lateral load resisting system consists of a three dimensional MRF on the perimeter of the building as shown in Figures 5.1 to 5.4. The gravity load is supported by the interior core columns in conjunction with the perimeter columns.

For the *six storied frame* the composite floor framing is made of 63.5 mm (2.5 inch) regular weight concrete fill over 76.2 mm (3 inch) metal deck on steel wide flange sections. The floor-floor height of the building is 3.8 m (12.5 ft.) for typical floors and 5.5 m (18 ft.) for the ground floor (Figure 3). The weight of a building floor, including partition, ceiling

and mechanical piping, is reported to be 4.8 kN/m^2 (100 psf) for typical floors and the roof. The exterior window wall system was assumed to weigh 1.7 kN/m^2 (35 psf) averaged over the exterior surface of the building. The design live loads were 3.83 kN/m^2 (80 psf) and 0.96 kN/m^2 (20 psf) for the typical floor and roof, respectively.

In case of twenty storied frame, the floor framing system is same as that for the 6 storied frame. The floor-floor height of the building is 3.8m (12.5 ft.) for typical floors and 5.5m (18 ft.) for the ground floor (Figure 4). The weight of a building floor, including partition, ceiling and mechanical piping, was assumed to be 4.8 kN/m^2 (100 psf) for typical floors and the roof. The exterior window wall system was assumed to weigh 1.7 kN/m^2 (35 psf) averages over the exterior surface of the building. The design live loads were 3.83 kN/m^2 (80 psf) and 0.96 kN/m^2 (20 psf) for the typical floor and roof, respectively.

The design seismic forces were calculated on the basis of lateral force procedure recommended by Structural Engineers Association of California [SEAOC, 1980]. The seismic dead load considered for base shear calculation includes dead load on the floor and weight of the façade. Live load was not considered in calculating the lateral force.

In the present study only one transverse frame has been analysed. It is assumed that 50% of the total lateral force is resisted by the frame. The base shear force is vertically distributed as recommended in SEAOC's provisions. The storey drift requirement are satisfied by modelling the supports of the frames as describe in the original report. SCWB design philosophy was adopted. Member sizes were evaluated based on the stress ratios and storey drifts, and are shown in Figures 5.3 and 5.4, for six storied and twenty storied frames, respectively.

Six storied frame is having fundamental period of 1.31 s and a corresponding base shear of $0.052W$ for calculating member forces. However, the story drifts were calculated based on reduced base shear corresponding to a period of 1.6 seconds. The final beam and column sections, and doubler plates details are shown in Figure 4.3. For the twenty storied frame the design shear force for panel zone was increased using the flexural strength of the beams framed into the joint rather than design bending moments. The final beam and column sections, and doubler plates details are shown in Figure 5.4.

Both designs of frames conforms to minimum thickness of column web or doubler plates as per IS 800 [IS 800: 2007], given by $t_{p,reqd.} = \frac{d_p + b_p}{90}$, where d_p is depth of JPZ between continuity plates and b_p is width of JPZ between column flanges

5.4 Modelling of Benchmark Moment Frames

The analyses of benchmark frames have been carried out using SAP 2000 software, and modeling parameters used are described below. The various components to be modelled are beams, columns and doubler plates. All the members were assumed to be of uniform cross-section.

The beams have been modelled as lineal frame elements with lumped plasticity by providing plastic hinges at beam ends with a rigid end offset (Figure 5.5). The moment rotation relationships at beam end hinges are modelled using both FEMA 356 recommendations (Figures 5.6, Table 5.1 and 5.2) and the proposed method (Figure 5.5, Table 5.3 and 5.4)

Along with the rigid end offsets, panel zone elements, in the form of doubler plates has been modelled to account for joint deformations in the frame. For a steel beam to column joints subjected to lateral loads, with beams of equal depth on both sides of the joint, the average shear stress in the column web due to the beam moment is calculated as

$$\tau_{avg} = \frac{V_y}{(d_c - t_{cf})t_{cw}} \quad (5.1)$$

$$\text{where, } V_y = \frac{\sum M_{pb}}{d_b} - H \quad (5.2)$$

The average shear strain, γ_{av} , in the panel zone before reaching the yield strain γ_y is

$$\gamma_{av} = \frac{\sum M_{pb}(1-a)}{G(d_c - t_{cf})t_{cw}d_b} \quad (5.3)$$

The elastic rotational stiffness associated with shear deformation of the panel zone is

$$k_e = \frac{\sum M_b}{\gamma_{av}} = \frac{G(d_c - t_{cf})t_{cw}d_b}{(1-a)} \quad (5.4)$$

where, G is elastic shear modulus and α is ratio of depth of beam to story height. For practical purpose, the yield moment that causes shear yielding of the panel zone is

$$\sum M_y = \frac{\sigma_y t_{cw} d_c d_b}{\sqrt{3}} \quad (5.5)$$

$$\gamma_y = \frac{\sigma_y}{G\sqrt{3}} \quad (5.6)$$

For the proposed method, as the nonlinear behaviour of JPZ has been taken into consideration while estimation of hinge properties, the force deformation behaviour of JPZ and beams are defined as one nonlinear hinge at beam ends with no rigid end offset. However, for frames with FEMA 356 hinge properties, the moment-rotation relationship for panel zone has been modeled as per FEMA 356 recommendations as given in Table 5.2.

For both the proposed hinges and FEMA hinges, the columns are modelled similar to the beams, using lineal frame elements having uniform cross section, a lumped plastic hinge and a rigid (stiff) end offset. P-M2 steel hinge rotation model having a rigid-plastic hinge with axial load and moment interaction, along with a steel type yield surface has been used to model the column hinges. The $M-\theta$ relationship for column end hinges are modelled as per FEMA 356 recommendations (Tables 5.7 and 5.8).

5.4.1 Hinge Properties from the Proposed Method

For both the six storied and twenty storied benchmark frames, the hinge properties, obtained using the proposed method are presented in Tables 5.3 and 5.4 respectively. The beams are modelled, as uniform elastic lineal member as described in section 5.4. The only difference being the assignment of hinges at the joint itself (with zero rigid end offset).

5.4.2 FEMA 356 Hinge Properties

Generally, in nonlinear analysis, inelastic actions in MRFs are assumed to be localized at beam and column ends. To determine the response of a frame accurately, FEMA 356 (2000) recommends certain modelling parameters for assignment of the nonlinear hinges (Tables 5.1, 5.2 and 5.5). These hinge properties are assigned to the

frames as shown in Figures 5.6 and 5.8. The panel zone elements are assigned to the joints, only where the doubler plates are present. While, no panel zone element has been assigned to joints having no column web reinforcements.

The dead loads and live loads as described in the frame details have been applied and THA of both the benchmark frames are carried out. The ground motion applied to the six storied frame is N21E component of 1952 Kern County Earthquake scaled to a peak ground acceleration of 0.47 g by a factor of 3 (Figure 5.9). While the twenty storied frame has been subjected to EW component of the first eighty seconds of the original 1985 Mexico Earthquake which possessed a peak ground acceleration of 0.17 g (Figure 5.10). The THA have been carried out with both the proposed as well as the FEMA hinge properties, and the results obtained presented in the following section.

5.5 Results and Discussion

The results of THA of the benchmark frames are shown through Figures 5.10 - 5.13. It has been observed that the responses obtained by employing the nonlinear hinges as per the proposed method are fairly close to the published results.

Figure 5.10 shows the displacement profile of the six storied frame at maximum roof displacement. The displacement profiles obtained using the *FEMA hinges* and *proposed hinges* are compared with the corresponding reported displacement profiles [Tsai and Popov, 1988]. It can be observed that the displacement profile obtained using proposed hinges closely matches with the reported profile. Figure 5.11 depicts comparison of the floor displacement histories using the *proposed hinges* and *FEMA hinges*, with published results. The close correspondence of results compared establishes the effectiveness of the proposed method.

For the twenty storied frame, a comparison of roof displacement and base shear histories, obtained using *proposed* and *FEMA hinges* with reported results, have been shown through Figures 5.12 and 5.13, respectively. The Figures depicts the effectiveness of *proposed hinges*, as it closely matches the actual response of the frame.

As, the number of points of nonlinearity have been reduced from five (for conventional FEMA Hinges) to three (for proposed hinges), the computational effort

required to analyze the frames has reduced significantly. This results in enhanced computational efficiency in case of proposed method.

5.6 Conclusion

The results of THA, using the *proposed* and *FEMA hinges* and comparison thereof with the published results underlines the usefulness of the study. The Nonlinear Dynamic THA of frames with proposed hinges is computationally more efficient than the frames having conventional FEMA Hinges. This can be attributed to the reduction in number of points having nonlinearity from 5 in case of FEMA hinges to three in case of proposed hinges. Also, the response obtained using proposed hinge definition exhibits closer correspondence with the published results as compared to conventional FEMA hinges, hence, establishes the precision of the proposed method.

Table 5.1: Modelling parameters (Nonlinear Hinges) for Beam Elements [Table 5-6, FEMA 356, 2000]

Beams - Flexural Action	Modelling Parameters		
	Plastic Rotation Angle, rad		Residual Strength Ratio
	A	B	C
$\frac{b_f}{2t_f} \leq \frac{52}{\sqrt{F_y}}$ and $\frac{h}{t_w} \leq \frac{418}{\sqrt{F_y}}$	$9\theta_y$	$11\theta_y$	0.6
$\frac{b_f}{2t_f} \geq \frac{65}{\sqrt{F_y}}$ or $\frac{h}{t_w} \geq \frac{640}{\sqrt{F_y}}$	$4\theta_y$	$6\theta_y$	0.2

Table 5.2: Modelling Parameters (Nonlinear Hinges) for Panel Zone Element [Table 5-6, FEMA 356, 2000]

Panel Zone Shear Action	Modelling Parameters		
	Plastic Rotation Angle, rad		Residual Strength Ratio
	A	B	C
	$12\theta_y$	$12\theta_y$	1.0

Table 5.3: Manual (Proposed) Hinge Property Definitions for Exterior and Interior Joints for Six Storey Frame

S. No.	Joint Label	Yield Rotation (rad)	Yield Moment (kNm)	Rotation Ratio (Yield/Ultimate)	Moment Ratio (Yield/Ultimate)
1.	I2-3	0.00616	871.68	6.50	1.20
2.	I4-5	0.00608	627.53	6.58	1.53
3.	I6	0.00706	402.19	5.66	1.46
4.	E2-3	0.00803	845.13	4.98	1.34
5.	E4-5	0.00935	793.12	4.28	1.22
6.	E6	0.00898	487.25	4.46	1.32
7.	IR	0.00580	224.22	6.90	2.62
8.	ER	0.00705	341.36	5.67	1.69

Table 5.4: Manual (Proposed) Hinge Property Definitions for Exterior and Interior Joints for twenty Storey Frame

S. No.	Joint Label	Yield Rotation (rad)	Yield Moment (kNm)	Rotation Ratio (Yield/Ultimate)	Moment Ratio (Yield/ Ultimate)
1.	IG	0.00479	1,246.14	8.36	1.36
2.	I2 - I3	0.00433	1,246.14	9.25	1.36
3.	I4 - I9	0.00473	1,229.03	8.46	1.35
4.	I10 - I15	0.00517	1,213.05	7.74	1.38
5.	I16 - I19	0.00477	932.19	8.38	1.47
6.	I20	0.00562	739.43	7.12	1.40
7.	IR	0.00784	739.43	5.10	1.27
8.	EG	8.24	1.65	7.17	1.65
9.	E2 - E3	0.00486	1,174.34	8.24	1.65
10.	E4 - E5	0.00514	1,172.26	7.79	1.56
11.	E6 - E7	0.00553	1,169.99	7.24	1.48
12.	E - E9	0.00590	1,167.92	6.78	1.40
13.	E10 - E11	0.00634	1,166.48	6.31	1.32
14.	E12 - E13	0.00696	1,162.80	5.75	1.38
15.	E14 - E15	0.00789	1,160.15	5.07	1.35
16.	E16 - E17	0.00712	892.06	5.62	1.44
17.	E18 - E19	0.00804	890.82	4.98	1.43
18.	E20	0.00834	715.18	4.79	1.40
19.	ER	0.00853	715.18	4.69	1.31

Table 5.5: Modelling parameters (Nonlinear Hinges) for Column Elements [Table 5-6, FEMA 356, 2000]

Columns - Flexural Action	Modelling Parameters		
	Plastic Rotation Angle, rad		Residual Strength Ratio
for $P/P_{cl} < 0.2$	A	B	C
$\frac{b_f}{2t_f} \leq \frac{52}{\sqrt{F_y}}$ and $\frac{h}{t_w} \leq \frac{300}{\sqrt{F_y}}$	$9\theta_y$	$11\theta_y$	0.6
$\frac{d \cdot b_f}{2t_f} \geq \frac{65}{\sqrt{F_y}}$ or $\frac{h}{t_w} \geq \frac{460}{\sqrt{F_y}}$	$4\theta_y$	$6\theta_y$	0.2
for $0.2 < P/P_{cl} < 0.5$	A	B	C
$\frac{b_f}{2t_f} \leq \frac{52}{\sqrt{F_y}}$ and $\frac{h}{t_w} \leq \frac{418}{\sqrt{F_y}}$	$11\{1 - (\frac{1.7P}{P_{cl}})\}\theta_y$	$17\{1 - (\frac{1.7P}{P_{cl}})\}\theta_y$	0.2
$\frac{b_f}{2t_f} \geq \frac{65}{\sqrt{F_y}}$ or $\frac{h}{t_w} \geq \frac{640}{\sqrt{F_y}}$	θ_y	$1.5\theta_y$	0.2

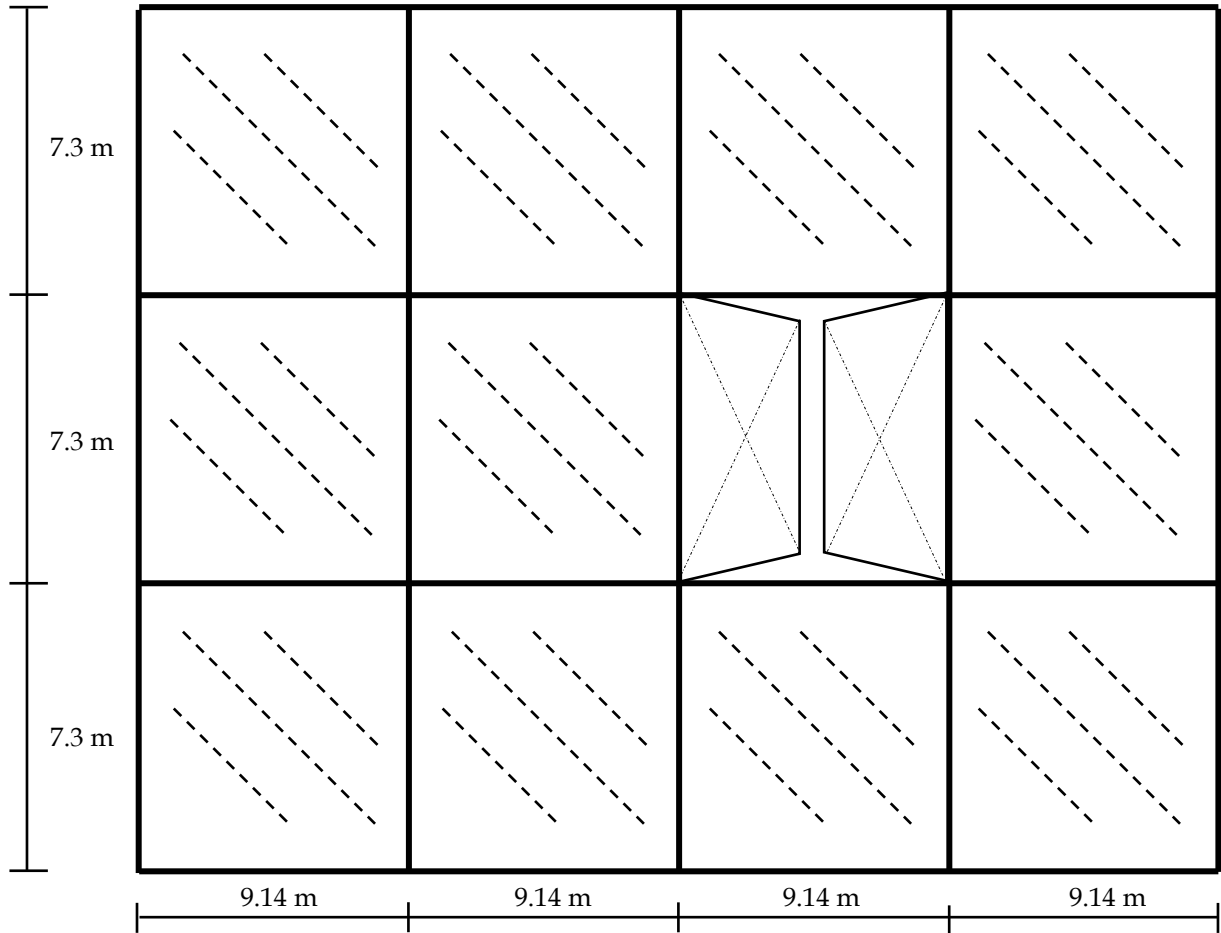


Figure 5.1: Plan of Six Storey Building Frame

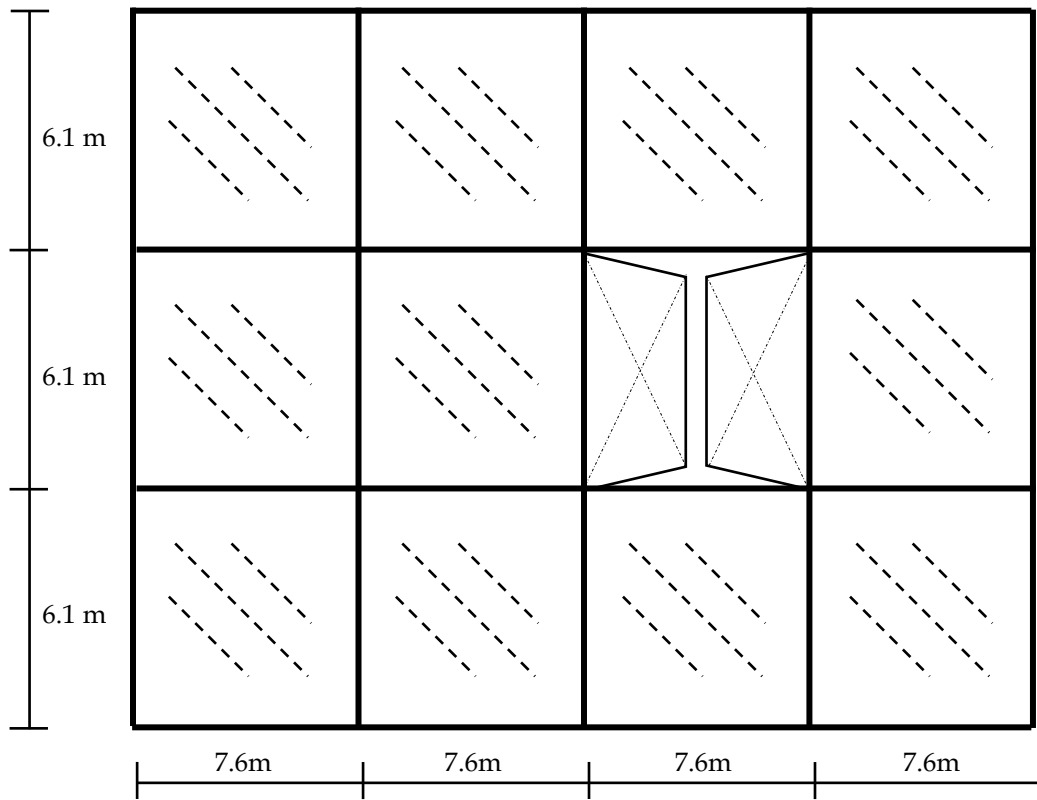


Figure 5.2: Plan of Twenty Storey Building Frame

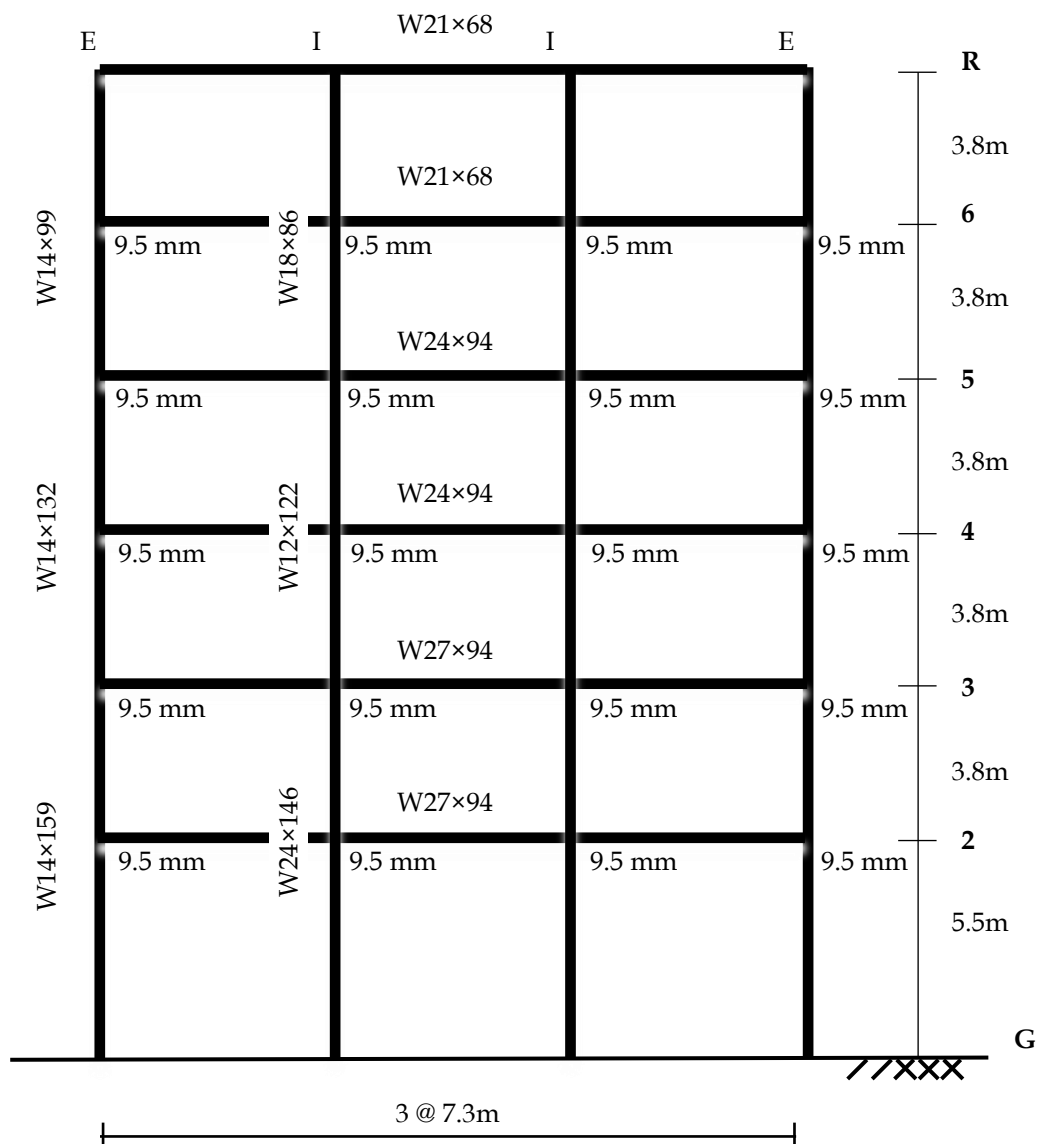


Figure 5.3: Six Storey Benchmark Frame [Tsai and Popov, 1988]

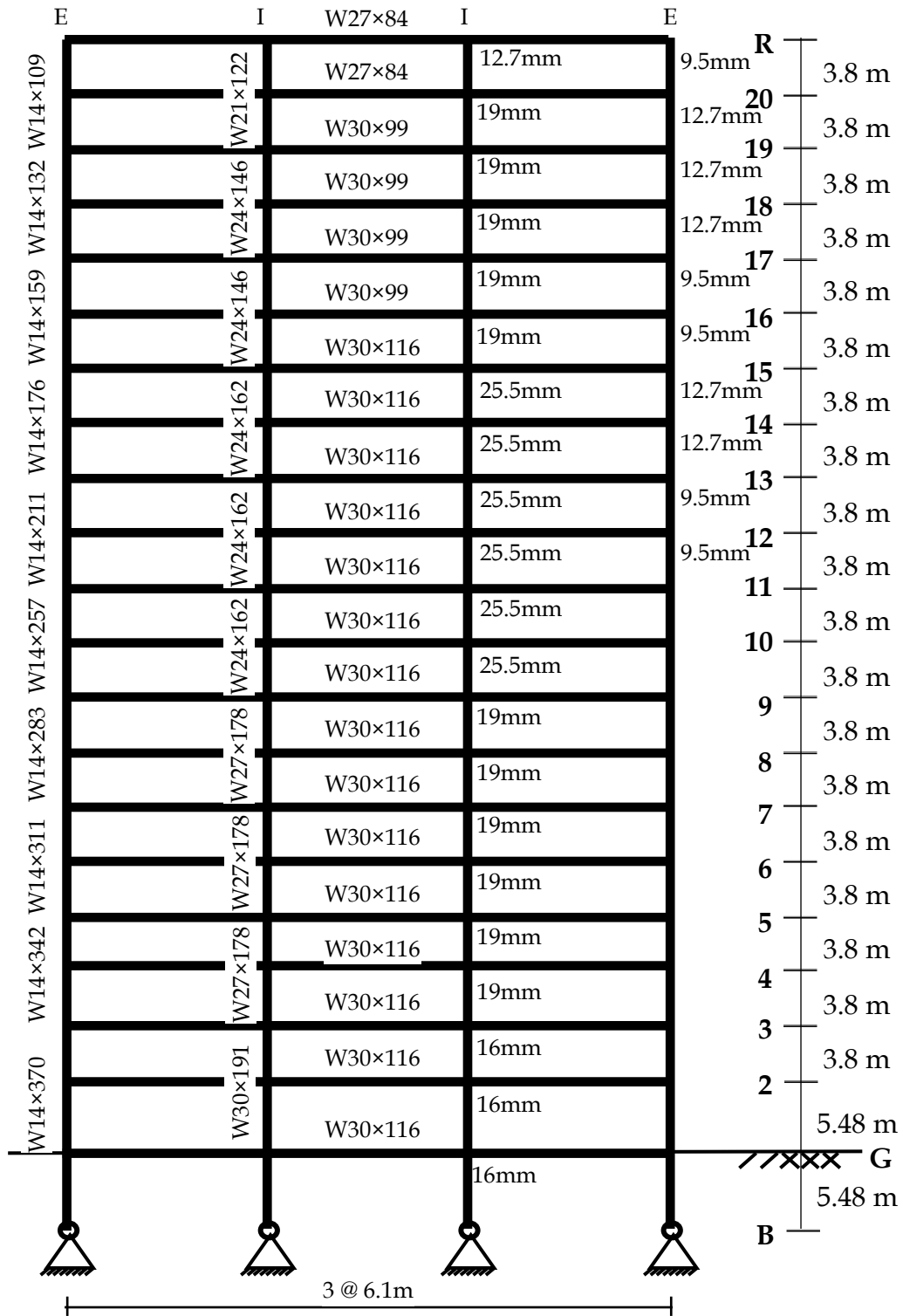


Figure 5.4: Twenty Storey Benchmark Frame [Tsai and Popov, 1988]

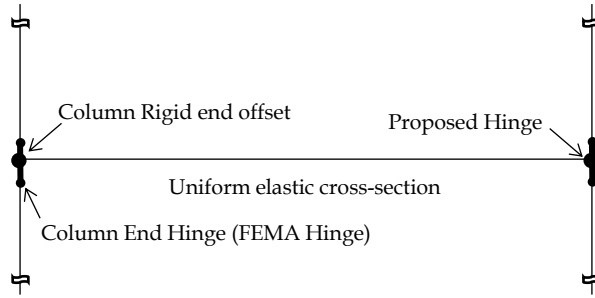


Figure 5.5: Assignment of Proposed Hinges. The proposed hinges are assigned to the beams of benchmark frames as M3 (Moment) hinges, with isotropic Hysteretic Rule. The rigid end offset of the proposed hinges are kept to be zero, so that the nonlinearity is assigned at the joint.

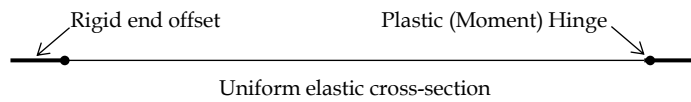


Figure 5.6: Typical Beam compound element modelling

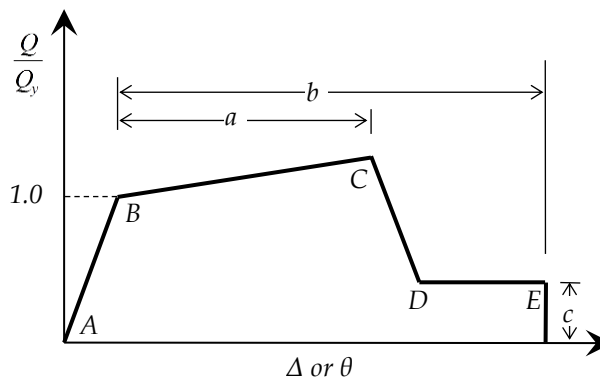


Figure 5.7: General Force Deformation Curve. Used for both FEMA and Proposed Hinge assignments.

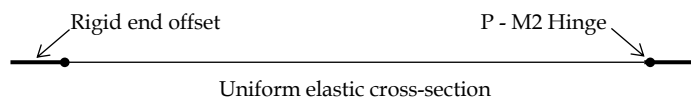


Figure 5.8: Typical Column compound element

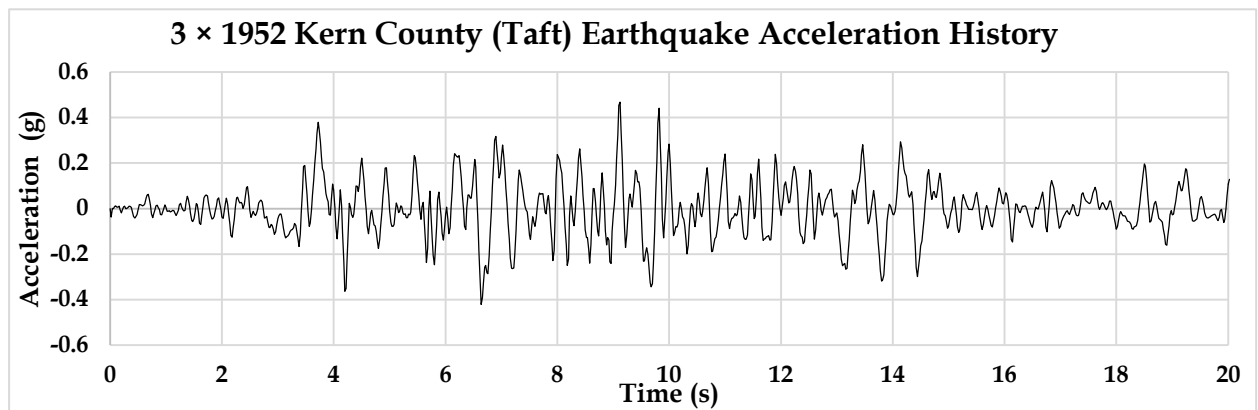


Figure 5.9: Ground Acceleration time history for 3× TAFT earthquake. The Six Storied Building frames is analysed using this ground motion.

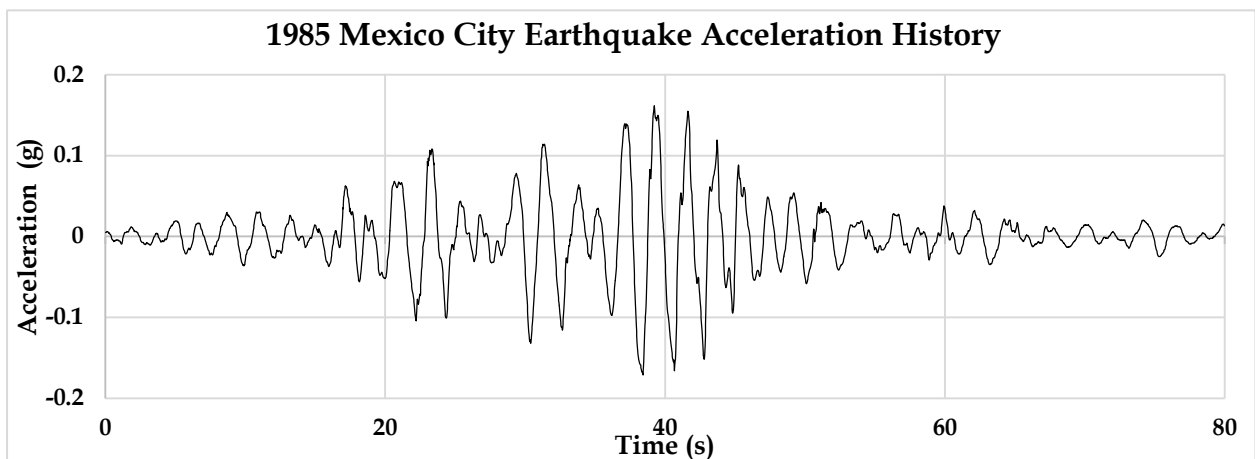


Figure 5.10: Ground Acceleration time history for Mexico City earthquake. The Twenty Storied Building frames is analysed using this ground motion.

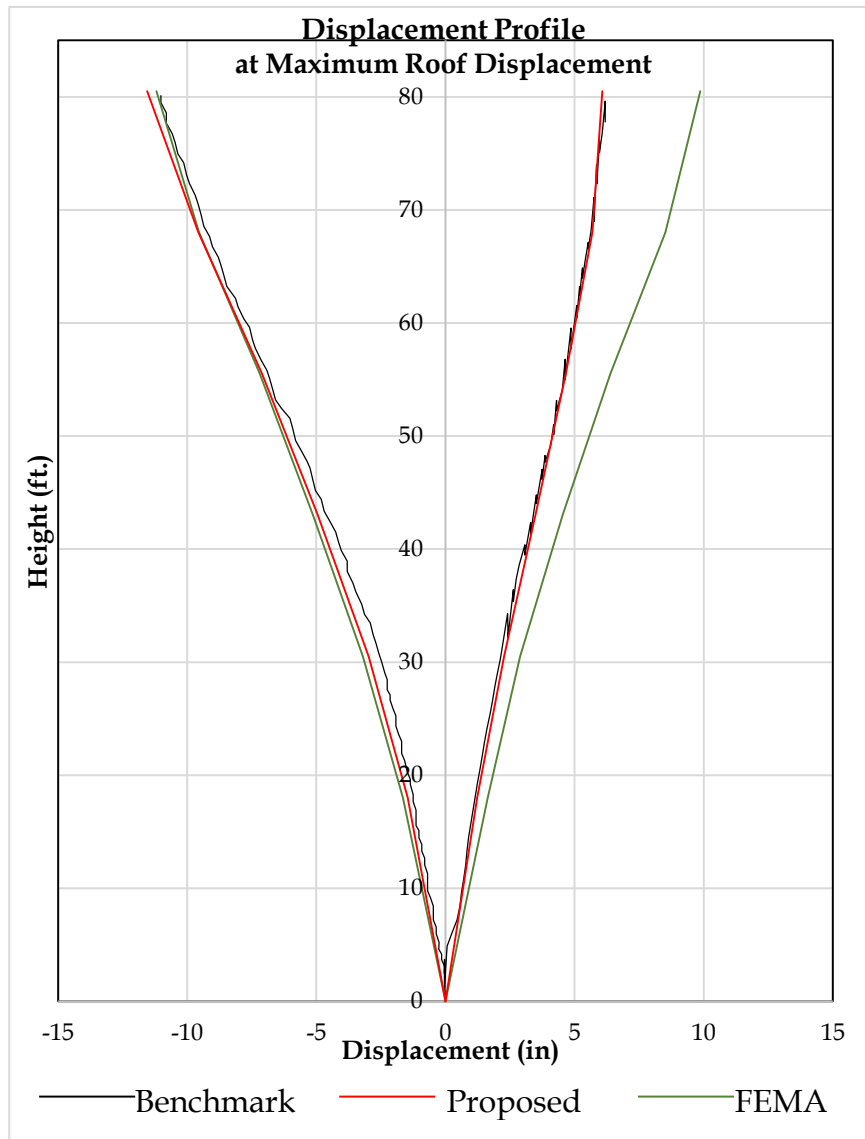


Figure 5.11: Displacement Profile at Maximum Roof Displacement for Six storied frame.

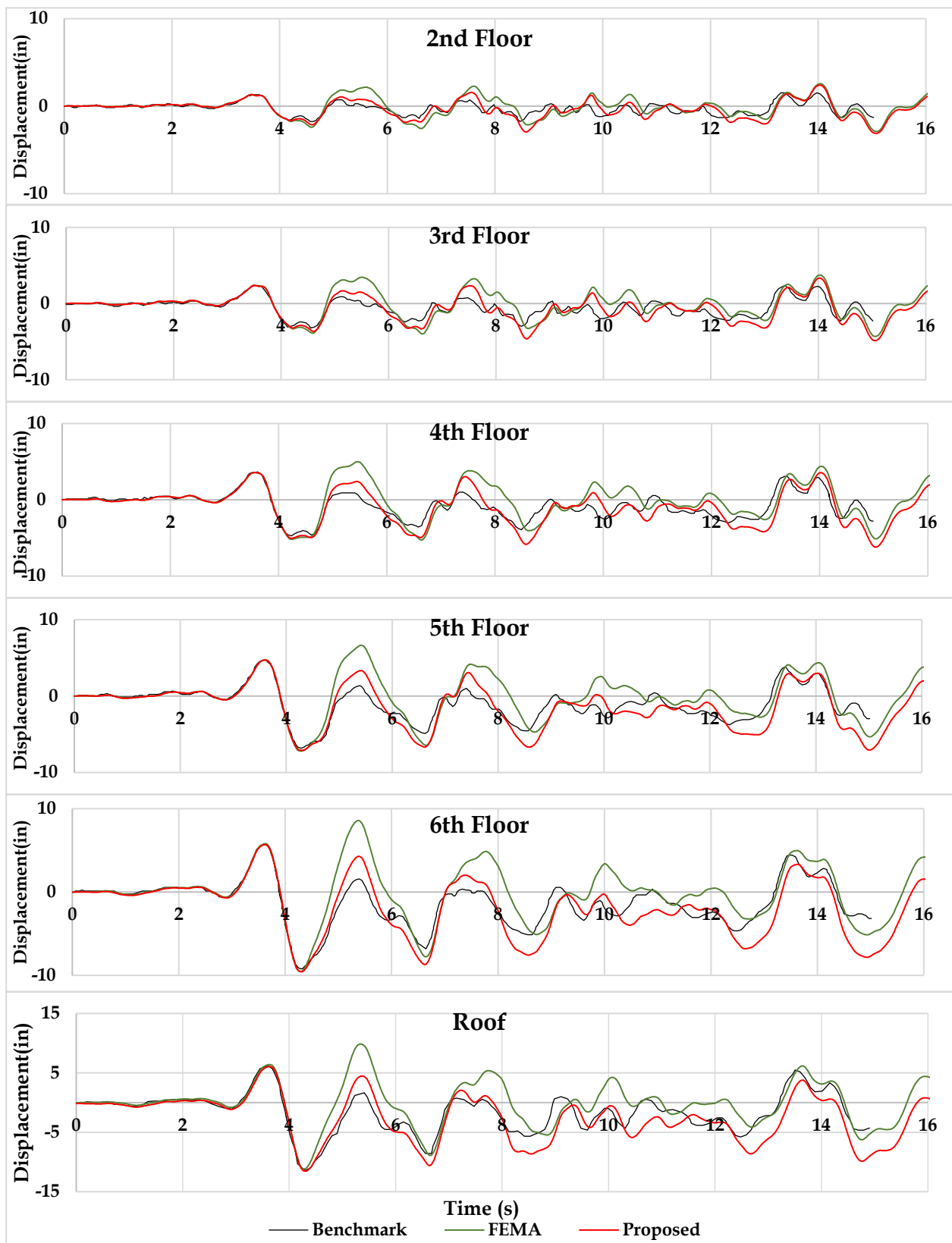


Figure 5.12: Floor Displacement Histories for Six storied frame

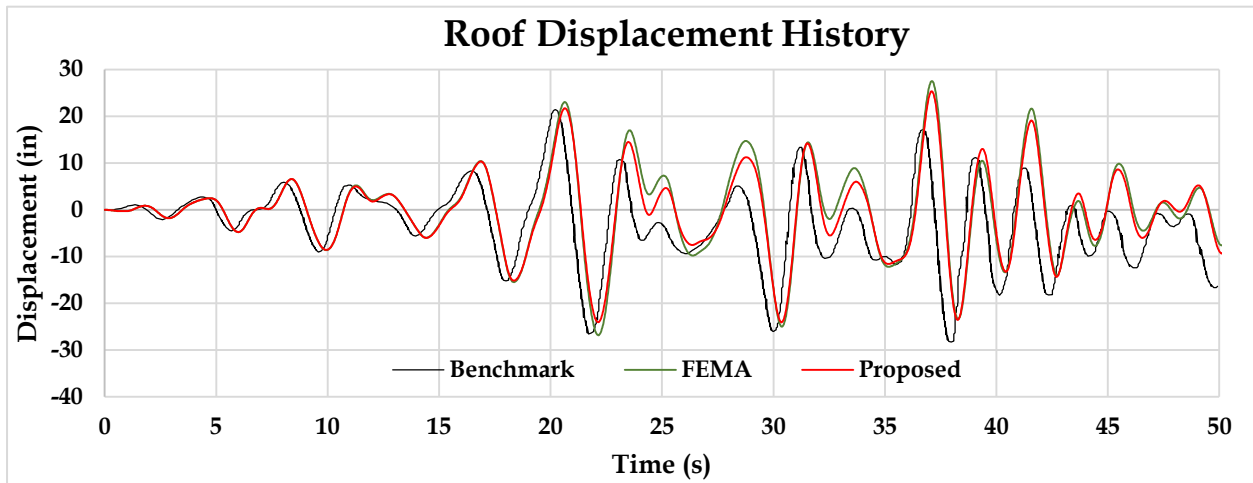


Figure 5.13: Roof Displacement History for Twenty storied frame

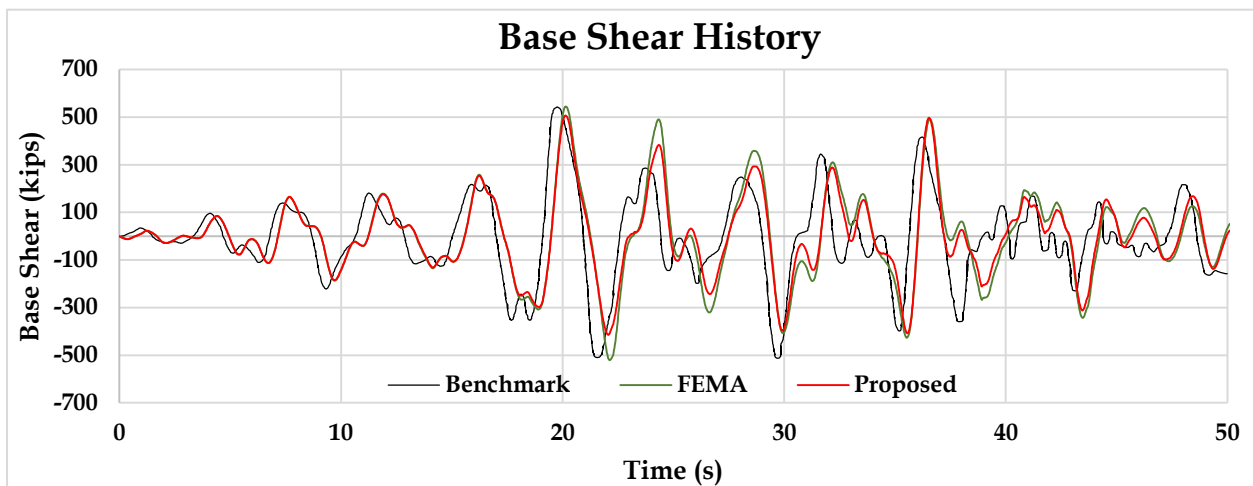


Figure 5.14: Base Shear History for Twenty storied frame

Chapter 6

Summary and Conclusion

6.1 Overview

When subjected to seismic excitations, steel moment resisting frames are supposed to dissipate the energy induced through rotation of members. The capacity design concept recommends that beams shall form flexural hinges, before inelasticity initiates in the columns. The role of joint panel zone in dissipation of inelastic energy is a much researched aspect in design of beam to column joint. Seismic behaviour of a beam to column joint depends on the performance of each of its components. The individual strength of each of these components can be determined using the principles of basic mechanics. This study presents a mechanics based hand calculation approach to determine the yielding sequence and corresponding drifts for a strong axis beam to column moment joint.

6.2 Summary

Beam to column joints in a moment resisting frame are locations of maximum concentration of stresses. The flow of forces between the components of a joint occurs on the basis of individual strength of these components. Adhering to the concept of capacity design, for maximum utilization of available ductility, a strength hierarchy has to be maintained between the members of a frame. The components of beam to column joints where damage is anticipated are (a) beam ends, (b) JPZ, (c) column ends and (d) beam to column connection; preferably in the same order. For steel moment resisting frames, it is recommended that, the beam to column joints shall be stronger than the beams, and the plastic moment capacity of columns shall be greater than that of the beams. However, there are, still, no unequivocal guidelines for the design of JPZ region.

Three possible design philosophies for JPZ are (a) strong JPZ design, (b) weak JPZ design and (c) balanced JPZ design. During past four decades, each of these have been carefully studied. AISC 360-10 recommends a balanced JPZ design approach,

which calls for simultaneous yielding of beam ends (flexural) and JPZ (shear). However, other design standards recommend different design criteria for JPZ design.

As the JPZ is an integral part of column, inelasticity in JPZ is deemed to be irreparable. Also, inelastic deformations in JPZ leads to uncontrolled permanent overall deformation of frames. The JPZ strength depends on the thickness of web of columns in a joint, and thus is a function of column to beam strength ratio (CBSR, represented by β) of a joint. The first part of present work aims at determining the minimum value of CBSR which renders the JPZ to undergo inelastic actions only after development of plastic hinges in beams. To achieve this, a parametric study has been carried out, with joints having CBSR varying from 1.2 to 3.89. Non-linear finite element analyses (FEA) of twelve, typical interior beam to column joint subassemblages has been carried out. The effects of two types of joint reinforcements, i.e. continuity and doubler plates, are also studied. The results suggest that CBSR upto 3.89 are not sufficient to prevent inelastic actions in JPZ region. Also, it has been observed that the location of onset of inelasticity remains within JPZ in the considered range.

Different components of beam to column moment joints undergoes inelastic actions on the basis of their individual strength. Using the principles of basic mechanics, it is possible to determine the yielding sequence of different components of a joint, a priori. This forms the basis of second part of the present work, where a mechanics based hand calculation method is proposed, to determine the force - deformation behaviour of a joint. The proposed method can be used for both interior and exterior beam to column joints, and takes into consideration, the effects of column web doubler plates. The efficacy of proposed method is verified by carrying out FEA for twenty-five combinations of both exterior and interior beam to column strong axis joint subassemblages. The results suggest that the proposed method accurately predicts the force deformation behaviour of joints. It has also been observed that for unreinforced moment joints, the minimum value of CBSR to prevent inelasticity in JPZ is 8.0.

The effectiveness of proposed method is further validated by carrying out non - linear dynamic time history analyses of two benchmark frames. The frames are

analysed with two types of non-linear hinge properties (moment rotation curves), which are, (a) obtained using the force deformation curves using the proposed method and (b) prescribed in FEMA 356 (2000). The time history analysis responses, using hinge properties based on proposed method agrees more closely than standard FEMA hinges, with responses reported in literature.

6.3 Conclusions

Based on the results of the numerical study following salient conclusion are drawn.

1. The joint panel zones inelasticity is the primary energy dissipation mechanism for joints having CBSR up to 3.9. Further, the inelastic actions in beams ends does not initiate upto a CBSR of 1.8. Also, a partial yielding of beam flanges is observed for joints having CBSR greater than 2.5.
2. The continuity plates are able to increase inelasticity in beam flanges, though their effect is not very significant.
3. The column web doubler plates leads to de-localization of inelasticity from JPZ to the beam end region. This is attributed to increased shear capacity of the JPZ. It is also concluded that inelastic actions in JPZ can, at best, be delayed, and not prevented, by using column web doubler plates.
4. The proposed mechanics based hand calculation method provides a tri-linear force deformation behavior of beam to column joint subassemblages. The method is able to predict the sequence of three modes of yielding, namely, Beam Flange Yielding, Panel Zone Yielding and Formation of Plastic Hinges in beams; and the corresponding drifts. The comparison of results obtained from the method with FEA shows that the method is able to predict the force deformation behaviour with reasonable accuracy. The results of finite element analyses are in agreement with the predicted force deformation behavior of beam column joint subassemblages, for both interior and exterior joints.
5. The proposed method is computationally elegant and efficient and able to predict yield drift for three components of beam column subassemblage

without resorting to detailed FEA. The method can be used for design of strong and unyielding joint panel zone.

6. The results of FEA analyses indicate that, minimum value of CBR to prevent inelastic actions in JPZ is as high as eight, for both exterior and interior joints.
7. The results of THA, using the proposed and FEMA hinges and comparison thereof with the published results underlines the usefulness of the study. The THA of frames with proposed hinges is computationally more efficient than the frames having conventional FEMA Hinges. Response computation using proposed hinge definition exhibits closer correspondence with the published results as compared to conventional FEMA hinges, hence, establishes the precision of the proposed method.

6.4 Recommendations

It has been observed that that for moment resisting frames with joints having CBR lesser than 8.0, JPZ goes into inelastic range before formation of beam plastic hinges. Also, inelastic actions initiates in the JPZ region at fairly low drift levels. On the basis of these observations, it is recommended that, in areas of high seismicity, moment frame buildings have inherent limitations, and suitability of other structural systems needs to be explored. Also, in areas where low to moderate level of seismic shaking is anticipated, moment frame buildings may be constructed, only if anticipated drift intensities are lower than those required to render the JPZ inelastic.

6.5 Limitations

The present work has following major limitations:

1. The possibility of inelastic actions in columns has not been taken into consideration while the formulation of proposed method.
2. The effect of gravity loads on the inelastic behaviour of the frames are ignored.
3. Effects of axial compressive forces acting on the columns are not considered.
4. Brittle fracture of welds has not been studied.

6.6 Scope of Future Work

The following problems can be addressed in the future research:

1. A similar method to predict the force - deformation behaviour can be developed for other structural steel systems, like braced frames, steel moment frames with steel plate structural walls, etc.
2. The effects of axial forces, crack propagation in joints, fracture analysis of connections can be studied in detail.
3. The proposed method can be extended to incorporate the effects of column inelasticity and connection reinforcements.
4. Different JPZ reinforcement strategies, to prevent inelastic actions in JPZ can be studied.

References

1. AIJ, (1995), "Preliminary Reconnaissance Report of the 1995 Hyogoken-Nanbu Earthquake" English Edition, Architectural Institute of Japan, April, 1995.
2. AISC, (1973), Commentary on Highly Restrained Welded Connections," Engineering Journal, AISC, Third Quarter, pp. 61-73,1973.
3. AISC, (1990), Steel Design Guide Series 1 – Column Base Plates, American Institute of Steel Construction, Inc., Illinois, USA, 1990.
4. AISC, (1999), Metric Load and Resistance Factor Design Specifications for Structural Steel Buildings, American Institute of Steel Construction, Inc., Illinois, USA, 1999.
5. AISC, a. (2005). 360-Specification for Structural Steel Buildings; American Institute of Steel Construction, Inc.
6. AISC, A. S. D. (1989). Plastic Design Specifications for Structural Steel Buildings, American Institute of Steel Construction, Chicago, IL.
7. AISC, b. (2005). "AISC 341-05." Seismic provisions for structural steel buildings. Chicago (IL): American Institute of Steel Construction.
8. Allen, J., Richard, R. M., and Partridge, J., (1998), "Seismic Connection Design for Retrofitting Steel Moment Frames," Proceedings of the NEHRP Conference and Workshop on Research on the Northridge , California Earthquake of January 17, 1994, Vol IIIB, pp, 449-468, California Universities for Research in Earthquake Engineering, CA, 1998.
9. American Society of Civil Engineers (ASCE), (2000), "Prestandard and commentary for the seismic rehabilitation of buildings." FEMA-356, Washington, D.C.
10. Anderson, J, C., and Xiao, Y., (1998), "Repair/Upgrade Procedures for Low Rise Steel Moment Frames," Proceedings of the NEHRP Conference and Workshop on Research on the Northridge , California Earthquake of January 17, 1994, Vol. IIIB, pp, 469-477, California Universities for Research in Earthquake Engineering, CA, 1998.

11. Anderson, J. C., (1997), "A Welded Moment Connection for Low Rise Steel Frames," Proceedings of the EERC-CUREe Symposium in Honor of Vitelmo V. Bertero, USC/EERC-97/05, pp. 75-83, CA, USA, 1997.
12. Anderson, J. C., Duan, J., Xiao, Y., and Maranian, P., (2002), "Cyclic Testing of Moment Connections Upgraded with Weld Overlays," Journal of Structural Engineering, ASCE, Vol. 128, No. 4, pp. 509-516, 2002.
13. Arlekar, J. N. and C. Murty (2004). "Improved truss model for design of welded steel moment-resisting frame connections." Journal of Structural Engineering 130(3): 498-510.
14. ASTM, (1996), Annual Book of ASTM Standards, Vol. 01.04, American Standards for Testing and Materials, USA, 1996.
15. Becker, R. (1975). "Panel zone effect on the strength and stiffness of steel rigid frames." Engineering Journal, AISC 12(1): 19-29.
16. Bertero V. V., Popov E. P., and Krawinkler H. (1972). "Beam-column subassemblages under repeated loading." Journal of the Structural Division 98(5): 1137-1159.
17. Bertero, V.V., Anderson, J. C. and Krawinkler, H. (1994). Performance of steel building structures during the Northridge earthquake, Earthquake Engineering Research Center, University of California.
18. Blodgett, O. W., (2000), "Lessons Learned in the Field," Modern Steel Construction, February 2000.
19. Brandonisio, G., et al. (2011). "Shear instability of panel zone in beam-to-column connections." Journal of Constructional Steel Research 67(5): 891-903.
20. Bruneau, M. and S. A. Mahin (1991). "Full-scale tests of butt-welded splices in heavy-rolled steel sections subjected to primary tensile stresses." Engineering Journal 28(1): 1-17.
21. Castro, J. M., Elghazouli, A. Y. and Izzuddin, B. A. (2005). "Modelling of the panel zone in steel and composite moment frames." Engineering Structures 27(1): 129-144.

22. Castro, J. M., Dávila-Arbona, F. J. and Elghazouli, A. Y. (2008). "Seismic design approaches for panel zones in steel moment frames." *Journal of Earthquake Engineering* 12(S1): 34-51.
23. Challa, V. and J. F. Hall (1994). "Earthquake collapse analysis of steel frames." *Earthquake Engineering & Structural Dynamics* 23(11): 1199-1218.
24. Cheng, J. J. R., Yura, J. A. and Johnson, C. P. (1988). "Lateral buckling of coped steel beams." *Journal of Structural Engineering* 114(1): 1-15.
25. Choi, S. W. and H. S. Park (2012). "Multi-objective seismic design method for ensuring beam-hinging mechanism in steel frames." *Journal of Constructional Steel Research* 74: 17-25.
26. Civjan, S. A., Engelhardt, M. D. and Gross, J. L. (2001). "Slab effects in SMRF retrofit connection tests." *Journal of Structural Engineering* 127(3): 230-237.
27. Uniform Building Code (1997). UBC. 1997. International Conference of Building Officials, Uniform Building Code, Whittier, California.
28. Committee, A. (2010). "Specification for Structural Steel Buildings (ANSI/AISC 360-10)." American Institute of Steel Construction, Chicago-Illinois.
29. Degenkolb, H. (1994). "Connections (Interview by Stanley Scott)." Oakland, EERI Oral History Series, EERI.
30. Dooley, K. L. and J. M. Bracci (2001). "Seismic evaluation of column-to-beam strength ratios in reinforced concrete frames." *Structural Journal* 98(6): 843-851.
31. Dubina, D., Ciutina, A. and Stratan, A. (2001). "Cyclic tests of double-sided beam-to-column joints." *Journal of Structural Engineering* 127(2): 129-136.
32. El-Tawil, S. (2000). "Panel zone yielding in steel moment connections." *Engineering Journal-American Institute of Steel Construction* 37(3): 120-131.
33. El-Tawil, S., Vidarsson, E., Mikesell, T. and Kunnath, S. K. (1999). "Inelastic behavior and design of steel panel zones." *Journal of Structural Engineering* 125(2): 183-193.
34. El-Tawil, S., Mikesell, T. and Kunnath, S. K. (2000). "Effect of local details and yield ratio on behavior of FR steel connections." *Journal of Structural Engineering* 126(1): 79-87.

35. Engelhardt, M. D. and A. Husain (1992). Cyclic tests on large scale steel moment connections. Proceedings of the 10th World Conference on Earthquake Engineering.
36. Engelhardt, M. D. and T. A. Sabol (1998). "Reinforcing of steel moment connections with cover plates: benefits and limitations." *Engineering Structures* 20(4): 510-520.
37. Engelhardt, M. D., Winneberger, T., Zekany, A. J. and Potyraj, T. J. (1996). "The dogbone connection: Part II." *Modern Steel Construction* 36(8): 46-55.
38. Englekirk, R. E. (1999). "Extant panel zone design procedures for steel frames are questioned." *Earthquake Spectra* 15(2): 361-369.
39. EQE, (1989), "The October 17, 1989 Loma Prieta Earthquake: A Quick Look Report," EQE International, San Francisco, California, 1989.
40. EQE, (1994), "The January 17, 1994 Northridge, California Earthquake: An EQE Summary Report March 1994," EQE International, San Francisco, California, 1994.
41. FEMA, f. (2000). "350-Recommended Seismic Design Criteria for New Steel Moment-Frame Buildings." Washington (DC): Federal Emergency Management Agency.
42. Fenves, S. J. (1973). "Decomposition of Provisions of Design Specifications." *Decomposition of Large Scale Problems*: 43-56.
43. Fielding, D. (1994). "Frame Response Considering Plastic Panel Hinges." *Engineering Journal-American Institute of Steel Construction Inc.* 31(1): 31-37.
44. Fielding, D. J. and W. F. Chen (1973). "Steel frame analysis and connection shear deformation." *Journal of the Structural Division* 99(1): 1-18.
45. Hall, J. F. (1997). "Seismic response of steel frame buildings to near-source ground motions." Report, Earthquake Engineering Research Laboratory, California Institute of Technology.
46. Hall, J. F., (1994), "Northridge Earthquake of January 17, 1994 - Preliminary Reconnaissance Report," EERI Publication Number 94-01, Earthquake Engineering Research Institute, CA, USA, 1994.

47. Hamburger, R. O., Malley, J. O., Mahin, S. A., (1998), "Development of Guidelines for Evaluation, Repair, Upgrade, Design and Construction of Moment-Resisting Steel Frames," Proceedings of the NEHRP Conference and Workshop on Research on the Northridge , California Earthquake of January 17, 1994, Vol. IIIB, pp. 578-587, California Universities for Research in Earthquake Engineering, CA, 1998.
48. Ibarra, L. F., Medina, R. A. and Krawinkler, H. (2005). "Hysteretic models that incorporate strength and stiffness deterioration." *Earthquake Engineering & Structural Dynamics* 34(12): 1489-1511.
49. Jin, J. and S. El-Tawil (2005). "Evaluation of FEMA-350 seismic provisions for steel panel zones." *Journal of Structural Engineering* 131(2): 250-258.
50. JSCM, (1995), "Preliminary Report on The Great Hanshin Earthquake January 17,1995," Japan Society of Civil Engineers, Japan, 1995.
51. Kasai, K. and E. P. Popov (1986). "General behavior of WF steel shear link beams." *Journal of Structural Engineering* 112(2): 362-382.
52. Kato, B. (1982). "Cold formed welded steel tubular members." *Axially compressed structures*: 149-180.
53. Krawinkler, H. (2000). "State of the art report on systems performance of steel moment frames subject to earthquake ground shaking." Report no. FEMA-355C, SAC Joint Venture.
54. Krawinkler, H. and E. P. Popov (1982). "Seismic behavior of moment connections and joints." *Journal of the Structural Division* 108(2): 373-391.
55. Krawinkler, H., Anderson, J., Bertero, V., Holmes, W. and Theil Jr, C. (1996). "Steel buildings." *Earthquake Spectra* 12(S1): 25-47.
56. Kuntz, G. L. and J. Browning (2003). "Reduction of column yielding during earthquakes for reinforced concrete frames." *Structural Journal* 100(5): 573-580.
57. Lee, C. H., Jeon, S. W., Kim, J. H. and Uang, C. M. (2005). "Effects of panel zone strength and beam web connection method on seismic performance of reduced beam section steel moment connections." *Journal of Structural Engineering* 131(12): 1854-1865.

58. Lee, D., Cotton, S. C., Hajjar, J. F., Dexter, R. J., Ye, Y. and Ojard, S. D. (2005). "Cyclic behavior of steel moment-resisting connections reinforced by alternative column stiffener details II. Panel zone behavior and doubler plate detailing." *Engineering Journal-American Institute of Steel Construction* 42(4): 215.
59. Lee, K. H., Goel, S. C., and Stojadivod, B., (1998), "Boundary Effects in Welded Steel Moment Connections," 61st U.S. National Conference on Earthquake Engineering, 1998.
60. Liu, X. G., Tao, M. X., Fan, J. S. and Hajjar, J. F. (2014). "Comparative study of design procedures for CFST-to-steel girder panel zone shear strength." *Journal of Constructional Steel Research* 94: 114-121.
61. LRFD, A. (1994). "Manual of steel construction, load and resistance factor design." Chicago: American Institute of Steel Construction.
62. Malley, J. O. and K. Frank (2000). Materials and Fracture Investigations in the FEMA/SAC PHASE 2 Steel Project. 12th World Conference on Earthquake Engineering.
63. Manual, A. U. S. (2010). "Version 6.10." ABAQUS Inc.
64. Matos, C. and R. Dodds (2000). "Modeling the effects of residual stresses on defects in welds of steel frame connections." *Engineering Structures* 22(9): 1103-1120.
65. Mazzolani, F. and V. Piluso (1996). Theory and design of seismic resistant steel frames, CRC Press.
66. Mele, E., et al. (2001). "Cyclic behaviour of beam-to-column welded connections." *Steel and Composite Structures* 1(3): 269-282.
67. Miller, D. K. (1998). "Lessons learned from the Northridge earthquake." *Engineering Structures* 20(4): 249-260.
68. Miyakoshi, J., Hayashi, Y., Tamura, K. and Fukuwa, N. (1997). Damage ratio functions of buildings using damage data of the 1995 Hyogo-Ken Nanbu earthquake. Proceedings of the 7th international conference on structural safety and reliability (ICOSSAR).

69. Nader, M. N. and A. Astaneh-Asl, (1993), "Seismic behavior and design of semi-rigid steel frames", Earthquake Engineering Research Center, University of California.
70. Nakashima, M. and S. Sawaizumi (2000). Column-to-beam strength ratio required for ensuring beam-collapse mechanisms in earthquake responses of steel moment frames. Proceedings, Citeseer.
71. Nasrabadi, M. M., Torabian, S. and Mirghaderi, S. R. (2013). "Panel zone modelling of Flanged Cruciform Columns: An analytical and numerical approach." *Engineering Structures* 49: 491-507.
72. Oстераas, J. and H. Krawinkler (1989). "The Mexico earthquake of September 19, 1985-Behavior of steel buildings." *Earthquake Spectra* 5(1): 51-88.
73. Oстераas, J. D. and H. Krawinkler (1990). Strength and ductility considerations in seismic design, Earthquake Engineering Center.
74. Pan, L., Chen, Y., Chuan, G., Jiao, W. and Xu, T. (2016). "Experimental evaluation of the effect of vertical connecting plates on panel zone shear stability." *Thin-Walled Structures* 99: 119-131.
75. Partridge, J. H., Allen, J. and Richard, R. M., (2002), "Failure Analysis of Structural Steel Connections in the Northridge and Loma Prieta, California Earthquakes," Proceedings of the 7th National Conference on Earthquake Engineering, Paper No 00157. HI-RI, Boston, 2002.
76. Popov, E. P. (1988). "Seismic moment connections for MRFs." *Journal of Constructional Steel Research* 10: 163-198.
77. Popov, E. P. and B. Pinkney (1969). "Cyclic yield reversal in steel building connections." *Journal of the Structural Division*.
78. Popov, E. P. and R. M. Stephen (1972). "Cyclic loading of full-size steel connections."
79. Popov, E. P. and R. M. Stephen (1977). "Capacity of columns with splice imperfections." *Engineering Journal* 14(1).
80. Popov, E. P., Tsai, K. C. and Engelhardt, M. D. (1989). "On seismic steel joints and connections." *Engineering Structures* 11(3): 148-162.

81. Richard, R. M., Allen, J., and Partridge, J. E. (1997), "Proprietary Slotted Beam Connection Designs," *Modern Steel Construction*, pp. 28-33, March, 1997.
82. Roeder, C. (2000). "State of the art report on connection performance." FEMA 355d. Washington DC: Federal Emergency Management Agency.
83. Roeder, C. W. and D. A. Foutch (1996). "Experimental results for seismic resistant steel moment frame connections." *Journal of Structural Engineering* 122(6): 581-588.
84. Roeder, C. W., Schneider, S. P. and Carpenter, J. E. (1993). "Seismic behavior of moment-resisting steel frames: analytical study." *Journal of Structural Engineering* 119(6): 1866-1884.
85. SAC, (1996), "Notice to Building officials and Design Professionals in the San Francisco Bay Area" SAC Steel Project, September 1996.
86. Salmon, C. G., and Johnston, B. G., (1990), *Steel Structures - Design and Behavior*, 3rd Edition, Harper Collins Publishers Inc.. NY, USA, 1990.
87. Sarraf, M. and M. Bruneau (1998). "Ductile seismic retrofit of steel deck-truss bridges. II: Design applications." *Journal of Structural Engineering* 124(11): 1263-1271.
88. Schneider, S. P. and A. Amidi (1998). "Seismic behavior of steel frames with deformable panel zones." *Journal of Structural Engineering* 124(1): 35-42.
89. Schneider, S. P., Roeder, C. W. and Carpenter, J. E. (1993). "Seismic behavior of moment-resisting steel frames: experimental study." *Journal of Structural Engineering* 119(6): 1885-1902.
90. Seismic, A. (2010). *Seismic Provisions for Structural Steel Buildings*, (ANSI/AISC 341-10), American Institute of Steel Construction, Chicago, IL.
91. Specifications, F. R. (2000). "Quality Assurance Guidelines for Steel Moment Frame Construction for Seismic Applications." FEMA-353. Federal Emergency Management Agency, USA.
92. Tsai, K. C, and Popov, E. P., (1988), "Steel Beam-to-Column Joints in Seismic Moment Frames," Report No. UCB/EERC-88-19, Earthquake Engineering Research Center, College of Engineering, University of California at Berkeley, 1998.

93. Tuna, M. and C. Topkaya (2015). "Panel zone deformation demands in steel moment resisting frames." *Journal of Constructional Steel Research* 110: 65-75.
94. Uang, C.-M. and D. M. Bondad (1996). Static cyclic testing of pre-Northridge and haunch repaired steel moment connections, Division of Structural Engineering, University of California, San Diego.
95. Venture, S. J. (1999). "Interim guidelines advisory No. 2 supplement to FEMA-267." FEMA Publication 267b.
96. Wilson, E. and A. Habibullah (1998). "SAP2000 – Structural Analysis Users Manual." Computers and Structures, Inc.
97. Xue, M., Kaufmann, E. J., Lu, L. W., and Fisher, J. W., (1996), "Achieving Ductile Behavior of Moment Connections - Part II," *Modern Steel Construction*, June, 1996.
98. Yang, T.-S. and E. P. Popov (1996). Analytical studies of pre-Northridge steel moment-resisting connections. *Proceedings of 11th World Conference on Earthquake Engineering*.
99. Youssef, N. F. G., Bonowitz, D., and Gross, J. L., (1995), "A Survey of Steel Moment- Resisting Frame Buildings Affected by the 1994 Northridge Earthquake," Building and Fire Research Laboratory, National Institute of Standards and Technology, MD, USA, 1995.
100. Youssef, N. F., Bonowitz, D., and Gross, J. L. (1995). A survey of steel moment-resisting frame buildings affected by the 1994 Northridge earthquake, US National Institute of Standards and Technology.
101. Zekioglu, A., Mozaffarian, H. and Uang, C. M. (1997). Moment frame connection development and testing for the city of hope national medical center. *Building to Last*, ASCE.

Appendix-A

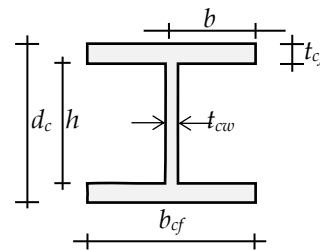
Illustrative Example: Force Deformation Behaviour Using Proposed Method

The proposed method to obtain force deformation behaviour is explained for an interior beam to column strong axis joint. The joint subassemblage considered consists of column (W27×235) having a clear height of 3.8m between supports, and two beams (W16×100) of 3m length from column centerline. The sections selected are AISC standard sections. Column to Beam Strength Ratio for the selected beam to column joint subassemblage is 3.89.

The design constants required in the proposed method are Modulus of Elasticity (E): 200,000 MPa), Poisson's ratio (ν): 0.26 and yield strength (f_y): 250MPa) for A36 steel. The stepwise procedure for obtaining the force deformation behaviour is given below:

I. Properties of Column Section:

Depth of Column Section, $d_c = 729$ mm,
 Thickness of Column Web, $t_{cw} = 23$ mm,
 Width of Column Flange, $b_{cf} = 361$ mm,
 Thickness of Column Flange, $t_{cf} = 41$ mm,



1. Check for Column section class:

$$a. \frac{b}{t_{cf}} = 4.4 < 15.83 \left(= 0.56 \sqrt{\frac{E}{f_y}} \right) \text{ and } \frac{h}{t_{cw}} = 28.13 < 42.14 \left(= 1.49 \sqrt{\frac{E}{f_y}} \right)$$

Thus, the section selected is a non-slender section as per AISC 361-10.

$$2. \text{ Moment of Inertia of Column Section, } I_c = \left\{ \frac{b_{cf} \times d_c^3}{12} + \frac{(b_{cf} - t_{cw}) \times (d_c - 2 \cdot t_{cf})^3}{12} \right\}$$

$$= 4026239063 \text{ mm}^4;$$

$$3. \text{ Elastic Section Modulus of Column Section, } Z_{ec} = \frac{I_c}{(d_c/2)} = 11045923 \text{ mm}^3;$$

4. Plastic Section Modulus of Column Section,

$$Z_{pc} = 2 \left\{ \frac{t_{cw} \left(\frac{d_c}{2} - t_{cf} \right)^2}{2} + b_{cf} t_{cf} \left(\frac{d_c}{2} - \frac{t_{cf}}{2} \right) \right\}$$

$$= 11045923 \text{ mm}^3;$$

$$5. \text{ Shape Factor for Column Section, } S_c = \frac{Z_{pc}}{Z_{ec}} = 1.14;$$

$$6. \text{ Plastic Moment Capacity of Column Section, } M_{pC} = \frac{f_{yc} Z_{pc}}{1000000} = 3147.52 \text{ kNm.}$$

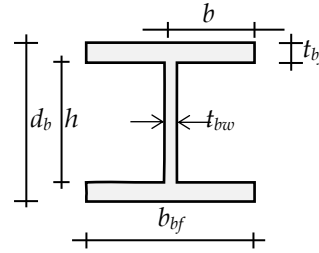
II. Properties of Beam Section:

Depth of Beam Section, $d_b = 432 \text{ mm}$,

Thickness of Beam Web, $t_{bw} = 15 \text{ mm}$,

Width of Column Flange, $b_{bf} = 264 \text{ mm}$,

Thickness of Column Flange, $t_{bf} = 25 \text{ mm}$,



7. Check for Beam section class:

$$a. \frac{b}{t_{bf}} = 5.28 < 10.75 \left(= 0.38 \sqrt{\frac{E}{f_y}} \right) \quad \text{and} \quad \frac{h}{t_{cw}} = 25.47 < 106.35$$

$$\left(= 3.76 \sqrt{\frac{E}{f_y}} \right)$$

Thus, the section selected is a compact section as per AISC 361-10.

$$8. \text{ Moment of Inertia of Column Section, } I_b = \left\{ \frac{b_{bf} \times d_b^3}{12} + \frac{(b_{bf} - t_{bw}) \times (d_b - 2 \cdot t_{bf})^3}{12} \right\}$$

$$= 617007910 \text{ mm}^4;$$

$$9. \text{ Elastic Section Modulus of Column Section, } Z_{eb} = \frac{I_b}{(d_b / 2)} = 2856518 \text{ mm}^3;$$

10. Plastic Section Modulus of Column Section,

$$Z_{pb} = 2 \left\{ \frac{t_{bw} \left(\frac{d_b}{2} - t_{bf} \right)^2}{2} + b_{bf} t_{bf} \left(\frac{d_b}{2} - \frac{t_{bf}}{2} \right) \right\} = 3233415 \text{ mm}^3;$$

$$11. \text{ Shape Factor for Column Section, } S_b = \frac{Z_{pb}}{Z_{eb}} = 1.132;$$

$$12. \text{ Plastic Moment Capacity of Column Section, } M_{pB} = \frac{f_{yb} Z_{pb}}{1000000} = 808.35 \text{ kNm.}$$

Thus, the Column to Beam Strength Ratio (CBSR) for selected interior joint subassembly is $CBSR = \frac{2 \times M_{pC}}{2 \times M_{pB}} = 3.89$.

13. If doubler plates are provided, the thickness of column web at the JPZ level increases. This increased thickness of JPZ is taken into consideration as, $t_{pz} = (t_{cw} + t_{dp})$ where t_{dp} is the total thickness of doubler plates provided.

III. Yielding Modes and Sequence:

For Interior beam to column joint subassemblages,

$$14. \text{ Beam Flange Yield Strength, } F_{y,bf} = \frac{f_y \times b_{bf} \times t_{bf}}{1000} = 1650 \text{ kN}$$

$$15. \text{ Panel Zone Yield Strength, } V_{y,pz} = \frac{\left(\frac{f_y}{\sqrt{3}} \times d_c \times t_{pz} \right)}{1000} = 2420 \text{ kN}$$

16. Beam Flange force, corresponding to plastic flexural strength of beam, M_{pB} :

$$F_{p,bf} = \frac{M_{pB}}{(d_b - t_{bf}) \times 1000} = 1986.13 \text{ kN}$$

Since, $V_{y,pz} < 2 \times F_{y,bf} < 2 \times F_{p,bf}$, the yielding sequence will be

- a. JPZ Yielding,
- b. Beam Flange Yielding,
- c. Beam Plastic Hinge formation.

IV. Yield Forces:

17. Shear Force in Beam corresponding to its plastic flexural strength is

$$V_{pB} = \frac{M_{pB}}{\left(\frac{L_b - d_c}{2} \right) \times 1000} = 306.72 \text{ kN}$$

18. Beam end force required for shear yielding of JPZ (P),

$$V_{y1} = \left(\frac{V_{y,pz}}{2} \right) \times \left(\frac{d_b - t_{bf}}{L_b/2 - d_c/2} \right) = 186.87 \text{ kN}$$

19. Beam end force for beam flange yielding (BFY), $V_{y2} = \frac{F_{y,bf} (d_b - t_{bf})}{(L_b/2 - d_c/2)} = 254.81 \text{ kN}$

20. Beam end force for formation of plastic hinge in beams (BPH),

$$V_{y3} = \frac{F_{p,bf}(d_b - t_{bf})}{(L_b/2 - d_c/2)} = 306.72 \text{ kN}$$

V. Post-Yield Stiffnesses:

21. Beam Stiffness:

a. Post- first (flange) yielding: $K_{b1} = \frac{\left(\frac{1}{12} \times t_{bw} \times d_b^3\right)}{I_b} = 0.16$

b. Post formation of plastic hinges: $K_{b2}=0.05$ (Assumed)

22. Panel Zone Stiffness:

a. Immediately following yield: $K_{pz1}= 0.07$ (Literature [Krawinkler, 1978])

b. Post significant yield: $K_{pz2}=0.03$ (Literature [Krawinkler, 1978])

VI. First Yield Event:

At the initiation of first yield,

23. Beam end force, $V_{y1} = \frac{V_{y,pz}}{2} \times \frac{(d_b - t_{bf})}{(L_b/2 - d_c/2)} = 186.87 \text{ kN}$

24. Bending Moment in Column, $M_{c1} = \frac{2 \times V_{y1} \times (L_b/2)}{1000} = 1121.21 \text{ kNm}$

25. Rotation of Columns, $\theta_{c1} = \frac{(M_{c1}/2) \times 1000000 \times (L_c/2)}{3 \times E \times I_c} = 0.00044092 \text{ rad}$

26. Shear in JPZ, $V_{pz,1} = \frac{2 \times V_{y1} \times (L_b/2 - d_c/2)}{(d_b - t_{bf})} = 2420.11 \text{ kN}$

27. JPZ deformation, $\gamma_{pz1} = \frac{V_{pz,1} \times 1000}{G \times d_c \times t_{pz}} = 0.00181865 \text{ rad}$

28. Drift in Column, $\Delta_{c1} = \theta_{c1} \times \frac{L_b}{2} = 1.323 \text{ mm}$

29. Drift in JPZ, $\Delta_{pz1} = \gamma_{pz1} \times (L_b/2 - d_c/2) = 4.793 \text{ mm}$

30. Drift in Beam, $\Delta_{b1} = \frac{V_{y1} \times 1000 \times (L_b/2 - d_c/2)^3}{3 \times E \times I_b} = 9.240 \text{ mm}$

$$31. \text{ Total drift at first yield, } \Delta_{total1} = \Delta_{c1} + \Delta_{pz1} + \Delta_{b1} = 15.356 \text{ mm}$$

$$32. \text{ Percentage drift at first yield, } \%D_1 = \frac{\Delta_{total1}}{L_b/2} \times 100 = 0.512\%$$

VII. Second Yield Event:

Post first yield,

$$33. \text{ Beam end force, } V_{y2} = \frac{F_{y,bf} (d_b - t_{bf})}{(L_b/2 - d_c/2)} = 254.81 \text{ kN}$$

$$34. \text{ Bending Moment in Column, } M_{c2} = \frac{2 \times V_{y2} \times (L_b/2)}{1000} = 1528.86 \text{ kNm}$$

$$35. \text{ Rotation of Columns, } \theta_{c2} = \frac{(M_{c2}/2) \times 1000000 \times (L_c/2)}{3 \times E \times I_c} = 0.00060123 \text{ rad}$$

$$36. \text{ Shear in JPZ, } V_{pz,2} = \frac{2 \times V_{y2} \times (L_b/2 - d_c/2)}{(d_b - t_{bf})} = 3300 \text{ kN}$$

$$37. \text{ JPZ deformation, } \gamma_{pz2} = \gamma_{pz1} + \frac{(V_{pz,2} - V_{pz,1}) \times 1000}{(0.07 \times G) \times d_c \times t_{pz}} = 0.0112646 \text{ rad}$$

$$38. \text{ Drift in Column, } \Delta_{c2} = \theta_{c2} \times \frac{L_b}{2} = 1.804 \text{ mm}$$

$$39. \text{ Drift in JPZ, } \Delta_{pz2} = \gamma_{pz2} \times (L_b/2 - d_c/2) = 29.688 \text{ mm}$$

$$40. \text{ Drift in Beam, } \Delta_{b2} = \frac{V_{y2} \times 1000 \times (L_b/2 - d_c/2)^3}{3 \times E \times I_b} = 12.600 \text{ mm}$$

$$41. \text{ Total drift at first yield, } \Delta_{total2} = \Delta_{c2} + \Delta_{pz2} + \Delta_{b2} = 44.091 \text{ mm}$$

$$42. \text{ Percentage drift at first yield, } \%D_1 = \frac{\Delta_{total2}}{L_b/2} \times 100 = 1.47\%$$

VIII. Third Yield Event:

At initiation of third yield event,

$$43. \text{ Beam end force, } V_{y3} = \frac{F_{p,bf} (d_b - t_{bf})}{(L_b/2 - d_c/2)} = 306.72 \text{ kN}$$

$$44. \text{ Bending Moment in Column, } M_{c3} = \frac{2 \times V_{y3} \times (L_b/2)}{1000} = 1840.3 \text{ kNm}$$

$$45. \text{ Rotation of Columns, } \theta_{c3} = \frac{(M_{c3}/2) \times 1000000 \times (L_c/2)}{3 \times E \times I_c} = 0.0007237 \text{ rad}$$

$$46. \text{ Shear in JPZ, } V_{pz3} = \frac{2 \times V_{y3} \times (L_b/2 - d_c/2)}{(d_b - t_{bf})} = 3972.25 \text{ kN}$$

$$47. \text{ JPZ deformation, } \gamma_{pz3} = \gamma_{pz2} + \frac{(V_{pz3} - V_{pz2}) \times 1000}{(0.03 \times G) \times d_c \times t_{pz}} = 0.028104 \text{ rad}$$

$$48. \text{ Drift in Column, } \Delta_{c3} = \theta_{c3} \times \frac{L_b}{2} = 2.171 \text{ mm}$$

$$49. \text{ Drift in JPZ, } \Delta_{pz3} = \gamma_{pz3} \times (L_b/2 - d_c/2) = 74.068 \text{ mm}$$

$$50. \text{ Drift in Beam, } \Delta_{b3} = \Delta_{b2} + \frac{(V_{y3} - V_{y2}) \times 1000 \times (L_b/2 - d_c/2)^3}{(3 \times E \times I_b) \times 0.16} = 28.315 \text{ mm}$$

$$51. \text{ Total drift at first yield, } \Delta_{total3} = \Delta_{c3} + \Delta_{pz3} + \Delta_{b3} = 104.554 \text{ mm}$$

$$52. \text{ Percentage drift at first yield, } \%D_1 = \frac{\Delta_{total3}}{L_b/2} \times 100 = 3.485\%$$

IX. Bilinear Idealization:

This method provides a tri-linear curve, representing the force deformation behaviour of the beam to column joint considered for this illustration (Figure A-1). To utilize this proposed curve for Nonlinear Dynamic Time History Analysis of frames, a bilinear idealization of the force deformation behaviour is required. The method of idealization adopted for the present study is presented in this section.

53. Beam End Force at first yield,

$$V_{y1} = 186.67 \text{ kN}$$

54. Total drift at first yield, $\Delta_{total1} = 15.356 \text{ mm}$

55. Average of Second and Third yield forces,

$$V_{y2}' = \frac{V_{y2} + V_{y3}}{2} = 280.77 \text{ kN}$$

56. Target Drift required, $\Delta_t=120\text{mm}$

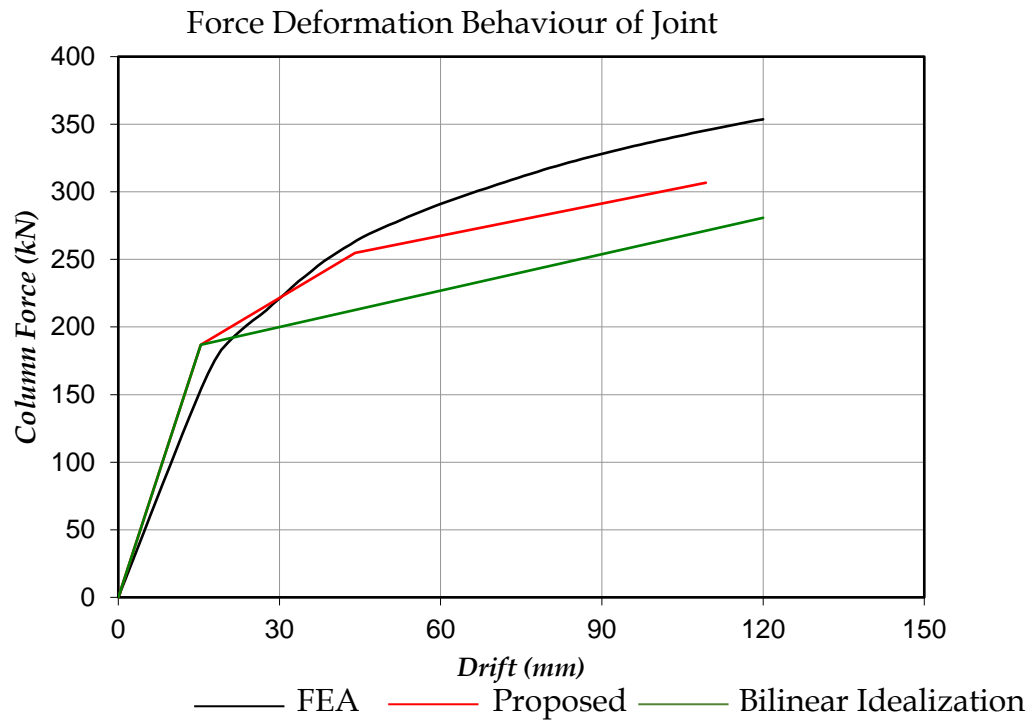


Figure A-1: Force Deformation Behaviour of an interior beam to column joint subassembly.

BIO-DATA

The author is a regular PhD Research Scholar at Malaviya National Institute of Technology Jaipur, Jaipur (Rajasthan) since 2012. He obtained his Bachelor's Degree in Civil Engineering from Jabalpur Engineering College, Jabalpur (Madhya Pradesh) in 2010. He completed his Master's Degree in Structural Engineering with dissertation on "**Seismic Hazard Mitigation of Multi Storied Building using Semi Active MR Damper**", from Malaviya National Institute of Technology Jaipur, Jaipur (Rajasthan) in 2012. His area of specialization is "Earthquake Engineering".

Following is the list of the publications from his Doctoral work.

1. A A Kasar, R. Goswami, S D Bharti and M K Shrimali, (2015) "Influence of Joint Panel Zone on Seismic Behaviour of Beam to Column Connections", *Advances in Structural Engineering*, *Advances in Structural Engineering: Dynamics (Refereed)*, Volume Two, pp. 933-943, ISBN: 978-81-322-2192-0 (Print) ; 978-81-322-2193-7 (Online)
2. A A Kasar, R Goswami, S D Bharti and M K Shrimali, (2014), "Parametric Analysis of Moment Connection Based on Beam-to-Column Strength Ratio", 15th Symposium on Earthquake Engineering (Refereed), *Proceedings of 15SEE*, Elite Publishing House Pvt. Ltd.; IIT Roorkee, pp. 621-632.